Recent advancement and applications of mass spectrometry imaging

Bharath S. Kumar Ph.D., MRSC*
Independent Researcher
21, B2, 27th street, Nanganallur, Chennai, India
*bskumar80@gmail.com
ORCID: 0000-0002-3594-7881

Abstract

Analysis concerning the spatial distribution of biomolecules in complex surfaces can be accomplished with mass spectrometry imaging [MSI]. The in situ direct determination of the abundance of lipids, peptides, proteins, and metabolites in segments of tissues enables MSI to be an effective technique. Molecule-specific visualization can be accomplished utilizing a variety of ionization techniques, each of which generates data with great spatial and mass accuracy and is suitable for a particular application. A chemical microscope that may be utilized for straightforward biomolecular assessment of histopathological tissue surfaces is generated through the integration of molecular classification with regional assessment. MSI effectively enables label-free identification and mapping of a variety of biological compounds, the presence or absence of which may be an obvious indication of disease pathogenesis. The MSI protocol's several phases must be carefully adhered to if one wants to detect the target analytes with the necessary spatial resolution. When combined with other imaging modalities, MSI can be used to ascertain the connection between changes in the spatial distribution of essential chemicals and other differences in the properties of the tissue. The findings of the examined empirical research illustrate how MSI represents a viable experimental approach with an assortment of applications. The paper will concentrate on technical developments, applications, challenges, and MSI's prospects moving forward.

Background

The unfulfilled requirement for exceptionally precise illness diagnosis techniques presents new difficulties for laboratory medicine advancements. Biomedical diagnostic procedures must be completed accurately and quickly to support clinical judgment and enhance patient care. Over the past few decades, the continual advancement of novel analytical techniques and practices has had a significant impact on the early diagnosis of diseases and the creation of effective therapeutic regimens. The identification of molecular pathways that underlie protein pathology in illnesses continues to be a challenge, which has a negative impact on the advancement of effective therapeutic approaches. The lack of biochemical tools with the required precision, sensitivity, and spatial- and temporal resolution to define molecular mechanisms at cellular length scales is one factor that contributes to the inadequate comprehension of the fundamental molecular processes in diseases.[1] Techniques for chemical imaging are vital bioanalytical tools for understanding molecular alterations on a subcellular scale. Different biochemical imaging tools, such as immunoassays, can be used to examine spatial variations of various molecular targets *in vivo* and *in situ*.[1] While immunoassays are used most frequently in in vitro testing for

identifying an intended analyte, some drawbacks of this approach (low sensitivity, inadequate dynamic range, and frequently costly and lengthy processing times) have prompted researchers to look for superior alternatives using alternative strategies.[2] These strategies should be highly accurate, precise, and provide high throughput. Due to its extremely high sensitivity, which can reach the femtomolar range, mass spectrometry [MS] can perform more effectively in diagnosing molecular pathology than conventional biochemical assays.[3]

In the field of biomedical science, MSI has gained prominence as a technique for in situ mapping of the spatial distribution of chemical species. By applying this method, the in situ distribution characteristics of metabolites, lipids, peptides, and proteins can be comprehensively and untargetedly characterized.[4] MSI refers to processes that gather both chemical and spatial data to interpret and display the outcomes as chemical illustrations.[4] Both 2D and 3D images can be captured using the experiment. Due to its great chemical specificity and comparatively simple use, MSI has become a promising technology in many fields, including health care, material sciences, and forensics.[5-9] Metabolite analysis and morphological traits are displayed in a single image by fusing the robust rapid examination of high-throughput capabilities of MS with spatial chemical data. MSI can be employed to analyze metabolic profiles qualitatively and quantitatively, and it can offer visual evaluation of spatial distribution data of intricate biological and microbial environments.[10] MSI offers label-free, non-targeted chemical imaging. Prior to analysis, molecular species are not required to be chosen, and quite often, compounds can be recognized without being chemically altered or using labeling substances. This stands in stark contrast to traditional histological procedures, which attach labels to target structures to visualize structural components of cells, tissues, or organs.[11] Despite MSI's nontargeted nature, histological information can be effectively extracted from the data set, often even exceeding the amount of knowledge provided through histochemical staining procedures.[11] Discovering illness biomarkers of different dimensions and polarity requires knowledge of how ions are formed.[11] To microscopically see unlabeled molecular components in or on biochemical or ecological specimens, several MS techniques—including MALDI, DESI, LAESI, SIMS, etc.—have emerged or continue to be widespread. Other approaches, such as combinations with post-ionization units, liquid extraction concepts, and surface activation approaches, are also known in addition to these key techniques. All these techniques have unique principles, attributes, and performances, and each one has at least one benefit over the others.

Mass spectrometry imaging (MSI)

MSI is an innovative, label-free analytical approach that can collect chemical data that is spatially resolved by detecting the m/z of several molecular species across the tissue specimen. [12] Without the need for any prior knowledge, MSI allows label-free assessment of the prospective target species, unlike other, more proven methods of biochemical imaging.[1] By mapping key biomolecules, MSI, an ex vivo molecular visualization technology, can give researchers a better understanding of biochemical reactions taking place in the tissue.[1] Several illnesses exhibit molecular dysregulation as a defining feature.[13-16] Consequently, new avenues for diagnosis and treatment are opening because of MSI investigations of the biomarkers connected to these illnesses. This is especially helpful when conventional histopathology's morphological markers

are ambiguous and tissue chemical analysis seems to offer more quantitative data about the illness.[12] Even though MSI studies are untargeted, the preparation of samples can be customized for multiple categories of desired molecules of interest. [1]

Key features of MSI over other imaging modalities

1) It is possible to acquire several distinct molecular distributions at once: The vast array of chemical species that can be examined is one of the features of MS. This capability allows for the possibility of documenting the biodistribution of many phospholipid groups at once or viewing all the metabolites in depth. Additionally, it is feasible to identify drugs, peptides, phospholipids, and their metabolites concurrently. [17]

2) Visualizing ionizable materials is possible. The intensity dispersion of the ions found on the specimen surface after ionization can be observed in MSI. As a result, after ionization, the ions can be observed. It can seem typical, but if ionization is conceivable, even a very slight difference in m/z can be seen as a distinct image. As a result, making use of an FT-ICR-MS, it is now possible to provide imaging data by peak isolation with extremely high mass resolution. [18,19]

3) Even compounds that are not visible to antibodies can nonetheless be recognized. [17]

The two common types of MSI approaches include a) scanning MSI and b) stigmatic MSI.

Scanning MSI

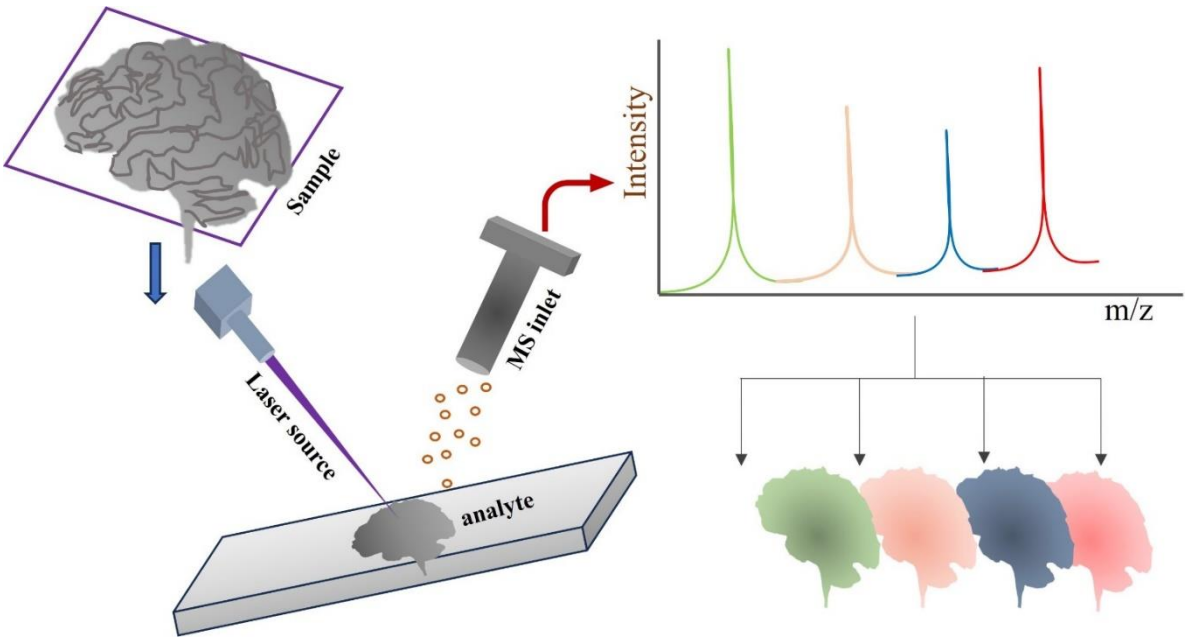

Figure 1. Schematic illustration of MSI workflow

In a scanning MSI, imaging is carried out by scanning the tissue surface in two planes, then recording the MS output pixel-by-pixel (Figure 1). The ion signatures associated with chemical species, however identified, can be merged with their spatial characteristics to create their ion images. MS data are gathered across the tissue surface. 2 The intensity gradient at a specific m/z is collected from the obtained mass spectrum.[17] The diameter of the irradiation spot and the spot

spacing determine the spatial resolution of the image in the scanning type. "Oversampling" occurs when the spacing is less than the spot diameter. The acquisition of several mass spectra is required to scan for an image with a high spatial resolution.[17]

Stigmatic MSI

Ionization is done as a surface with stigmatic-type MSI rather than as a point. The ionized ions in the stigmatic MIS reach the detector while still being distributed across the tissue surface. Thus, a high-spatial-resolution detector can be used to produce an image with excellent resolution. By placing an ion optical system before the detector, it is also feasible to identify the image as a changing magnification image.[17]

McDonnell and Heeren (2007) state that complementary benefits and drawbacks set apart the various ionization processes employed in MSI that mostly relate to spatial resolution, mass accuracy and resolution, chemical precision, specificity, and molecular mass spectrum.[6] Typically, two factors are prioritized: (i) spatial resolution and (ii) molecular mass range, while evaluating the performance and applicability of MSI for the investigation of various molecular species in various tissues and in diverse biological settings.[1] Both characteristics depend on the desorption technique, including the probe's size, the construction of the mass detector, and most crucially, the sample preparation. The purpose of this review article is to provide a succinct summary of the key developments and applications of MSI, as well as acclimate the reader to the course of an experiment, instrumental developments, and methodological problems. [1]

Sample preparation

The processing of MSI samples involves several different factors, from sample collection to surface pretreatment and analysis. Tissue harvest from either human or animal origins and preserving tissues are the most significant aspects determining the reliability of the collected information across all MSI studies.[1] After surgical excision, tissue must be handled carefully and quickly to avoid molecular fragmentation and spatial rearrangement.[20] Although FFPE fixed and fresh-frozen tissue are both capable of being evaluated by MSI, fresh-frozen tissue is the form that is most commonly used. The primary rationale for this is that chemical infusion and preservation methods are difficult to incorporate into MS-based studies because they interfere with MS detection. However, recent studies have shown that lipids, peptides, and even metabolites are capable of being effectively detected in FFPE-fixed specimens[21-23], which is opening a wide range of possibilities for MALDI MSI-based histology investigations on substantial unhealthy specimen sizes that are available through tissue banks.[24,25] For MSI, the most popular technique for molecular analysis of ex vivo tissue specimens remain the use of fresh-frozen tissue.[1] Rapid freezing is necessary to prevent cell wall ripping, which would otherwise alter tissue architecture and the functioning of proteins at the cellular and subcellular levels. As a result, rather than forming a crystalline structure, water solidifies, resulting in an amorphous, vitreous state.[1] The amount of tissue exposed to the cooling agent is increased when sliced sections are rapidly frozen in liquid nitrogen, which supposedly allows for the fastest cooling rate.[1] Nevertheless, if a vapor barrier develops on the topmost layer of warm tissue,

inconsistent freezing might take place. Isopentane that has been cooled with liquid nitrogen or, rarely, with dry ice is also used for larger samples, like whole rat brains.[1]

Thin, flat platforms are required for MSI analysis. The temperature of cryo-sectioning, which is frequently used to prepare specimens on a microtome, varies depending on the type of tissue (fatty versus water-based tissues). The dissected tissue segments can be placed simply on a conductive surface for thorough tissue imaging. An alternate approach is the sample stretching technique. In this case, the tissue segment is positioned onto parafilm with embedded glass beads and extended symmetrically in two dimensions. The parafilm is held in place by being attached to a glass slide. The stretching method improves analyte extraction and spatial resolution without requiring concern about diffusion.[26,27] In either method, the specimen might need to be appropriately prepared after mounting the tissue section onto a target. Matrix deposition, enzymatic digestion, and washing methods can all be used, depending on the type of MS, ionization method, and desired molecule class. Since lipids and salts are frequently broken down by common washing solvents, washing shouldn't be performed if these molecules are the target compounds. It is advised to perform many wash procedures ahead of protein or peptide matrix deposition.[28] When salts that can react with it are taken out, the matrix can uniformly crystallize, which increases the ionization effectiveness of peptides and proteins. While implementing the matrix for neuropeptide MSI, sophisticated multistep rinsing procedures are often used. These involve pH-optimized organic and aqueous washes designed to precipitate proteins and peptides, remove lipids, and wash away ions that may impede the MSI signal. However, using abrasive cleaning methods could harm the sample and remove peptides that are important for analysis. It is advised to optimize the matrix and washing processes on adjacent slices to establish the best sample preparation protocol to use for every kind of sample. For DESI-MSI, samples are often not pretreated.

The matrix deposition process must be consistent, reproducible, sensitive, and straightforward to implement. The dimension of the matrix crystals additionally influences how much spatial resolution can be obtained. Matrix deposition for biological samples can be carried out with or without pre-cleansing procedures.[28] DHB (2,5-dihydroxy-benzoic acid), SA (22 sinapinic acid), [29] 2,5-DHA (2,5-dihydroxy acetophenone), [30] and HHCA (4-hydroxy-alpha-cyano-cinnaminic acid) are frequently employed as matrices for protein and peptide analysis.[31] It has been illustrated that MALDI-MSI based on the DHB matrix is a reliable technique for reliable and reproducible MS imaging.[32] Many matrices share the same crystal size, which influences spatial resolution and demands careful calibration. Some matrices, like DHB, also yield larger crystals than others. Nevertheless, with appropriate solvent settings and the optimal nebulizer parameters, the problem can be resolved.

Data assessment

The complicated nature and substantial data footprint of the spectral data generated through studies make them difficult to evaluate.[33] To solve these problems, a large amount of computing resources is needed. For instance, hundreds of thousands of individual pixels make up an average high spatial resolution MALDI-IMS experiment, where each pixel represents a spectrum made up of hundreds of thousands of tiny m/z bins. To produce a composite array of pseudo-colored

images for each potential m/z of interest, these spectra need to be processed through various stages such as thresholding, normalization, and spatial mapping. Adding to this complexity, cross-platform assessments and data sharing have historically been challenging because the majority of MSI instruments use vendor-specific software for initial data processing.[34] To analyze imzML data, the common MSI file format, vendor neutral MSI processing software alternatives have recently emerged.[35-38] This standard format enables the integration of several MSI datasets from various systems, even with vendor-specific applications.

To examine MSI data sets for unbiased segmentation, a variety of multivariate analysis (MVA) techniques can be used.[39-42] Essentially, via multivariate statistics, this technique examines each pixel spectrum as a separate sample in multivariate space, allowing it to determine the most significant differences and co-variation, respectively, which are then recorded in the corresponding factor of the study. The variables, i.e., mass peaks and their intensity, that contribute most to the variation reflected in the factor are obtained from the corresponding loading values. In a similar vein, cluster analysis looks for commonalities that enable the grouping of pixel spectra according to comparable characteristics that fundamentally correspond to comparable peak patterns. This method allows for the identification of chemical variances and similarities throughout the tissue region that is being scanned. The next step is to use the statistics to correlate the chemical patterns that are obtained with the anatomical features and the region of interest (ROI) to do a targeted, comparative statistical analysis of the ROI spectral data further. Many research report combining multiple MVA methods, for example, PCA and maximum autocorrelation factor analysis (MAF), PCA and hierarchical cluster analysis,[43] or PCA, NMF, MAF, and probabilistic latent semantic analysis (PLSA).[44] According to Norris et al. (2007), baseline correction, intensity standardization, smoothing, recalibration, and spectrum alignment are the most crucial phases in the processing of spectra.[45] When using MVA techniques for data processing, recalibration and alignment are especially crucial. In addition to MSI data, fusion can be applied to data from other imaging modalities, including Raman, fluorescence, and FT infrared spectroscopy (FTIR). This helps to overcome the limitations of each method, take advantage of their complementary information, and even pave the way for novel findings in biology. [46,47]

Implementation of orthogonal imaging modalities, such as autofluorescence scans, N-glycan IMS data, and magnetic resonance imaging with autofluorescence microscopy, are new to the field. These modalities allow for the connection of glycosylation differences to pathological features or biomarkers of interest.[48-51]

The relative novelty of N-glycan MSI meant that fewer computational resources were initially available for peak assignment, in contrast to the more established peptide, lipid, and small molecule imaging.[52] To assign N-glycan structures to mass spectra, most laboratories currently use shared online databases like GlyConnect or GlyTouCan, or internal database created with software like GlycoWorkbench or GlycoMod.[53-56] Although there is still much to learn about automated peak selecting software for N-glycans from MSI generated spectra, recent systems like Bruker Daltonic's Metaboscape have showed promise in aligning mass spectra peaks to a vast repository that contains known N-glycan masses with corresponding structures. [57]

Ionization sources

MALDI

The matrix dependent MALDI (Figure 2) method offers high spatial resolutions. The low molecular weight matrix is applied to tissue samples during the MALDI preparation process. The crystallized matrix is then exposed to a laser beam, which causes the matrix to change from a solid to a gaseous state. The sample is then ionized by energy.[58] Images of metabolites are formed and detected using MSI. As it offers a good compromise between sample preparation, chemical sensitivity, and spatial resolution, MALDI is one of the most utilized ionization techniques associated with MSI.[59] Which analytes are detectable depends on the mixture's chemical make-up and the way they are distributed within the sample.[60] Depending on the laser beam, the matrix composition, and the distribution of analytes in the specimen, MALDI-MSI has a spatial resolution that ranges from 5 to 50 µm. [12]

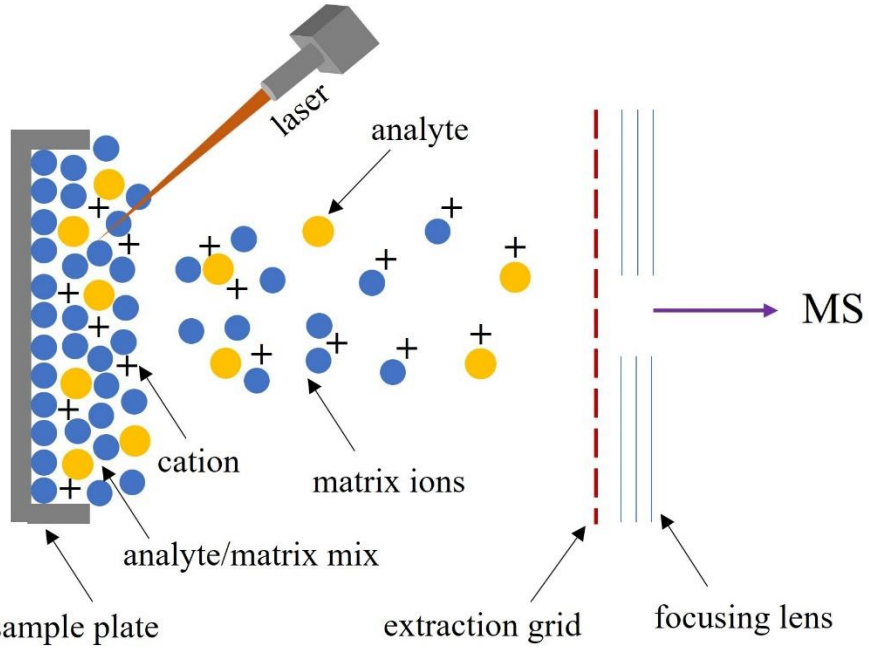

Figure 2. Schematic illustration of MALDI source

Researchers can reliably determine hundreds of metabolites using high-resolution MALDI-MSI with a spatial resolution of 10µm.[61,62] With ambient pressure AP-MALDI, a spatial resolution of 1.4µm can be achieved.[63] However, ion production often falls when the diameter of the laser focus size shrinks to attain a finer spatial resolution.[59,64] Consequently, to carry out spatial metabolomics investigations, investigators still need to strike a balance between obtaining sufficient signal intensities and maintaining finer spatial resolutions. For some molecular species, MALDI-2's sensitivity has increased 100-fold with the inclusion of an additional laser. [59,65]

The ion source section of MALDI-MSI has thus far primarily been operated at high vacuum. From a practical perspective, high vacuum has some drawbacks, such as challenging sample

introduction, matrix chemical volatility, loss of small volatile substances, and changes in specimen morphology. Ion stability has been found to be enhanced by higher pressures up to ambient conditions owing to collisional cooling. The loss of resolution brought on by delocation, which represents molecules flowing through and away from the tissue, is one of the other downsides of MALDI-MSI. Due to these restrictions, multimodal imaging has become increasingly important, which entails computationally superimposing additional imaging information to increase resolutions.[59,64]

Ambient ionization sources

Mass spectrometry (MS) has become extensively employed in analytical and bioanalytical research. This remarkable accomplishment is mostly attributable to MS's unparalleled abilities to identify, capture, and describe molecules and atoms of diverse types, compositions, and sizes.[66] The combination of high sensitivity, selectivity, and speed has long been regarded as one of MS's main advantages. The range of molecules and compounds that MS is capable of handling has also significantly increased in recent years. This means that it is now capable of working with nearly every kind of biological molecule, as well as comparatively small and thermally inert organic molecules, inorganic and organic salts, and organisms like viruses and bacteria.[67-73]

To identify and quantify an extensive array of mixtures, MS must facilitate successful ionization to produce diagnostic ions—ideally for each individual component—that can be transferred to the high vacuum setting of the instrument.[75] There were several challenges to get around when transferring the analyte molecules from their "natural" ambient setting—where target molecules typically exist often in condensed states in complex mixtures to the clean vacuum MS environment.[74]

The introduction of ambient ionization mass spectrometry (AMS), which enables rapid direct analysis of substances in their natural state, completely transformed the discipline of analytical chemistry. Since AMS's introduction, the analytical chemistry community has played a critical role in its advancement, driven by the various benefits it provides over traditional MS.[74] Rapid sample assessment is made possible by the lack of chromatography; ambient ionization sources' adaptability makes them ideal for remote analysis when paired with portable instruments; and lengthy extraction and concentration processes can be minimized or eliminated. Consequently, the prospective applications of AMS have been recognized by an increasing number of scientific disciplines, especially in the fields of environmental sciences, forensics, and illness diagnostics.[75]

DESI

DESI (Figure 3) is an ambient ionization mass spectrometric technique for examining small molecules in the tissues of a living organism that have been dissected[76] or undissected[77]. In comparison to other ionization techniques (such as MALDI, SIMS, etc.) in MSI, DESI has an advantage because it may work in ambient settings and requires little to no sample preparation, making the process extremely rapid.[12] The technique utilizes an affordable solvent spray, which makes it easier to operate than MALDI or SIMS. Additionally, it doesn't require a vacuum for ionization. The DESI probe holds great potential for use in point-of-care diagnostics as it can instantly extract molecular fingerprints from samples of live organs, skins, tissues, biological

fluids, and volatiles when applied directly to those surfaces. [12] In the DESI-MSI, nitrogen is used as the nebulizing gas, and a solvent is electro sprayed at a high voltage to create a stream of fast-moving charged microdroplets that are bombarded onto an area of tissue (10–15 μm).[78,79] The droplet solvent dampens the tissue surface by dissolving biochemical species (mostly lipids and metabolites) found in the tissue. Following the arrival of primary droplets, this liquid layer is splashed, creating secondary microdroplets that extract the biological species. These droplets are then transformed into gaseous ions for identification using mass spectrometry.

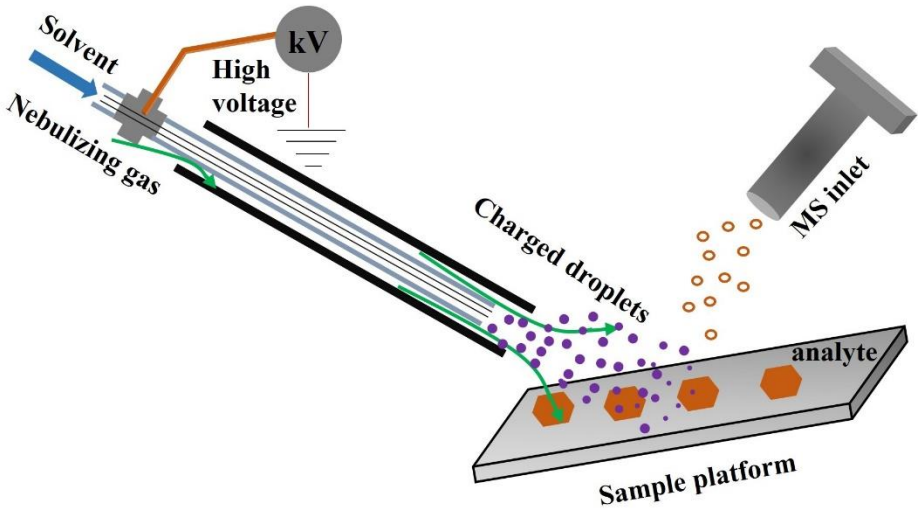

Figure 3. Schematic illustration of DESI source

nano-DESI

A liquid bridge created between two capillaries is utilized in nano-DESI (Figure 4) to perform localized liquid extraction from the specimen.[80,81] The extracted species are ionized by ESI after being transported to a MS inlet via a short nanospray capillary.[82] With only minimum sample preparation and a spatial resolution of 10 μm, nano-DESI MSI allows quantitative imaging of several molecules in biological samples. [82]

EESI

In contrast to conventional ambient MS techniques, EESI (Figure 5) isolates the sample from an electric field and minimizes contamination caused by chemical regents.[83] The primary characteristics of EESI-MS are as follows: (1) instantaneous and remote monitoring; (2) in vivo examination; (3) identification of polar and non-polar substances; (4) tolerance of complicated matrices; (5) absence of chemical contamination; (6) absence of complex sample pretreatment; (7) monitoring ion-molecule or ion-ion reactions; (8) appropriate for investigating liquids, gases, aerosols, surfaces, etc.; and (9) simple to apply with a variety of instruments.[83] Additionally, EESI-MS has demonstrated satisfactory results in in vivo metabolism analysis, offering a practical means of exploring deeply into human body dynamics through the fingerprinting of volatile and nonvolatile analytes in breath samples and real-time assessment of human pharmacokinetic profiles. [84-86]

Internal-EESI [iEESI], a variation of the EESI technique, is frequently used for determining volumetric data concerning molecules within bulk food specimens at the molecular level.[83] Using a capillary and a specific low rate, extractive solutions driven by a high voltage are directly injected into the bulk sample. The extracted analytes were transported by the solvent to the nearby MS for further investigation, following the gradient of the electric field inside the bulk sample.[83] The advantages of i-EESI include: i) direct chemical evaluation across bulk specimens as opposed to the surface; ii) the solvent used is easily variable; iii) a minimal amount of pre-sample treatment; iv) no sheath gas; v) faster analysis time; vi) limited sample consumption; and vii) ease of integration with different types of MS. [83]

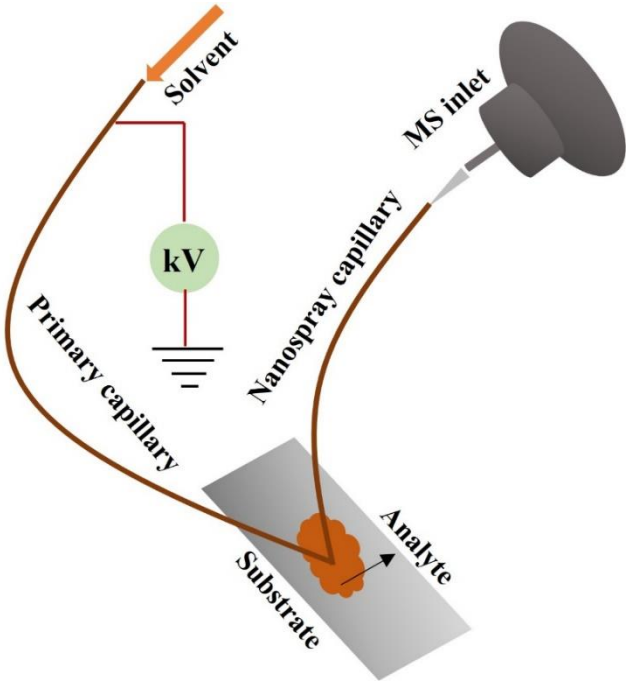

Figure 4. Schematic illustration of nano-DESI source

AFADESI

Like DESI, AFADESI (Figure 6) ionizes the material instantaneously via an electrospray stream.[87]Airflow is subsequently utilized to move ions over a distance.[88] Apart from gaining the benefits of DESI-MSI, AFADESI-MSI can also attain a large coverage of the metabolites under investigation. It can identify thousands of molecules at once in an untargeted experiment.[89] Additionally, it permits whole-body section imaging.[90] Due to the ability to examine and compare many metabolites simultaneously, this coverage significantly increases the potential applications of spatial metabolomics.[83] When the gap between the MSI inlet and the ion transport tube is adjusted, AFADESI can attain picomolar sensitivity. [91]

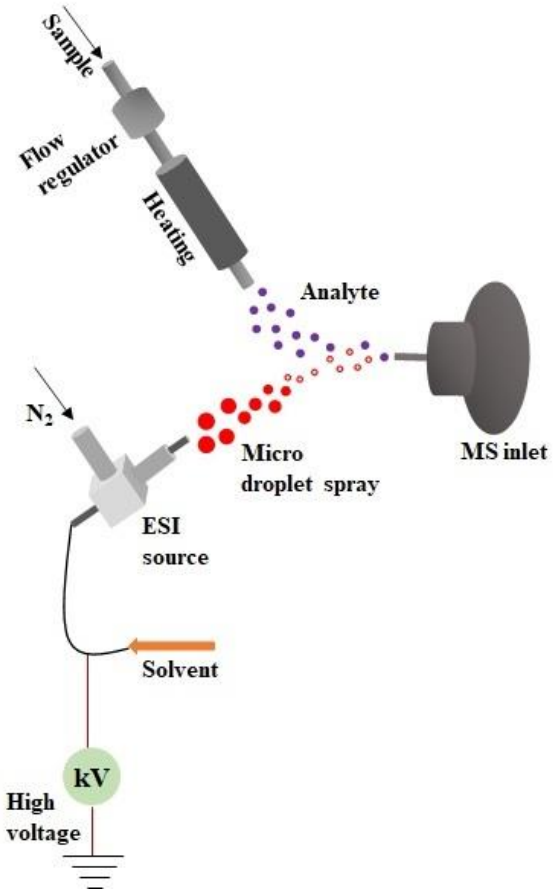

Figure 5. Schematic illustration of EESI source

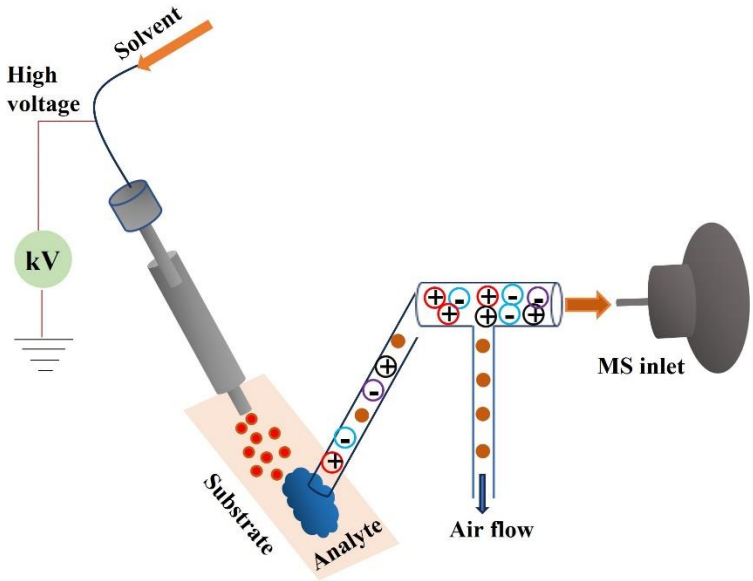

Figure 6. Schematic illustration of AFADESI source

LAESI & IR-MALDESI

Ambient ionization mass spectrometry has also been investigated with laser ablation techniques, which often use UV or IR laser sources. Since lasers may be optically focused to produce extremely efficient desorption at better spatial resolution and pulse frequencies compared to what can be accomplished by solvent- and plasma-based desorption techniques, the use of lasers to promote sample desorption is quite compelling. Of the laser ablation methods, two have continued to be widely used: matrix-assisted laser desorption electrospray ionization (MALDESI) and laser ablation electrospray ionization (LAESI).[92,93]

LAESI

By ablating a sample surface with a mid-IR laser, LAESI produces a plume of predominantly neutral molecules. The concentrated laser beam diameter determines the spatial resolution of LAESI, which is typically operated at approximately 200 μm.[94] Following laser ablation, an electrospray beam intercepts the molecules' plume, ionizing them and directing them in the direction of the mass spectrometer's (MS) intake. Polar molecules are intended targets of ionization, as is the case with other ESI-based techniques. Although there is no need for sample preparation or matrix addition with LAESI, the samples must have a high water content to absorb the IR laser and excite the target appropriately.[92] Verapimil and arginine were among the polar and less-polar analytes analyzed by LAESI during the same experiment. This was accomplished by adjusting the solvent gradient in the ESI source.[95] In an effort to increase sensitivity during remote LAESI—a variant of the technique in which the sample under study is situated further away from the MS inlet—. This approach frequently leads to a loss of sensitivity in comparison to traditional LAESI.[96,97]

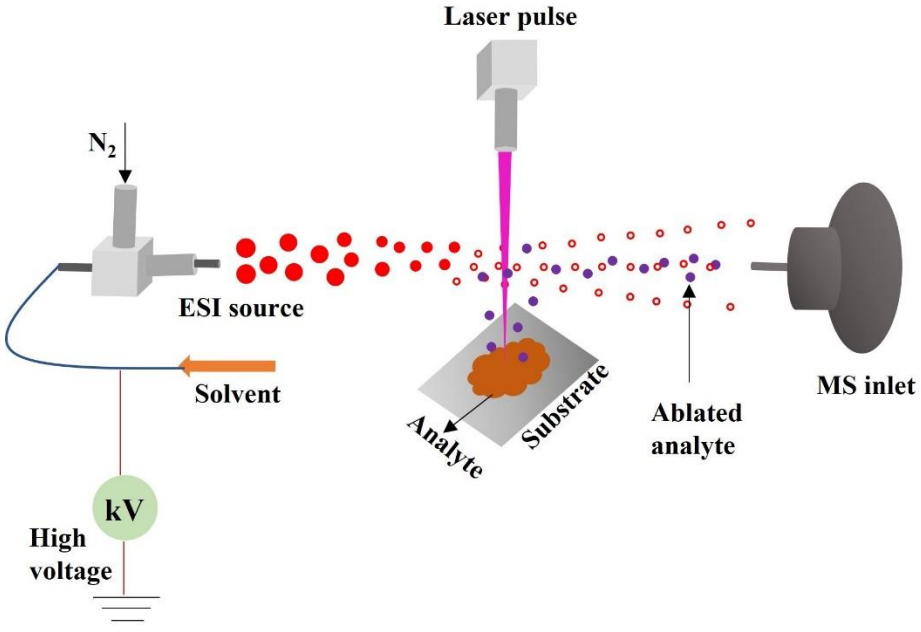

Figure 7. Schematic illustration of IR-MALDESI source

IR-MALDESI

The objective of MALDESI was to combine the laser ablation and MALDI sample preparation processes using an ESI source to ionize. Therefore, to facilitate laser desorption, the specimen had to be co-crystallized with an organic matrix. This was followed by UV laser ablation and subsequent ionization of the plume using an orthogonal ESI beam.[93] The primary objective of MALDESI's development has been technical advancements for imaging applications, particularly regarding its spatial resolution.[98,99] Prior to this, IR-MALDESI's (Figure 7) spatial resolution was limited to about 150 μm, primarily because of restrictions in the IR laser spot size. Higher lateral resolution for tissue imaging purposes was made possible by the laser focal point being narrowed to a 50 μm spot size using a multielement optical system.

Applications of mass spectrometry imaging (MSI) across disciplines

Neuroscience

Recent advances in neurochemical investigations have provided significant insights into the chemical composition of the brain and the involvement of complex molecular machinery with the spatial and temporal orientation of different types of neurotransmitters and other chemicals in it during cognitive disorders.[100] Misfolded proteins can accumulate into hazardous deposits inside or outside of cells, causing neuronal degeneration that progresses in a number of neurodegenerative diseases, including Parkinson's disease, Huntington's disease, Alzheimer's disease, and amyotrophic lateral sclerosis.[101] Understanding the molecular pathways behind neurodegenerative illnesses is aided by the absence of biochemical instruments possessing the necessary responsiveness, selectivity, and temporal and spatial resolution at the cellular level. For this reason, a precise molecular representation of the human brain is essential to comprehending biology and developing efficient monitoring, therapeutic, diagnostic, and predictive techniques for a range of neurodegenerative diseases.[102] Brain analysis has been heavily influenced by the development of contemporary healthcare imaging technologies such as computed tomography, PET, and MRI, in addition to their variants. Though these approaches have revolutionized medical imaging since their debut, none of them are able to directly evaluate the tissue at a high enough resolution to disclose the cellular and molecular characteristics associated with the disorder's severity and subtype.[100] Chemical imaging modalities are essential bioanalytical tools for understanding molecular processes at the subcellular level. Numerous biological imaging modalities may be used to study the spatial variations of distinct molecular targets both in vivo and in situ.[103] In particular, chemical probes and spectroscopy methods, as well as immunohistochemistry and in situ hybridization.[104,105] However, achieving sufficient resolving power while retaining a high level of molecular flexibility, sensitivity, and precision is a significant challenge.[103] Certainly, recent advancements in ex vivo tissue imaging techniques have opened up promising avenues for clinical study.[100] The use of mass spectrometry imaging [MSI] for determining the spatial distribution of biological molecules in situ has grown in popularity in biomedical research. The method allows for the comprehensive and unfocused characterization of the properties of proteins, metabolites, lipids, and peptides' in-situ distribution. Superior molecular specificity provides MSI with a notable advantage over conventional histochemical techniques. The use of MSI has increased significantly in recent years. This type of molecular imaging is not possible with other methods and can map hundreds of biomolecules' distribution in a tissue specimen at once and at a high resolution. Empirical

research, the neuro-domain, important metabolites, metabolic pathways, ionization source, and the MS-analyzer are all listed in Table 1.

Table 1. Empirical studies on MSI in neuroscience.

Domain	Ionization	Authors	Key metabolites	Metabolic pathway	MS analyzer
pharmacokinetics and pharmacodynamics	AFADESI-MSI	Liu et al (2022)	adenosine, histamine, GABA, taurine, glutamine	drug metabolism	Q-orbitrap
Alzheimer's disease	MALDI-TIMS-MSI	Michno et al (2021)	lysophosphatidicacid,glycerolipids, glycerophospholipids, phosphatidylcholine, sphingolipids,phosphoinositol	lipid metabolism	TIMS-TOF
Quantification of Dopamine	nano-SIMS	Rabasco et al (2021)	NA	drug metabolism	NR
Neuroinflammation & N-glycosylation	MALDI-MSI	Rebelo et al (2021)	sialylated and fucosylated structures	N-glycosylation	Q-TOF
Alzheimer Plaque Heterogeneity	MALDI-MSI	Wehrli et al (2022)	lipids and peptides	NA	TOF
Glioblastoma multiforme	MALDI-TOF-MSI	Kampa et al (2020)	lactate, glutamine, N-acetylaspartate, taurine, ascorbic acid	Purine & pyrmidine metabolism	TOF
N-Glycosylation	MALDI-MSI	Heijs et al (2020)	N-glycans	N-glycosylation	QTOF
Temporal Lobe Epilepsy	DESI-MSI	Ajith et al (2021)	phosphatidylcholine, phosphatidyl-ethanolamine	Lipid metabolism	Ion-trap
Glioblastoma tumor	MALDI-FTICR-MSI	O'Neill et al (2022)	Cardiolipins, phosphatidylinositol, ceramide-1-phosphate, and gangliosides	Lipid metabolism	FT-ICR
L-dopa, Parkinson's disease	MALDI-MSI	Fridjonsdottir et al (2021)	L-dopa, 3-o-methyldopa	L-dopa metabolism	FT-ICR
Alzheimer's disease	MALDI-MSI	Strnad et al (2020)	gangliosides,phosphatidylinositols	Lipid metabolism	TOF
blood brain barrier & antipsychotic drug	MALDI-qMSI	Luptakova et al (2021)	risperidone, clozapine, and olanzapine	drug metabolism	FT-ICR
glycoproteomics & N-glycosylation	MALDI-MSI	Malaker et al (2022)	HexNAc4-Hex5-NeuAc2	N-glycosylation	TOF
Neurotransmitters	LDI-MSI	McLaughlin et al (2020)	acetylcholine, dopamine, epinephrine, glutamine, norepinephrine, and serotonin	NA	TOF
Parkinsons diesease-neuropeptides alteration	MALDI-MSI	Hulme et al (2020)	dynorphins, enkephalins, tachykinins, and neurotensin	NA	TOF & FT-ICR
glioblastoma	MALDI-MSI	Duhamel et al (2022)	protein biomarkers	NA	TOF
Ganglioside metabolism - Alzheimers disease	MALDI-MSI	Kaya et al (2020)	monosialogangliosides	Ganglioside metabolism	TOF

Alzheimer's disease

The development of amyloid plaques, a crucial component in the pathophysiology of the disease, is a characteristic of Alzheimer's disease (AD). Patients who display amyloid pathology but retain cognitive normalcy tend to have diffuse architectural properties in their Aβ deposits, suggesting that plaque development is primarily linked to cognitive decline and the pathophysiology of AD.[106] Neuronal malfunction and synaptic loss have been linked to diffuse and neuritic plaques in the brain, which are formed when Aβ oligomers accumulate.[107,108] According to a recent study, this approach may block the deterioration of oligodendrocytes and the lipid-rich myelin sheath seen in the brains of AD patient groups and transgenic AD mouse models.[109] As a result, there has been a lot of discussion about the connection between intracellular lipid deposits, lipid biochemistry, myelin breakdown, and amyloid pathology in AD pathogenesis.[110-115]

In a recently published study, Michno et al. (2022) examined the lipidomic microenvironment connected to the structural polymorphism of the Aβ deposit in mutant mouse models of AD using MALDI-TIMS (trapped ion mobility spectrometry)-TOF in conjunction with hyperspectral imaging. [116] The examination of multivariate imaging data revealed alterations in several lipid species, with widespread trends of enrichment or depletion linked to Aβ.[117] Through the use of hyperspectral imaging, a unique distribution of phosphatidicacid, phophoethanolamine, and phosphoinositol lipids, which are clustered Aβ fibrillary structures inside individual Aβ plaques at different stages of developing plaque disease, was further demonstrated. Additionally, the researchers found a specific cardiolipin deficit that could not have been resolved with a traditional MALDI-TOF setup.[116] The study also showed that a marker of plaque progression is elevated phosphoinositol accumulation.[116] When taken as a whole, these results demonstrate how multidimensional imaging methods can be used to overcome the limitations of conventional MS imaging methods.[116] This made it possible to connect these distinct lipid components to amyloid plaque polymorphs associated with disease and to observe how they varied in a complex environment.

In a recent study, Wehrli et al. (2023) comprehensively analyzed multidimensional MSI and microscopy data to investigate molecular histopathology in complex tissue samples using a spatial chemometrics technique.[118] The method's potential was demonstrated by the study's application of the technique to pinpoint chemical traits of AD pathology.[118] Using trimodal MALDI-MSI and hyperspectral fluorescence microscopy, the spatial distribution changes in lipids and proteins associated with A malfunction in mutant AD mice were investigated.[118] The identification of covariance structures and specific chemical variations during the acquired image resolution was made possible by the use of unsupervised cross-modal chemometrics simulation and multiblock complementary component assessment, which conventional techniques could not accomplish.[118] Researchers will be able to better understand how the multidimensional methodology interacts with the underlying biochemistry thanks to the methodologies that are laid out for correlative molecular imaging.[118]

Brain tumor

Adults with glioblastoma multiforme (GBM) have the highest incidence of major malignant brain tumors. It is classified as a stage 4 neoplasm by the World Health Organization [WHO].[119] Despite efforts at surgery and treatment, the prognosis for glioblastoma is not good; the average survival rate is about fifteen months post diagnosis.[120] The failure of the therapy intervention in glioblastoma is attributed to intratumor variability. High intratumoral[121] and intertumoral variability, glioblastoma cell malleability,[122,123] and a highly immune-suppressive tumor micro-environment [TME], comprising MDSCs[124-127], microglia, and phagocytes, all have an impact on the cancer entity's high resistance to therapy. The cellular variety of glioblastoma within the TME must be understood to develop medications that could potentially treat the disease. Tryptophan [Trp] metabolism is a major regulator of treatment resistance in glioblastoma and other tumor types.[128] Tryptophan catabolic enzymes, or TCEs, have been connected in two distinct ways to the emergence of immunodeficiency and malignancies. Two things can happen when Trp is broken down: (a) cells and their surroundings may be deprived of this vital amino acid, leading to immunosuppressive effects in the TME; and (b) bioactive secondary metabolites are produced because of Trp breakdown. Several metabolites, such as kynurenine (Kyn) and kynurenic acid, can trigger AHR, a ligand-activated transcription component that promotes the replication of AHR target genes.[129] The production of Kyn, which triggers AHR and improves cancer cell mobility while decreasing immune cell proliferation and functionality in the TME, is brought about by high tryptophan-2,3-dioxygenase [TDO2] translation in glioblastomas.[130] Therefore, to fight therapeutic resistance and determine which patients might react best to therapies that center on TCEs and AHR, a fuller understanding of Trp degradation in glioblastoma is needed.

Panitz et al. (2021) examined tryptophan degradation in glioblastoma multiforme patients' blood and tumors using MALDI-MSI.[131] Serum Trp levels are lower in glioblastoma patients than in the general population. Interestingly, Trp concentrations of metabolites also decreased. Less drops were the consequence of increased enzymatic interactions among Trp and its metabolites, indicating that the amounts of Trp's systemic metabolites are regulated by Trp supply.[131] Utilizing MALDI-MSI, it was demonstrated that glioma tissues exhibited heterogeneous Trp degradation. The evaluation of scRNA-seq data demonstrated that almost all glioblastoma cell types exhibited Trp metabolism-related genes and that many different cell types, including macrophages and T cells, had AHR activation. 97% reduced life expectancy rate and elevated AHR activity were associated with the glioblastoma TCGA data.

The categorization of brain malignancies based on DNA methylation has in the meantime developed into a thorough machine learning techniques that has influenced the current WHO classification and resulted in the determination of additional unusual methylation categories of glioblastoma.[132] Even though they can detect and assess the results of modified genomes and transcriptomics and might more accurately describe the triggering of pathways,[133-135] proteomic techniques have not been studied as frequently. To determine proteomic variations between grades and genetic changes, proteomic investigations of gliomas have been carried out.[136] Although glioblastomas are very heterogeneous tumors, a spatially detailed proteomics approach could provide new insights into their biology and improve classification. Finding proteomic markers may improve the capacity to differentiate between the many glioblastoma subtypes and offer therapeutic recommendations.[137]

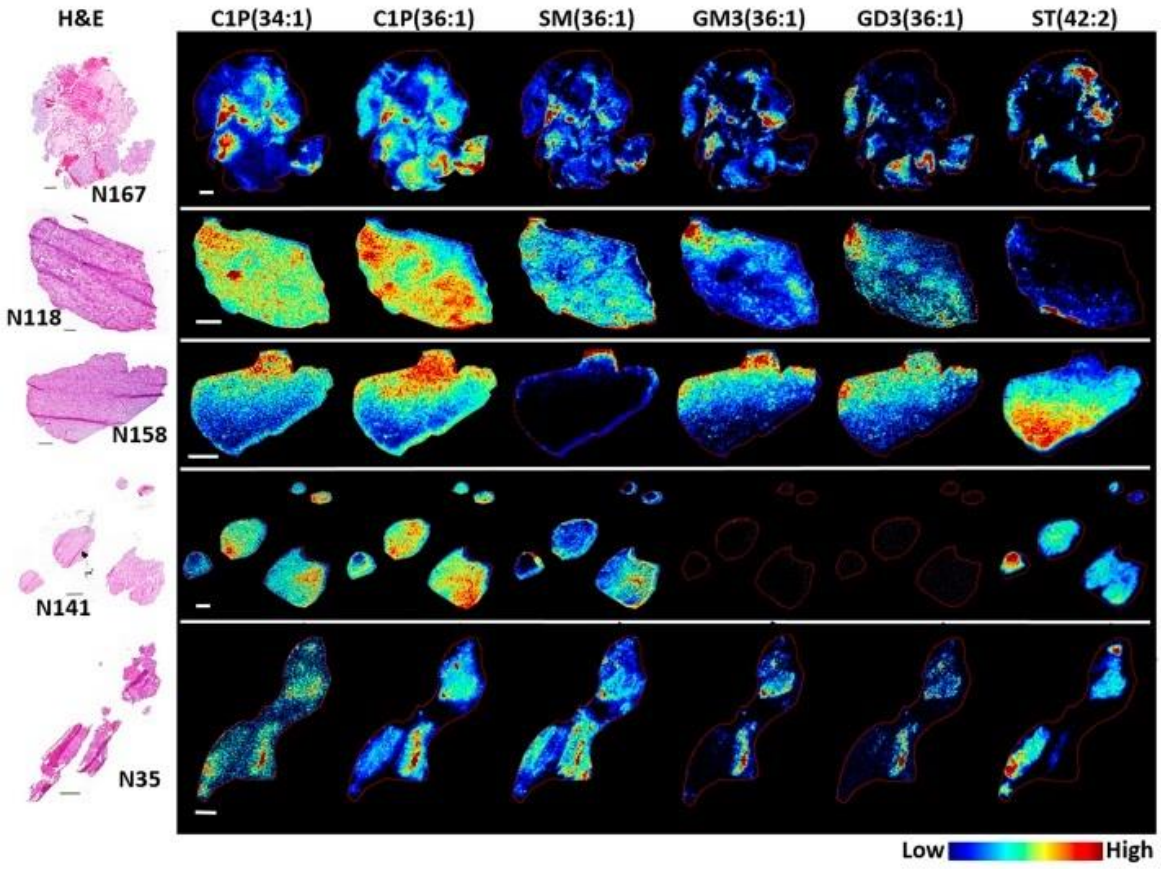

Figure 8. Representative MS images for several sphingolipid species. Sphingolipid subclasses include ceramide1-phosphate (C1P), sphingomyelin (SM), mono- and di-sialodihexosylganglioside (GM3 and GD3 respectively) and sufatide (ST). C1P(34:1) and (36:1) correspond to m/z 616.471 and 644.502, respectively. SM(36:1) corresponds to m/z 715.578. GM3(36:1) and GD3(36:1) correspond to m/z 1179.741 and 1470.830, respectively. ST (42:2) corresponds to m/z 888.624. Images were acquired at 30 µm pixel resolution from 5 µm thick sections; the H&E stained section of each sample is shown in the left panel. Scale bars are 1 mm. [Reproduced with permission from O'Neill et al., (2022), Nature Portfolio.]

An approach for spatially specified proteome analysis was studied by Duhamel et al. (2022). A group evaluation was conducted on 96 glioblastoma patients who had different chances of survival.[137] Through non-targeted MALDI-MSI analysis and spatial division utilizing many methods, the molecular heterogeneity among these malignancies was brought to light.[137] Higher quantities of RPS14 and PPP1R12A have been found in cancer patients with greater chances of surviving, in contrast to the malignancies of individuals with short and moderate survival. Cancer in individuals with brief and moderate survival had higher levels of ANXA11 expression than those of patients who had a longer survival.[137] Proteomic indicators identified by the study provide insight into the intratumoral molecular diversity of glioblastoma tumors.[138] While similar symptoms have been linked to survival in prior research, the results of this study showed that these traits can appear multiple times in a single tumor., which makes them unsuitable for use as prognostic biomarkers.[137] In light of this extreme heterogeneity, scientists have shown that, upon validation in a distinct patient cohort, a number of common markers may be identified for

individuals with cancer with shorter overall survival times and, in contrast, for the malignancies of persons with longer survival times.[137]

Lipids are fundamental regulatory molecules that have roles in apoptosis, differentiation, and proliferation. Through primary and secondary signaling pathways, they are intimately associated with cell survival. Therefore, it is not surprising that variations in cellular composition and lipid degradation have been linked to treatment resistance, aggressiveness, metastasis, and cancer cell development. A component in determining cell fate, the sphingolipid rheostat, is also disturbed in glioblastoma, leading to a reduction in growth inhibition pathways and an increase in growth pathways.[138] To optimize the use of these novel treatments and develop a clinically effective treatment regimen, a comprehensive understanding of the abnormal lipidomic patterns inside the glioblastoma TME is essential.

In a recent study, the early intratumoral lipid diversity among cancer cell subgroups and the various kinds of microvascular forms were identified using high-resolution MALDI-FTICR-MSI.[139] Studies have demonstrated that cardiolipins, phosphatidylinositol, ceramide-1-phosphate, gangliosides, and the glioblastoma stem cell signal GD3 organize differently in endothelial and cancer cell subsections. Conversely, it was shown (Figure 8) that sphingomyelins and sulfatides were reduced in regions with malignant cells.[139] Understanding the relationship between lipid structure and function is essential because the amount of cellular aggregation in each lipid category is governed by the composition of its fatty acid residue.[139] The study's findings identified several lipids in the tumor microenvironment (TME) of glioblastoma, indicating the need for more investigation to produce biomarkers for prediction and lipid-based therapies.[139]

Epilepsy

Over 45 million people worldwide are afflicted with epilepsy, a neurological disorder that has distinct symptoms, a cause, and a propensity to progress.[140] Roughly 20% of all cases of epilepsy that are identified are of the most prevalent type, known as temporal lobe epilepsy [TLE].[141] TLE, which frequently results in the degeneration of the hippocampus. It is expected that TLE, like several other neurological conditions, will disrupt lipid homeostasis. Frequent occurrences of unprovoked, repeated focal epileptic seizures in the temporal lobe result in a range of clinical symptoms.[142] It is anticipated that TLE, like other neurological diseases, will disrupt lipid homeostasis. Numerous etiological factors, including physiological, biochemical, and genetic components, have been linked to TLE.[143] The majority of TLE cases still have unknown causes.

DESI-MSI has been widely used to identify a variety of malignancies by evaluating the spatially defined tissue metabolome.[144] Numerous studies conducted over the past ten years have proven its therapeutic implications for lipidomics assessment. DESI-MSI was utilized by Ajith et al. (2021) in a recent investigation to investigate the differences in hippocampal metabolic changes between TLE patients and non-TLE patients.[145]

The human TLE-HS (TLE-hippocampal sclerosis) showed lower levels of several important lipids, particularly [PC] phosphatidylcholine and [PE] phosphatidylethanolamine, when compared to several other studies on animal models of epilepsy (Figure 9).[145] A metabolic

pathway study suggests that TLE may have repressed the Kennedy pathway, leading to a significant decrease in PC and PE thresholds.[145] More in-depth investigation of the associated biochemical pathways and putative therapeutic targets of TLE is now feasible thanks to this discovery.[145]

Parkinson's disease

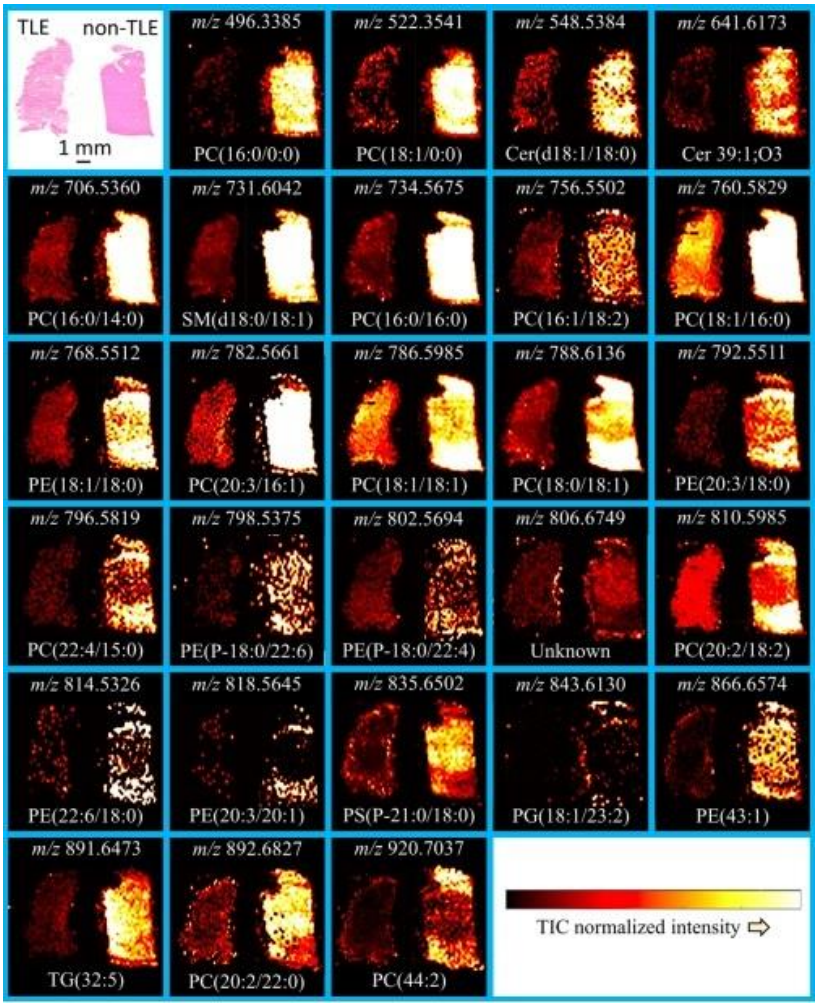

Figure 9. Representative positive ion mode DESI-MS images showing the spatial distribution of 27 lipid species in the human hippocampal section obtained from a TLE (shown on the left-hand side) and a non-TLE (shown on the right-hand side) patient. The upper left box shows optical images of the corresponding H&E-stained tissues. Image data are total ion current (TIC) normalized. [Reproduced with permission from Ajith et al (2021), ACS]

Aberrant neuropeptide synthesis and biotransformation have been linked to several neurological conditions, including Parkinson's disease (PD). PD is characterized by symptoms unrelated to movement, such as stiffness, bradykinesia, and a decrease in balance.[146] One of the main pathogenic features of PD is the degeneration of dopamine-producing neurons in the substantia nigra pars compacta [SNc], which extends to the stria. Disruption of SNc-striatum transmission affects connections with other neuronal circuitry of the basal ganglia that descends, such as the

interior and outer parts of the globus pallidus.[147] PD has been linked to alterations in the production or concentration of the neuropeptides tachykinin, neurotensin, and opioid.[148,149] It is unknown precisely what the converted peptides are and how their synthesis is altered in PD due to measuring problems. The neurotransmitters in the basal ganglia are endogenously liganded by these modified peptides.

Apart from having the ability to distinguish between neuropeptides with identical amino acid sequences and post-translational modifications [PTMs], MALDI-MSI can also identify uncharacterized neuropeptides. In a recent investigation, researchers discovered that numerous neuropeptides underwent significant changes because of 6-OHDA (6-hydroxy dopamine) lesioning and L-DOPA therapy.[150] The neuropeptides known as CPu (caudate-putamen) are especially affected by 6-OHDA lesioning, whereas the neuropeptides known as GP (globus pallidus) are greatly affected by L-DOPA therapy. The MALDI-MSI technique clearly illustrated how these therapies affected the neuropeptides in specific brain regions.[150] Elevated levels of many neuropeptides generated by PENK (proenkephalin) were detected in the 6-OHDA-lesioned CPu, corroborating the findings of prior mRNA studies.[151,152] In a similar vein, animals given L-DOPA and saline showed greater amounts of several PENK-generated peptides in the GP in the injured compared to the undamaged half.[150] The researchers also found that the neuropeptide enkephalin's concentrations were altered by L-DOPA therapy. There were decreased concentrations of several peptides produced from PENK in the GP and LH of rats treated with L-DOPA, both in the lesioned and unlesioned halves.[150] After 6-OHDA lesioning, the distinct dorsal sub-region of the GP exhibited the highest increase in neurotensin concentrations.139[150] To sum up, the method shown here greatly raised the detection threshold and broadened the range of neuropeptides that could be analyzed using MALDI-MSI.[150]

L-3,4-dihydroxyphenylalanine, or L-DOPA, has been used to treat PD and remains the most effective medication for reducing symptoms.[153] The therapeutic properties of L-DOPA are due to the conversion of L-DOPA into dopamine [DA] following decarboxylation by the aromatic L-amino acid decarboxylase enzyme. Although prolonged therapy is particularly beneficial in the early days of PD, it can lead to L-DOPA-induced dyskinesia (LID), which 10% of patients experience annually while on treatment.[153] The most serious motor adverse effect of DA substitution therapy is called LID, and it dramatically reduces the therapeutic benefit of administering L-DOPA. Dyskinesia appears to be specifically associated with the 5-hydroxytryptamine [5-HT] system. Research has demonstrated that when 5-HT neurons are exposed to L-DOPA, they can release DA as a fictitious neurotransmitter.[154-157] Not only can modification lead to LID, but it may also be involved in nonmotor disorders caused by L-DOPA.[158]

MALDI-MSI was used to map the spatial dispersion of L-DOPA in the brains of both dyskinetic and non-dyskinetic monkeys.[159] Extremely high L-DOPA levels in LID mice caused an increase in DA and its metabolites in extra-striatal areas. Furthermore, it was demonstrated that 3-OMD (3-methyl dopamine), the principal metabolite of L-DOPA, was substantially elevated in LID, indicating a disruption in the breakdown of L-DOPA in this condition.[159] Extra-striatal areas had higher amounts of DA due to heightened L-DOPA concentrations in LID; DA was primarily metabolized by COMT (catechol-O-methyl transferase).[159] The increased levels of dopamine in

extra-striatal regions may alter brain-wide signaling, which could impact biological processes and result in a range of adverse effects from L-DOPA treatment.[159]

The above-mentioned studies (Table 1) have contributed to our growing knowledge of molecular neuroanatomy and have assisted us in determining the molecular origins of some neurological conditions. Furthermore, the application of MSI to carry out a spatially oriented in situ examination of analytes (biochemicals) in tissue has immense potential for the study of neuropathology. The gold standard for identifying the nature and magnitude of the condition is frequently the examination of tissue specimens, even though new modalities and advanced imaging techniques are constantly being used to increase the effectiveness of image-guided therapy and treatment.[1] It has been widely documented that MSI in brain cancers and neurological illnesses can be extended to mouse models. These studies should be extended to human subjects.

Enhancing image resolution for localized cellular and sub-cellular features is currently a crucial aspect of MSI. In that sense, applying gold nanoparticles to MSI techniques is becoming more and more common.[160] Post-ionization isolation procedures need to be developed to resolve the issue of isomeric species clarification or isolating the poorly ionized species from MSI noise. It is highly desirable to develop distinctive and efficient sample preparation and ionization processes to capture an array of species in a single MSI scan. Research on the precise characterization and comprehensive assessment of metabolites from tissue specimens is necessary to expand the application of MSI.

Oncology

Cancer is among the most widespread causes of mortality and illness worldwide, claiming the lives of almost 10 million individuals annually. Cancer is still a challenging and lethal medical condition, in part due to its diverse nature, even with the ongoing research and development of new medications. For example, more customized treatment is required due to the significant intratumoral and inter-tumor heterogeneity of malignancies such as gliomas, lung cancer, and breast cancer. The intricacy of the pathogenesis and etiology of cancer has a significant impact on the disease's heterogeneity. Genetic mutations and epigenome alterations often accumulate and cause cancer.[161-163] The alteration of metabolic processes is one of the most obvious characteristics of tumor tissues. Poor treatment outcomes are often attributed to the metabolic variations among cancer and healthy cells within the TME.[164] Research on the many attributes of cancer tissues is crucial to comprehending the biology of cancer and creating effective treatments. Utilizing frozen section histology to determine the surgical margin of a tumor in a patient is a time-consuming, arduous, and usually arbitrary process. Thus, understanding the origins, characteristics, and susceptibilities of numerous cancers has been made possible by research on spatial metabolomics. Recent developments in MSI have made it possible to monitor ion images in tissues concurrently, which is significantly more effective than optical tissue image analysis, a technique commonly utilized in traditional histopathological evaluation. Table 2 lists significant empirical studies, cancer types, metabolites, metabolism pathways, and clinical importance.

Table 2. An overview of empirical studies on spatial metabolomics in cancer research.

Author	Diagnosis	Metabolites	Representative ions (m/z)	MP	CR	% Agt
Berman et al (2019)	Prostate cancer	fatty acids & phospholipids	LysoPE (16:0) (452.7), LysoPE (18:1) (478.2),PI (37:6) (867.5), PCh (O-40:2), PC (P-40:1) (826.7), FA22:4 (331.2)	Krebs cycle	Prostate cancer metabolism and surgical guidance	97.0
Tamura et al (2019)	Renal cell carcinoma	lipids and fatty acids	azelaic acid (187.1), [FA(16:1)] (253.2) (palmitoleic acid), [FA(18:2)] (279.2) (linoleic acid), [FA(18:1)] (281.2) (oleic acid)	Warburg effect	Therapeutic strategy for targeting cancer cell metabolism	NR
Santoro et al (2020)	Breast cancer	lipids	taurine (124.0), uric acid (167.0), glycerophospholipids (PE (P-16:0/22:6, 746.5, PS (38:3), m/z 812.5)	*De novo* lipogenesis	breast cancer pathogenesis	NR
Ghadi e al (2020)	esophageal adenocarcinoma	Glycerol phospholipids	PG 36:4 (769.5), PG 38:6 (793.5), PG 40:8 (817.5), PI 34:1 (835.5),	*De novo* lipogenesis	early diagnosis of cancer	NR
Benussan et al (2020)	adenocarcinoma (ADC) and squamous cell carcinoma (SCC)	Glycero phospholipids	FA (20:4) (303.2), PG (36:2) (773.5), PI (34:1) (835.5), PS (36:1) (885.5)	NR	classification of ADC and SCC subtypes	87.5
Zhang et al (2020)	Renal Oncocytoma vs renal cell carcinoma	free fatty acids (FFA) and monoradylglycerolipids (MG)	ascorbic acid (175.0), hexose (m/z 215.0), FA(18:1) (281.2), FA (20:4) (303.2), cardiolipin (CL) (723.4 & 737.4)	NR	discrimination of renal tumors	99.5
Vijaya lakshmi et al (2020)	Renal cell carcinoma	small metabolites, fatty acids and lipids	N-acetyl glutamate (187.0), 2-hydroxy butyrate, (103.0), creatinine (112.9)	metabolic alterations	surgical margin assessment	88.0
Song et al (2020)	Oral cancer	amino acids, carbohydrates, glycerolipids, glycerophospholipids, sphingolipids	putrescine (89.1), betaine (156.0), phosphocholine (259.9), linoleic acid (317.1), hypoxanthine (175.0)	arginine/ proline metabolism, histidine metabolism	satisfy the need for point-of-care testing	88.9
Fala et al (2021)	Murine lymphoma	metabolites	pyruvate and lactate	Pyruvate metabolism	investigate pyruvate delivery and lactate labeling	NR

Table 2. (continued)

Author	Diagnosis	Metabolites	Representative ions (m/z)	MP	CR	% Agt
Song et al (2022)	TNBC	metabolites	arginine (175.1), lysine (147.1), N, N-dimethyl arginine (203.1), N, N, N-trimethyl lysine (189.1)	NR	rapid diagnosis of TNBC	88.8
Strittmatter et al (2022)	Pancreatic cancer	Gemcitabine	Ceralasertib (451.3), 2',2'-Difluorodeoxycytidine (302.0),2',2'-Difluorodeoxyuridine (299.0)	Gemcitabine metabolism	visualizing drug metabolites	NR
Kauffmann et al (2022)	Colorectal cancer (CRC)	fatty acids	phosphatidylserines (810.5, 812.535, 766.536), phosphatidylethanolamines (PE) (726.5)	*De novo* lipogenesis	CRC diagnosis and prognosis	97.0
Vaysse et al (2022)	Oral cavity cancer	metabolites	ether-phosphatidylethanolamine PE(O-16:1/18:2) (698.5)	OSCC keratinization	in vivo tissue recognition	96.8
He et al (2022)	Thyroid tumor	amino acids,fatty acids, nucleotides, lipids	arachidonic acid (303.2), phosphatidylinositols (885.5), lysophospholipids (568.3)	pathogenesis mechanisms	improve diagnosis accuracy	93.0
Mondal et al (2023)	Breast cancer	lipids, fatty acids	phosphatidylcholine (PC), phosphatidylethanolamine (PE), ceramide (Cer), sphingomyelin (SM), diacylglycerol (DG)	*De novo* lipogenesis	therapeutic and diagnostic developments	100.0
Pan et al (2023)	Brain tumor	small metabolites	Glutamine, hexcer (d42:2)	endogenous metabolic pathways	tumor research	NR
Aramaki et al (2023)	Luminal breast cancer	lipids and fatty acids	phosphatidylcholine (PC), triglycerides (TG), phosphatidylethanolamine, sphingomyelin, and ceramide	cancer metabolism	describe heterogenity of cancer	NR

MP – metabolic pathway, CR – clinical relevance, % Agt – percent agreement, NR – not reported.

Renal carcinoma

Renal cell carcinoma, or RCC, was identified in almost 90% of renal cancer patients with recorded cases of malignancy.[165] Renal tubular epithelial cells in the proximal region give rise to RCC. In 2015, there were over 140,000 kidney cancer fatalities globally, and 430,000 new cases were anticipated to be identified with the disease.[166] Effective comprehensive therapies, such as tyrosine kinase antagonists and immune checkpoint inhibitors, have been demonstrated to significantly improve the prognosis of patients with metastatic RCC.[167-170] But there isn't enough data to support the decision of which treatments are best for particular patients. New biomarkers are therefore required for the early identification of RCC in patients. Furthermore, the search for

molecules that can predict the course or fate of a disease leads to the discovery of new biomarkers and improves therapeutic results. Metabolomics research indicates that survival and multiplication of cancer cells are influenced by the immune system, nutritional deficiency, and hypoxia.[171] Clear-cell RCC (ccRCC) is the most prevalent histological subgroup, accounting for around 70% of the various RCC types. High amounts of triacylglycerol and/or cholesterol ester have been found in the tumor tissue of ccRCC. *In vivo* proliferation of RCC cells is inhibited by phosphatidylethanolamine overexpression resulting from ethanolamine.[172-173]

DESI-MSI was employed by Vijayalakshmi et al. (2020) to identify and predict clear ccRCC at the molecular level.[174] 17 pairs of tumor and normal tissues were analyzed individually as a cohort.[174] The authors observed changes in the distribution and quantity of TCA cycle-related minor metabolites in the m/z 50–200 range, which is consistent with previously documented altered metabolism in ccRCC.[174] Compared to healthy tissue, ccRCC displayed decreased concentrations of fumarate, succinate, and creatinine and higher concentrations of lactate, glucose, glutamate, N-acetyl glutamate, and 2-hydroxybutyrate.[174] There were discernible differences in peak abundance within the 200–1,000 m/z range. In comparison to normal tissue, ccRCC tissue has higher amounts of PG (glycerophosphoglycerol), glycerophosphoinositol (PI), and glycerophosphoserine (PS). In ccRCC tissue, aminophospholipids such as glycerophosphoethanolamine (PE) are less common. Lower levels of PS and PE can affect lipid trafficking across membranes and membrane asymmetry, which in turn affects both processes involved in programmed cell death: phagocytosis and apoptosis.[173,175] The work shows how spatial metabolomics and DESI-MSI can be used to accurately distinguish between malignant and healthy tissues.[174]

Zhang et al. (2020) used DESI-MSI in a related study to differentiate renal oncocytoma [RO], renal cell carcinoma variations, and healthy kidney tissues.[176] Of all renal tumors, RO is a common benign kidney neoplasm that accounts for 5–9% of cases and is most commonly detected in males over 50.[177] Because RO is asymptomatic, the diagnosis is often made by accident during normal medical exams. Preoperative core needle biopsies of renal lesions are not particularly commonly employed because of the significant histologic and immunophenotypic overlap between malignant chRCC and RO, which makes it challenging to distinguish between the two using cytological and histological assessment. As a result, to make certain that patients' renal neoplasms are handled effectively, it is crucial to differentiate ROs from RCCs, particularly the more closely related types such as chromophobe RCCs (chRCCs).[176] The RO samples displayed greater abundances of m/z 737.4 but lower abundances of the molecules at PS (20:4_18:0), PI (34:1), and 36:1 as compared to healthier renal tissues (Figure 10). When comparing RO and healthy tissues, RCCs displayed reduced abundance for m/z (392.0, 864.0) but the same abundance for Cer(d40:1), m/z (810.5, 835.5).[176] 99.47% patient and pixel accuracy overall for the various tissue types. Overall, the study shows that metabolic data gathered in conjunction with statistical methods permits renal tumor distinction, which may be utilized in the healthcare system to improve renal tumor patients' care.[176]

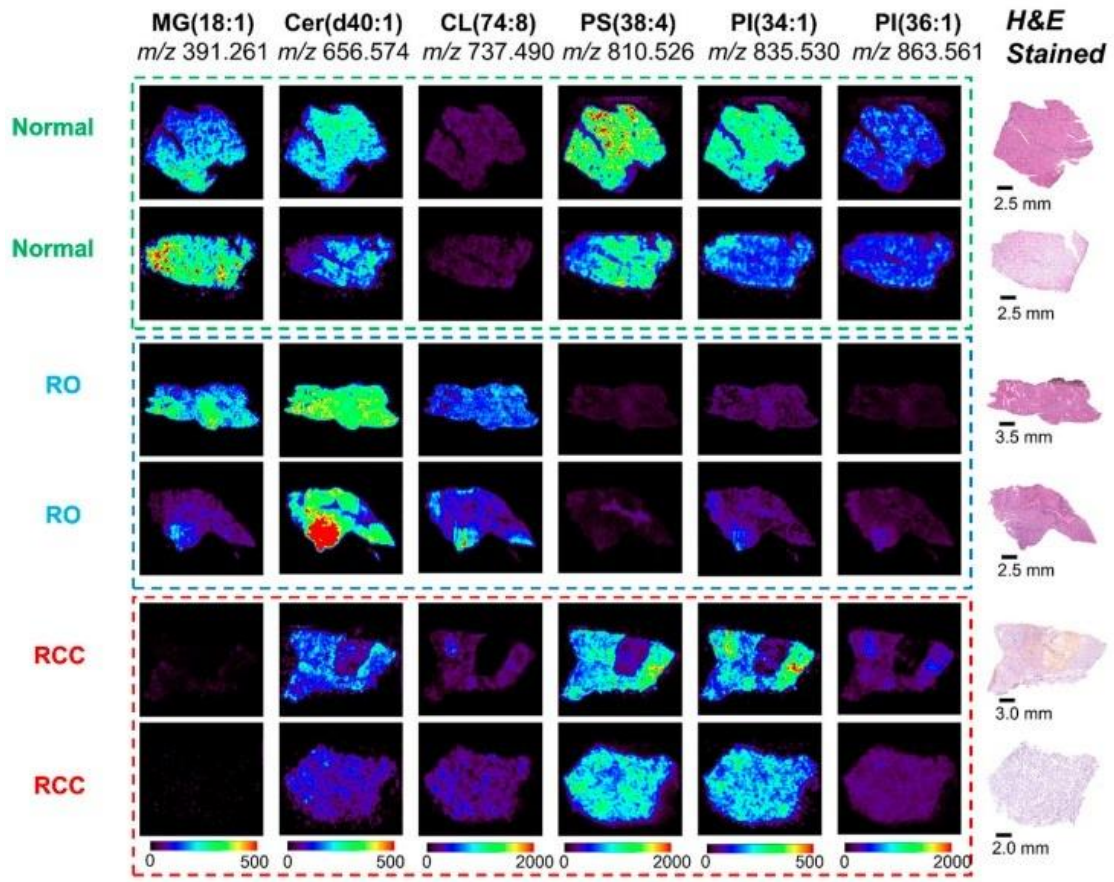

Figure 10. Representative DESI-MS ion images of normal kidney, RO, and RCC tissues. To better visualize the differences among the three tissue types for the six ions selected, the scale bars used are in unit of absolute intensity and were amplified by a factor of 4 (0–500 absolute intensity) for m/z 391.260, m/z 656.574 and m/z 835.530 of all the samples. [Reproduced with permission from Zhang et al (2020), Cancer Research PMC]

Oral cancer

Ocular squamous cell carcinoma, or OSCC, is by far the most fatal cancer of the oral cavity, with a mortality rate of over 50%. The early stage of OSCC is benign oral epithelial hyperplasia, which progresses to dysplasia and ultimately cancer. Even in individuals with OSCC who have had surgical resection, local recurrence is another risk that leads to treatment failure.[178] It can be challenging to monitor certain asymptomatic instances during or after surgery, even with relatively straightforward access to the oral cavity. Thus, there is a general desire to develop a practical tool for molecular identification in biological fluids. Although liquid,[179] gas,[180] and capillary electrophoresis-coupled mass spectrometry (MS)[181] technologies have been applied in the biomedical and clinical domains, they necessitate the time-consuming processing of complicated biological materials before analysis.

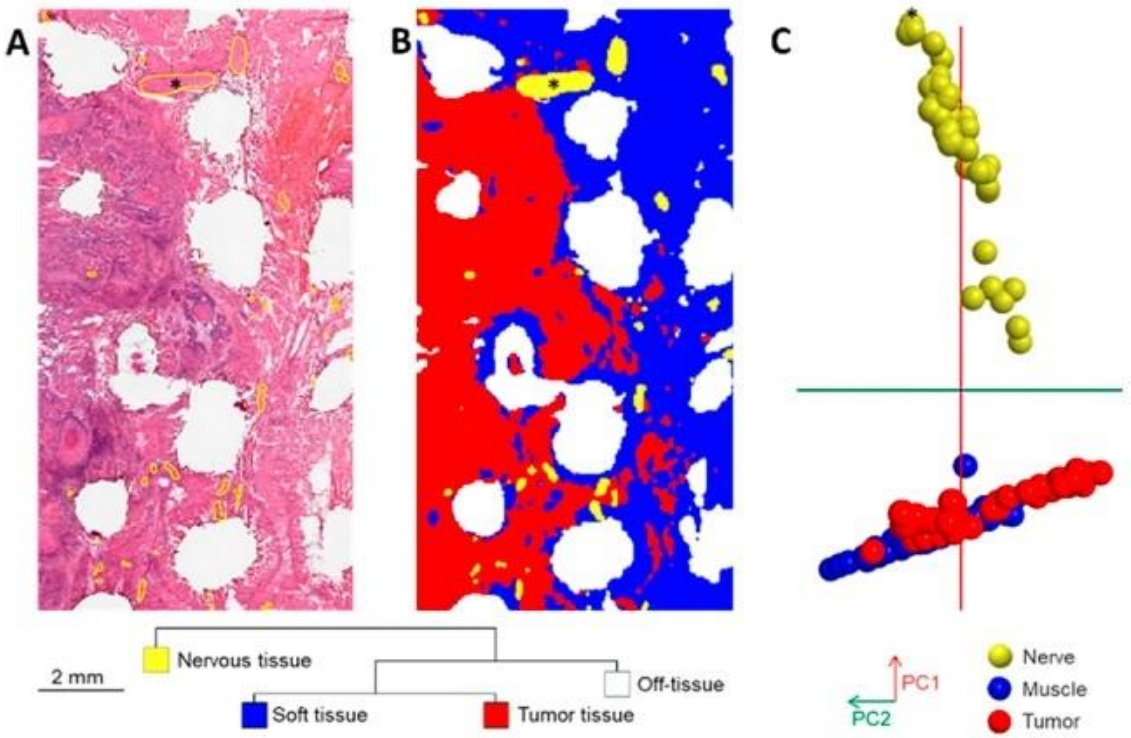

Figure 11. Distinct nerve metabolic profiles in oral cavity tissues by DESI-MSI. (A) Histology surrounding tissue defects of needle electrode-sampling for REIMS analysis surrounded by nerve features delineated in yellow on one resected specimen. (B) Segmentation analysis discriminating nervous tissue from the rest of the imaged areas based on DESI-MS profiles. (C) Principal component analysis score plot of DESI-MS profiles (55 nerve, 54 muscle, and 53 tumor) from tissue provided by six patients on the mass range m/z 600−1000 (PC1, which explains 80.3% of the variance of the data; PC2, 7.8%). [Reproduced with permission from Vaysse et al (2023), ACS]

Vaysse et al. (2022) applied rapid evaporative ionization mass spectrometry (REIMS) during oral cavity cancer surgery to identify cancer cells.[182] Electrocautery is frequently used as a surgical tool for resecting the oral cavity because of its hemostatic properties, which are required to cauterize the oral cavity's vascularized tissues. The process produces electrosurgical vapor as one of its byproducts. In this study, eleven individuals with OSCC have participated. By combining cross-validation and multivariate analytic techniques, the tissue was classified based on its metabolic characteristics and compared to histopathology in REIMS.[182] DESI-MSI was applied to six oral cavity sections to assess tissue heterogeneity, improving REIMS results. Using a unique cell-based experiment made up of several cell lines, the sensitivity of REIMS was assessed. REIMS detected cancer cells among 90% of myoblasts with a sensitivity and specificity of more than 80%.[182] In addition to the distinct metabolic characteristics of nerve properties, DESI-MSI highlighted the phosphatidylethanolamine PE (O-16:1/18:2) and cholesterol sulfate metabolic alterations ubiquitous to both mucosal development and OSCC variants (Figure 11). The evaluation of tissue heterogeneity with REIMS and DESI-MSI susceptibility with cell compositions highlighted sensitive metabolic properties during in vivo tissue characterization in oral cavity cancer procedures.[182]

Breast cancer

The most common type of cancer in women is breast cancer, an intricate group of diseases that differ greatly in their biologic aggressiveness and clinical presentations. Numerous clinical trials and advancements in genomic profiling have demonstrated the existence of therapeutically useful molecular subgroups.[183] Aggressive cancers are characterized by de novo lipogenesis, which is caused by genomic alterations that include the loss of chromosome 8p.[184-187] In healthcare facilities, histopathologic interpretation of H&E staining of tissue portions, specific immunohistochemistry (IHC) assays for ER and PR evaluation, and fluorescence in situ hybridization for HER2 gene amplification evaluation are commonly used in breast cancer evaluation and molecular subtyping. Even though H&E and IHC are very simple procedures, they require a lot of time and are subject to bias due to bias in information interpretation and reaction circumstances.

CPSI-MS, one of the notable ambient MS techniques, has been applied to evaluate biological fluids' metabolic properties.[188] Song et al. (2022) used machine learning and CPSI-MS to rapidly extract the metabolic signature from a ≤1μL liquid extraction of the TNBC tissue that had been biopsied.[189] The research utilized a four-phase methodology: 1) differentiation of metabolites in TNBC tissue; 2) TNBC-associated metabolite monitoring in serum and the development of metabolite-based machine learning models for fast serum monitoring and tissue identification, respectively; 3) pathway enrichment analysis to identify potential enzymes and carriers associated with the defective metabolites; and 4) expression verification of the enzymes or carriers responsible for the defective metabolites. DESI-MSI was used to confirm the targeted metabolites in tissues.[189] At the primary site of cancer, 76 distinct metabolite markers are recognized and are sufficiently trackable in serum. With rapid serum monitoring metabolites, CPSI-MS can identify tissue prognostic outcomes with 89% sensitivity and 90% specificity. In clinical settings, TNBC metabolism reprogramming can be promptly screened for, detected, and characterized because of the affordability of CPSI-MS technology.[189]

Aramaki et al. (2023) carried out cluster assessments of MSI data based on the characteristics of lipid molecules and the extent of their expression to investigate variance in luminal breast cancer biopsy specimens.[190] Phosphatidylethanolamine, sphingomyelin, phosphatidylcholine (PC), triglycerides (TG), and ceramide made up the clusters. It was determined that on HE pictures, the proportion of stroma and cancer was primarily linked with the concentration of TG and PC. The carbon makeup of this category of lipids varied from cluster to cluster as well.[190] This was consistent with the theory that cancer metabolism causes an increase in the overall number of enzymes that produce long-chain fatty acids. Increased carbon levels in PC aggregates could indicate serious cancer. These results may allow for the classification of cancers for whom genetic analysis on its own is inadequate by combining phenotypic heterogeneity with lipidomics.[190]

In a separate investigation, Mondal et al. (2023) used DESI-MSI to image fresh-frozen excision samples from 73 cancer patients who had lumpectomies. This included matched neighboring normal tissue and malignancy.[191] The findings show a significant metabolic increase of diacylglycerol, a lipid second carrier that stimulates the proliferation of cancer by activating protein kinase C (Figure 12). The investigation has found four distinct sn-1,2-diacylglycerols.[191]

When machine learning was applied to the whole dataset, diacylglycerols outperformed other lipid groups in the validation data set. This resulted in 100% reliability. Following the exclusion of diacylglycerol signals from the machine learning process, this accuracy significantly decreased. When lumpectomy cases have diacylglycerol, which may be an oncomarker, DESI-MSI should be employed in tandem with perioperative surgical pathology.[191]

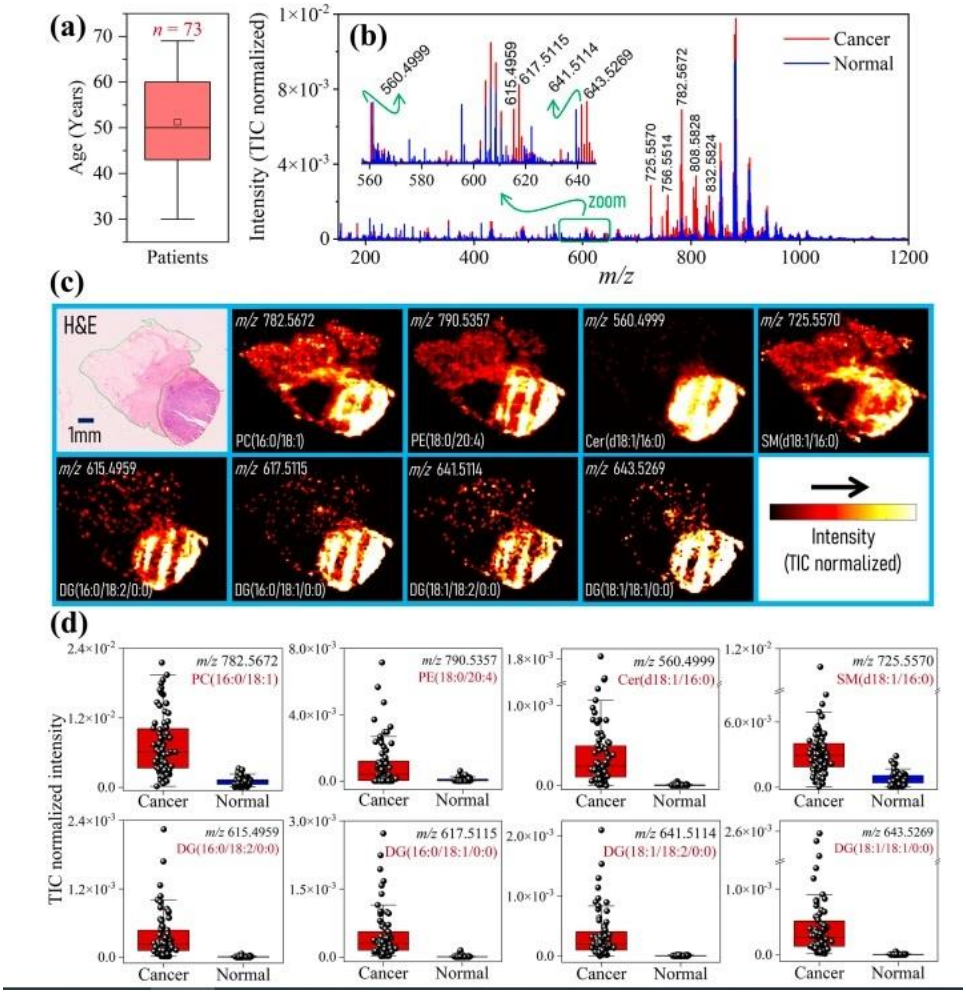

Figure 12. Positive ion mode DESI-MSI study with excision specimens obtained from lumpectomy of breast cancer patients. (a) Box−Whisker plot showing the age distribution of patients (n = 73) enrolled in this study. (b) Average mass spectral data collected from cancer (red spectrum) and adjacent normal (blue spectrum) specimens across all patients. Spectral averaging was performed using a total of 40 277 cancer pixels and 130 094 normal pixels across all MSI data of 73 patients. (c) Representative MSI showing spatial distributions of a phosphatidylcholine (PC), a phosphatidylethanolamine (PE), a ceramide (Cer), a sphingomyelin (SM), and four diacylglycerol (DG) molecules in a typical breast specimen that contains both cancer (red outline) and normal (green outline) areas as presented by the adjacent H&E-stained tissue (upper left). (d) Box− Whisker plots showing significant upregulation of those lipids in breast cancer compared to the adjacent normal tissue (p-values). [Reproduced with permission from Mondal et al (2023), ACS]

Esophageal cancer

Esophageal cancer (EA) is the eighth most frequent cancer globally, claiming the lives of almost 500,000 people annually.[192] EA is a type of cancer associated with acid reflux in the gastrointestinal tract that is most common in the West. Even with advancements in complete therapy, the 5-year survivability throughout all phases remains around 14%, and the 5-year fatality rate post-treatment with therapeutic objectives remains between 30 and 35%.[193] As a result, new instruments are needed to promote prompt diagnosis and effective care. While there has been a lot of research on the connection between metabolism and cancer, lipids, which make up about 70% of the human metabolome, have received little attention.[194-197] In bilayer membranes, many lipids are hidden away as GPLs (glycerophospholipids). Both their chemical and physical stability make them an ideal subject for biomarker studies. GPL diversity affects cellular signaling, membrane characteristics, and function. While phosphatidylinositols (PIs) promote phosphatidylinositol-3 kinase (PI3K) signaling, among the most disrupted pathways in EA, phosphatidylglycerols (PGs) have strong and opposing effects on the proliferation of squamous cells.[198,199] Finding the precise species composition is important, even though looking for GPLs could yield therapeutically useful diagnostic markers.

In their empirical study, Ghadi et al. (2020) compared the usual squamous and EA GPL features using DESI-MSI.[200] The investigators also investigated the following: In addition to serving as an extra validation cohort, the development of the EA GPL profile was examined between dysplastic, metaplastic, normal, inflammatory, and neoplastic cell types. These GPL markers were mechanistically based on the underlying genetics and associated fatty acid pool. It was determined that EA specimens had higher levels of polyunsaturated phosphatidylglycerols with longer acyl chains, along with various other abnormalities, with systematic enrichment in pre-malignant tissues. The characteristics of glycerophospholipid acyls and fatty acid acyls were similar, and there was a considerable increase in the expression of the genes encoding for the synthesis of both glycerophospholipids and fatty acids. By preventing the carbon exchange of ACLY in esophageal cancer cells, de novo lipogenesis is linked to the phospholipidome.[200]

Since the subject matter is still in its infancy, further research is required to determine the spatial information of the metabolites in different kinds of cancer. Such metabolite data may contribute to the creation of a thorough understanding of tumor biology in addition to the identification of novel biomarkers. Finding metabolic biological markers with spatially defined biochemical profiles linked to a range of disorders is essential to the successful application of this technology. The AMS technique is expected to have a significant positive effect since it can enhance the efficacy of cancer ablation or therapy, thereby facilitating the general acceptance of a therapy alternative that has a significantly lower risk of adverse effects. To enhance the diagnostic ability of AMS, new statistical methods must be created for quickly extracting comprehensive molecular data from ion images. Before AMS is introduced into standard pathology practice, it needs to be assessed on a large group of patients with varying kinds of cancers. Subsequent studies might evaluate more information and use innovative methods. For example, when additional spatial metabolomics information on different cancer specimens becomes available, it would be useful to associate metabolite localization between the stages of cancer. Through the comparison of the physiological and metabolic aspects of cancer growth, scientists can enhance their comprehension of the molecular pathways responsible for the advancement of tumors.

Finally, considering that multi-omics research is a highly pertinent domain of study, combining data from the omics domains (spatial metabolomics and proteomics) may possibly be an appealing move.

N-Glycosylation

Proteins undergo post-translational modifications called glycosylation, which is essential for biological activities such as modulatory mechanisms, morphological changes, and cell-cell interaction.[201] More precisely, the processes of secretion, molecular transport, and protein folding are influenced by glycoproteins.[202-204] Protein and lipid glycosylation is a necessary component of several innate and adaptive immune response regulation systems, including cell trafficking, cell proliferation and differentiation, T and B cell receptor activity, antigen distribution, and antibody functionality and clearance.[205-207] Membrane-bound glycoproteins serve as adhesive binding agents for both host-pathogen connections, which enable pathogens like viruses and bacteria to adhere to and enter mammalian cells, and host-host interactions, such as cell adhesion, receptor activation, and extracellular matrix chemicals.[208,209] Glycosylation is the process of covalently joining a sugar molecule (glycan) to the asparagine (N-linked) or serine/threonine (O-linked) domain of an amino acid. These sugars can form long, intricate chains or be linked as monomers. The specific sugar components that are used to make glycans are either synthesized by several metabolic processes or completely absorbed by the cell. These sugar components include, but are not limited to, glucose [Glu], mannose [Man], fucose [Fuc], N-acetylglucosamine [GlcNAc], and N-acetylgalactosamine [GalNAc].[210] These sugar chains combine to form the thick sugar architecture known as the glycocalyx, which is located on a cell's outermost layer.[211]

As a component of the secretory process, N-glycans are biosynthesized in the endoplasmic reticulum [ER] as a dolichol-linked sugar base, transferred to developing proteins during translation, and subsequently controlled by several enzymes in the ER and Golgi apparatus.[212] The results of this process are the three main N-glycan structural classes: complex, high mannose, and oligo- or hybrid. It has been found that N-glycosylation is significantly altered in cancer due to pathogenesis and its role as a direct regulator of cancer progression.[213] Many methods have been effectively developed to evaluate N-glycosylation.[214] Lectins are widely used in colorimetric, immunohistochemistry, and immunofluorescence techniques to detect N-glycans in tissues and molecules that are bonded to surfaces. These methods are effective, but they require lengthy sample processing steps that make it impossible to evaluate sizable batches of specimens in a reasonable amount of time for potential therapeutic or diagnostic applications. Extensive investigations into precise N-glycan structural relationships can be completed within timelines appropriate for high processing rates and therapeutic applications. Mass spectrometry imaging ["MSI"] adds to current techniques by capturing the spatial dimension of a glycan's distribution in situ, providing further insights into the composition and properties of biomolecules. An overview of the experimental studies, the type of ionization source and MS analyzer, the tumor type, sample type, related N-glycans found, and additional methodologies are shown in Table 3.

Table 3. Empirical studies on MSI in N-glycosylation research

Author	Tumor	Sample	Ionization	Analyzer	N-glycans associated(*)	ST
Vos et al (2022)	adenocarcinoma	endoscopic mucosal (FFPE)	MALDI-MSI	TOF/TOF	Hex6HexNAc5, Hex6HexNAc5NeuAc1, Hex7HexNAc6	H&E stain
Black et al (2022)	liver cirrhosis	Serum	MALDI-MSI	FT-ICR	Hex3dHex1HexNAc4+Na, Hex5dHex1HexNAc4+Na Hex4dHex1HexNAc4+Na	anitbody array
Ochoa-Rios et al (2023)	Cholangiocarcinoma (iCCA) & hepatocellular carcinoma (HCC)	Serum & iCCA/HCC tissue	MALDI-MSI	QTOF	single fucosylated N-glycan,double fucosylated N-glycan, double fucosylated with a galactose N-glycan,tetraantennary branched N-glycan,high mannose N-glycan	H&E stain
Jones et al (2022)	SARS-CoV-2	lung autopsy tissues	MALDI-MSI	QTOF	Hex2dHex1NAc2, Hex5dHex3NAc5,Hex8dHex2NAc7,Hex 6dHex3NAc6, Hex7dHex1HexNc6	IHC
Ščupáková et al (2021)	Breast cancer	cancerous tissue	MALDI-MSI	TOF & FTICR	high-mannose glycans, fucosylated and complex glycans.	IHC & GE
Rebelo et al (2021)	Neuroinflammation	brain tissue section	MALDI-MSI	QTOF	Sialylated, fucosylated N-glycans and oligomannose N-glycans	PET, IHC, UPLC, RT-qPCR
Drake et al (2019)	Clear-cell renal cell carcinoma (ccRCC)	ccRCC tissue	MALDI-MSI	FT-ICR	Hex7HexNAc6Fuc1, Hex5HexNAc5Fuc1-3, Hex6HexNAc6Fuc1-3	H&E stain
Blaschke et al (2021)	Prostate cancer	Urine and Prostatic Fluid	MALDI-MSI	QTOF	Hex5HexNAc4NeuAc1,Hex5HexNAc4Fuc1NeuAc1, Hex7HexNAc6Fuc2	HPLC, H&E stain
Boyaval et al (2022)	Colorectal cancer	Tissue sections	MALDI-MSI	TOF/TOF	H9N2,H8N2,H7N2,H6N2&H5N2	H&E stain, CE-ESI-MS/MS
McDowell et al (2021)	Pancreatic cancer	Pancreatic Cancer FFPE Tissues	MALDI-MSI	QTOF & FTICR	Hex6HexNAc5,Hex1HexNAc6,Hex9dHex1HexNAc8,Hex5dHex1HexNAc4,Hex7HexNAc6	IHC, IF
Ochoa-Rios et al (2022)	Nonalcoholic steatohepatitis	NAFLD/NASH tissue	MALDI-MSI	QTOF	fucosylated glycan	H&E stain
Conroy et al (2021)	Prostate cancer	Prostate Cancer FFPE Tissue	MALDI-MSI	TOF	high-mannose glycans,fucosylated, bisecting, and sialylated glycans	NA
Grzeski et al (2022)	Ovarian cancer	EOC FFPE tissue	MALDI-MSI	TOF	α2,6- and α2,3-sialylated N-glycans	H&E stain

Table 3. continued

Author	Tumor	Sample	Ionization	Analyzer	N-glycans associated(*)	ST
Briggs et al (2019)	Ovarian cancer	OC FFPE tissue	MALDI-MSI	TOF/TOF	(Hex)6 + (Man)3(GlcNAc)2,(Hex)2 (HexNAc)2 (Deoxyhexose)1 + (Man)3(GlcNAc)2	H&E stain, PGC-LC-ESI-MS/MS
Heijs et al (2020)	Neurological disorders	Cerebellum FFPE tissue	MALDI-2-MSI	timsTOF	[M − H]− N-glycans	H&E stain
Carter et al (2020)	Radiation-induced lung injury (RILI)	Lung tissue samples	MALDI-MSI	FT-ICR	Hex3HexNac5,Hex7HexNac2,Hex5HexNAc4,Hex5HexNAc4dHex1	H&E stain
Conroy et al (2020)	Prostate cancer	Prostate Cancer FFPE Tissue	MALDI-MSI	TOF	high mannose, tri- and tetra-antennary glycans	NA
Pace et al (2022)	Prostate cancer	Prostate Cancer FFPE Tissue	IR-MALDESI-MSI	Orbitrap	Sialylated N-glycans	NA
Lee et al (2022)	Osteoarthritis	osteochondral FFPE tissue	MALDI-MSI	TOF/TOF	(Hex)4(HexNAc)3, (Hex)4(HexNAc)4, and (Hex)5(HexNAc)4	H&E stain
Heijs et al (2020)	Myxoid liposarcoma (MLS)	FFPE MLS tissue	MALDI-MSI	TOF	Mannose N-glycans & tri- and tetra-antennary N-glycans	H&E stain
West et al (2020)	Prostate cancer	Prostate FFPE tissue	MALDI-MSI	FT-ICR	fucosylated N-glycans	SDS-PAGE
Boyaval et al (2021)	Colorectal cancer	FFPE fixed CRC tissue	MALDI-MSI	TOF/TOF	Hex7HexNAc2,Hex4dHex3HexNAc5,Hex5dHex1HexNAc4NeuAc	H&E stain
Delacourt et al (2021)	hepatocellular carcinoma	FFPE tumor tissue	MALDI-MSI	TOF & FTICR	Hex6dHex1HexNAc6,Hex7dHex2HexNAc6,Hex7dHex3HexNAc6,Hex6dHex2HexNAc5	H&E stain
Zhang et al (2022)	laryngeal tumor	FFPE human laryngeal cancer tissue	MALDI-MSI	TOF	Sialylated N-glycans	H&E stain
Angel et al (2021)	Aortic Valve Stenosis	FFPE tissue	MALDI-MSI	FT-ICR	sialic acid (N-acetylneuraminic acid) N-glycans w	Lectin stain
Lu et al (2023)	Prostate cancer	Tissues, cells & biofluids	MALDI-MSI	QTOF	alkyne-modified α2,3-linked sialic acid N-glycans.	H&E stain
Samal et al (2023)	Neuro disorder	FFPE mouse brain tissue	IR-MALDESI-MSI	Orbitrap	N-sialoglycans	NA

NA – not applicable; ST – supplementary techniques

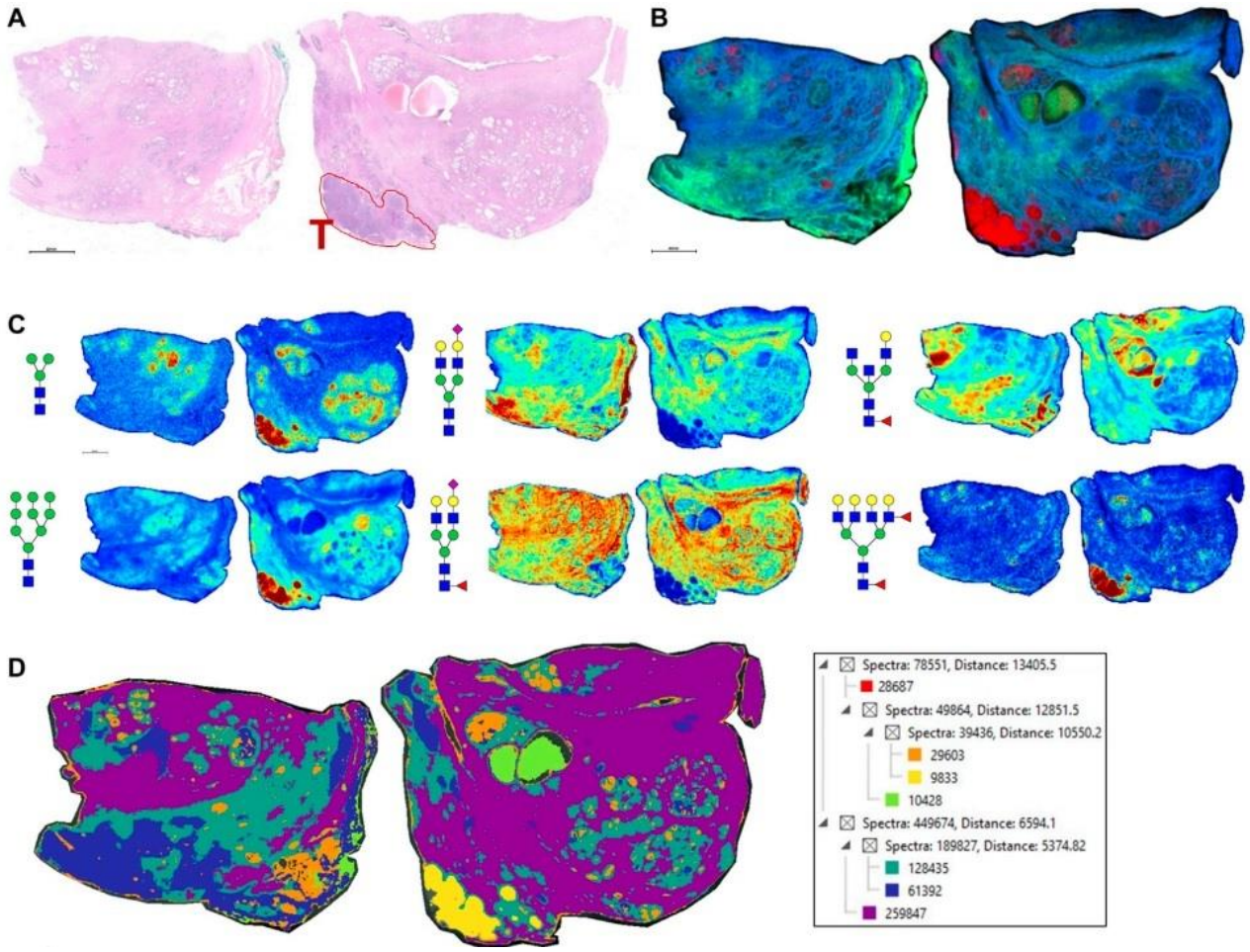

Figure 13. N-glycan imaging of FFPE prostate cancer and non-cancer tissues. (A) H&E stain of the two tissues from the same donor, non-cancer tissue on the left side and tumor on the right side. The tumor region, a Gleason grade 8/stage p3Tb, is highlighted with red outline and a red T. (B) An overlay MALDI image of three N-glycans, two stroma-associated ones, Hex5HexNAc4NeuAc1 in blue and Hex5HexNAc4Fuc1NeuAc1, and a tumor glycan Hex7HexNAc6Fuc2 (in red). (C) Six representative individual N-glycan images representative of different structural classes are shown, and glycan structure: a paucimannose (Hex3HecNAc2), high mannose (Hex5-Hex9HexNAc2), sialylated biantennary no fucose (Hex5HexNAc4NeuAc1), sialylated biantennary with fucose (Hex5HexNAc4Fuc1NeuAc1), bisecting GlcNAc biantennary (Hex4HexNAc4Fuc1) and branched fucosylated species (Hex7HexNAc6Fuc2). (D) Segmentation analysis, using Manhattan and k-bisecting classifications, was applied to the 73 N-glycans detected in the tissues. Spectra groupings are shown in the adjacent data tree. The N-glycan compositions are represented by blue squares for N-acetylglucosamine, green circles for mannose, yellow circles for galactose, purple diamonds for sialic acid, red triangles for fucose, and an "S" for sulfate. Reproduced with permission from Blaschke et al (2021), Frontiers in Chemistry.

Application of MSI in N-glycosylation research

Prostate cancer

The most common type of cancer diagnosed in men, prostate cancer also accounts for the second-highest number of cancer-related deaths in men worldwide.[215] A number of factors influence the start and progression of prostate cancer, including age, ancestry, ethnic origin, diet, and manner of life.[215] While there is a 99% five-year survival rate for patients with low-grade prostate tumors, the odds of survival are significantly reduced for those with higher-grade tumors and those who initially had distant metastases.[216] Because N-glycosylation plays a role in both metastasis and the epithelial-to-mesenchymal transition (EMT), establishing the N-glycosylation of prostate cancers may provide insight into the molecular mechanisms driving the growth of prostate cancer and may also be used to identify new markers or effective therapeutic interventions.[217]

"Expressed prostatic secretions in urine" (EPSu), proximal fluids from the prostate, are widely used in prostate cancer screening and prognostic studies.[218] These fluids contain a lot of extracellular vesicles (EVs) and glycoproteins (GP), which are secreted by the prostate gland. Because EVs and GPs can detect changes in their N-glycan composition as a sign of a problem, they may be new candidates for biomarkers.[218] Prostatic fluids, EPSu, and urine are rich sources of non-coding RNA and are used in several oligonucleotide-targeted diagnostic procedures for illnesses such as prostate cancer, in addition to being abundant in Evs.[219-221] Even though differences in the glycosylation of many other prostatic glycoproteins and prostate-specific antigen [PSA] are useful for diagnosis, the methods required to accurately determine N-glycans in urine specimens can be laborious and require several processing steps, which hinders their frequent clinical application.[222,223]

Blaschke et al. (2021) developed a technology for comprehensively analyzing the N-glycan elements of EPSu, prostatic fluids, and urine using MALDI-MSI.[218] Additionally, N-glycans in prostate cancer specimens have been discovered and histologically described, providing complementary findings (Figure 13). With urine, EPsu, prostatic fluids, and urine EPS-derived EVs, the approach is applicable and has been successful in identifying more than 100 N-glycan components.[218] To establish the heterogeneity in protein concentrations that might result in enhanced signal intensities and the determination of less abundant N-glycan species. N-glycan relative intensities were determined as the absolute intensity divided by the sum of the various absolute intensities of the N-glycans found in each sample being compared. The presence or absence of an N-glycan in every sample is discussed, and the amount of N-glycan in every individual sample is compared.[218] N-glycan structures were grouped into a class or classes based on theories about their structures. Through the addition of the relative intensities of the several N-glycans that comprise each class, the N-glycan classes were quantified. In N-glycan profiles, mannose, fucose, sialic acid, and sulfate were either present or absent, and each N-glycan was categorized into a group to contrast the classes' respective total relative intensities.

It is challenging to perform analytical studies to ascertain the biological significance of N-linked glycans due to their structural variability. Special challenges arise for N-linked glycans containing N-acetylneuraminic acid (sialic acid) due to the monosaccharide's lability and

ionization selectivity.[224] These limitations require novel analytic strategies that focus on these barriers to sufficiently investigate the biological relevance of N-linked glycans across various illnesses. Sialic acid contains a negative charge due to its carboxylic acid composition, which supports the negative ionization modality.[224] Since MALDI examinations have shown that negative mode investigations are less precise, glycan imaging has often employed a positive ionization technique.[225,226] Thus, an ionization approach like ESI could be appropriate for N-linked glycan imaging if further chemical derivatization processes are not used during sample preparation.

Pace et al. (2022) demonstrated the first in situ IR-MALDESI MSI assessment of N-linked glycans.[224] Following the enzymatic breakdown of N-linked glycans, negative ionization analysis was performed on FFPE human prostate tissue. 53 different N-linked glycans were successfully determined, dependent on prior identifications reported in the literature.[224] Sialic acid residues were found in over 60% of these identifications, indicating that IR-MALDESI can protect these susceptible molecules. GlycoHunter found a substantial number of doubly charged peaks in a single scan, indicating the presence of several chlorine-adducted molecules and potential sulfate and phosphate changes.[217] The work showed that chemical derivatization is not necessary for N-linked glycan imaging.[224]

When attached to asparagine sites on the glycoprotein framework, N-linked glycans can carry out a range of biological tasks because of their molecular diversity. Kuo et al. (2018) claim that the glycocalyx is a symbol of intrinsic cell wellbeing that is responsive to the temporal physiological state of the cell.[227] One characteristic that sets the glycocalyx apart is the presence of sialic acid [SA] carbohydrates on glycoproteins and glycosphingolipids, which are large glycoconjugate structures that are present on the extracellular matrix and the cell surface. SAs are known to be components of the well-known carbohydrate tumor antigens,[228] influenza virus binding receptors, and other transmissible illnesses. As components of glycoconjugates, they also participate in several biological processes.[229-230]

Azides and alkynes, two examples of bioorthogonal functional units, have been added to SAs together with extra sugar equivalents using a variety of metabolic, chemoenzymatic, or chemical tagging approaches.[231-233] Lu et al. (2023) manufactured bioorthogonal chemical labeling probes by substituting sialic acids linked at the α-2,3, and α-2,8 locations with alkyne or azide moieties.[234] The amidation reactions were further analyzed using pancreatic and prostrate FFPE specimens that had previously been characterized by N-glycan MSI.[235,236] The present procedures for amidation of bioorthogonal sugar azides and alkynes[237] and N-glycan MSI are streamlined by the study's application of the AAXL and AAN3 techniques, yielding novel techniques with unique features.[238,239] First off, amidation is not possible with α-2,6 sialic acids or other carboxylate-containing elements, but it is possible with α-2,3, and α-2,8 sialic acids in combination with proteins and lipids.[233] Second, without the aid of a living organism with an active metabolic process or of glycosyltransferases and substrates that are provided from outside, the AAXL and AAN3 reactions can bind an alkyne or azide to SAs. Third, the chemicals needed for the direct interactions between AAXL and AAN3 are readily available, reasonably priced, and covered by accepted practices for chemical labeling.[234] Merely four hours of sample preparation are needed for AAXL/AAN3, which can achieve conventional labeling efficiencies of 95% in clinical tissues and biofluids when added to a standard N-glycan IMS method.[234] All

things considered, the development of the bioorthogonal click chemistry components by AAXL and AAN3 makes it possible to conduct a number of cutting-edge studies focusing on glycoproteomic, labeling, identification, and illustration workflows for SA isomers.[234]

Liver cancer

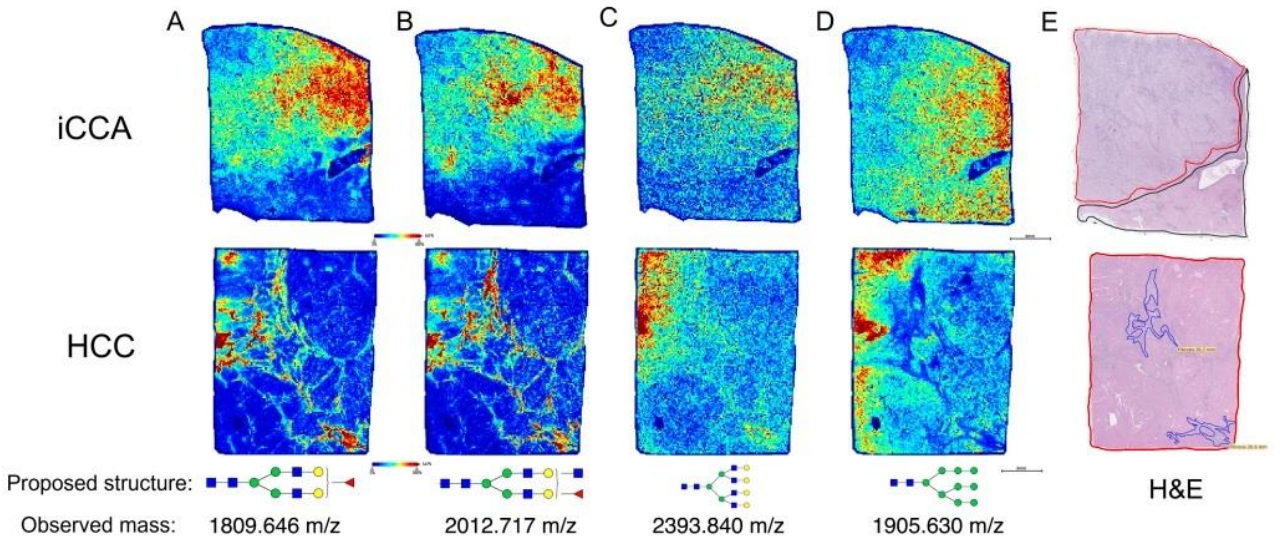

Figure 14. Bisected and biantennary fucosylated structures are highly expressed in iCCA tumor. Representative images of the relative intensity of biantennary fucosylated N-glycan (1809.646 m/z); (A) bisected fucosylated N-glycan (2012.717 m/z); (B) tetraantennary branched N-glycan (2393.840 m/z); (C) high mannose N-glycan (1905.630 m/z); (D) proposed N-glycan structures at the bottom correspond to the respective m/z value (observed mass). (E) H&E staining. Tumor regions are outlined in red, normal areas are outlined in black, and fibrotic regions are outlined in blue. Intrahepatic Cholangiocarcinoma (iCCA), and Hepatocellular Carcinoma (HCC). For N-glycans, red triangle, fucose; blue square, N-acetylglucosamine; green circles, mannose; yellow circles, galactose. Reproduced with permission from Ocha Rios (2022), AACR

Compared to other forms of cancer, hepatocellular carcinoma (HCC) was found to be more strongly associated with N-glycosylation changes.[240-242] HCC, the second most prevalent cancer in the world, is becoming more and more common in the US.

To determine the relationship between HCC-specific N-glycosylation modifications and genetic tumor characteristics, Delacourt et al. (2021) utilized MALDI-MSI to evaluate HCC tissue specimens while contrasting the spatial N-glycosylation to a commonly employed HCC molecular taxonomy.[243] Fucosylation in S2 tumors is particularly relevant since there is an apparent disparity in fucosylation trends between S1 and S2 cancers (Figure 16).[243] Comparing

S2 tumors to adjacent non-HCC liver tissue, fewer fucosylated components are present, in contrast to what can be detected in S1 tumors.[243] Fucosylated entities are expressed more in the nearby non-tumor liver tissue compared to an S2 tumor, but in S1 cancers, such structures have been observed to be strongly associated with tumors. Fucosylated structures, which are usually tumor-correlated in S1 cancers, are expressed at substantially higher concentrations in S1 tumors compared to S2 tumors, irrespective of the surrounding tissue.[243]

The epithelial cancer known as cholangiocarcinoma (CCA) arises in the lining of the biliary mucosa, which lines the ducts that transport bile from the liver to the small intestine.[244] CCA's classification as a distal CCA (dCCA), perihilar CCA (pCCA), or intrahepatic CCA [iCCA] subgroup depends on its anatomic position.[245] N-glycan MALDI-MSI was utilized by Ocha Rios et al. (2023) to identify the instantaneous modifications in tissue and blood samples from iCCA patients (Figure 14).[246] In order to acquire a better understanding of the histopathologic origin of the N-glycan components in the iCCA and HCC tissues, whole tissue examinations were carried out. In comparison to HCC and bile duct disorders such as primary sclerosing cholangitis, N-glycan changes were significantly more prevalent in iCCA tissue and serum samples.[246] The results of this study show that the biomarker approach improved the iCCA detection accuracy when compared to carbohydrate antigen, which is currently thought to be an adequate predictor of CCA. To identify serum biomarkers that can aid in the non-invasive detection of individual CCA, this study describes the N-glycan modifications that happen in iCCA tissue.[246]

Ovarian cancer

The most common cause of cancer-related mortality in women is ovarian cancer (OC), with gynecological cancers being the sixth most common cancer among women that results in death.[247] Due to ambiguous late-occurring symptoms as well as a lack of reliable early diagnostic signs, inadequate early diagnosis is the primary cause of a high mortality rate. Ninety percent of cases of ovarian cancer include the most common kind, called epithelial ovarian cancer, or "EOC." Genomic approaches can be used to differentiate EOC into two distinct groups. Group I is more likely to possess low-grade serous, endometrioid, mucinous, and clear cell carcinomas, while Group II is more likely to possess high-grade serous and endometrioid tumors.[248] By gathering spatial data, researchers can gain insight into tumor-specific N-glycan alterations in OC growth and progression, considering investigation into protein N-glycosylation has extensively revealed anomalies in the OC TME.[249]

Grzeski et al. (2022) utilized N-glycan MALDI imaging in association with chemical sialic acid derivatization to uncover tissue type-specific N-glycosylation in more unusual histotypes of EOC and non-malignant OC.[250] MALDI-MSI analysis revealed that EOC tissues are densely covered with sialylated glycan structures along with high-mannose N-glycans.[250] The distribution of in situ EOC tissue varies between 2,6- and 2,3-sialylated N-glycan structures, which emphasizes the significance of the sialic acid research unique to linkages. While further validation with a broader sample size is necessary, the data offer valuable insights into the molecular alterations occurring in EOC tissue.[250]

Colorectal cancer

Colon cancer (CRC) ranks as the fourth most prevalent type of cancer detected and the third lethal cancer overall, with both numbers continuously increasing over time.[251,252] In CRC, n-glycosylation undoubtedly has an oncological role. Utilizing CRC tissue homogenate, several CRC cell lines, and patient serum,[253] N-glycans have been investigated in studies employing MALDI-TOF MS.[254,255] These investigations discovered an array of N-glycan structural characteristics specific to CRC tumor tissue, including increased mannose levels, core fucosylation, sialylation, modified branching, and even sulfation.

Boyaval et al. (2022) employed MALDI-MSI to spatially identify the N-glycan species in a set of pT1 CRC tissues.[256] The structural features of the identified N-glycans were determined with CE-ESI-MS/MS. Using a range of 58 N-glycans, comparative intensities and glycosylation characteristics have been established.[256] Differential patterns were found between dysplastic, normal, and malignant sections. Increased cell proliferation is consistent with the presence of more high-mannose-type N-glycans in the dysplastic portion as compared to the cancer part.[256] Changes in the invasive front of the cancer were observed by the researchers, including increased expression of 2,3-linked sialic acids that correlated with the glycosylation pattern in the area. This study's capacity to discriminate between pre-tumors and malignant tumors may prove useful in the pathological characterization of cancer stages.[256]

Neuroscience

Seizures and dementia are examples of neuropathological symptoms associated with congenital glycosylation abnormalities.[257] Glycoprotein functions will be impacted by changes in N-glycosylation, which will ultimately cause disruptions to the cellular machinery.[257] Therefore, researching N-glycosylation changes in the context of neuroinflammation may open up new treatment options.[257] N-glycans are essential for myelinogenesis, synaptic expansion, and neuronal differentiation and progression, although little is known about their role in brain physiology.[258] A complete characterization of the brain's N-glycome is essential to understanding how glycosylation may be driving the etiology of neurological diseases, particularly in neurological conditions such as neuroinflammation.[257]

Samal et al. (2023) reported upon the application of IR-MALDESI-MSI for the detection of brain N-linked glycans.[259] An additional comparative analysis of the impact of tissue segment thickness on glycan imaging and characterization was offered by the study.[259] Because of IR-MALDESI's enhanced sensitivity for N-glycan identification, the study estimated that the mouse brain had 136 N-glycans.[259] Half of the N-glycans that were identified had residues of sialic acid, which is almost three times higher than the percentage observed in previous studies.[259] It has been established that sulfated N- and O-glycan epitopes are essential for several pathological effects and biological recognition mechanisms.[260-262] Additionally, the study published the initial glycan MSI analysis to record the N-sulfoglycans in the brain tissue analysis (Figure 15).[259] It has been determined that sulfated glycoproteins are species with multiple charges. It is important to note that the corpus callosum, which can be recognized by the presence of a myelinated nerve fiber cluster, has more of these sulfated N-glycans compared to any other location.[263] The role of sulfated N-glycans in the peripheral nervous system's myelination has

been demonstrated.[264] Irreversible neurological damage is promoted by demyelinated axons, causing axonal malfunction. Axonal activity tuning is dependent on myelination.[265,266] The brain's myelin-rich corpus callosum's spatial distribution of sulfated glycans emphasizes the significance of spatial glycan signals in the pathophysiology of several myelin-related disorders. Finally, while preserving sialoglycans without chemical derivatization, IR-MALDESI-MSI provides a very sensitive platform for glycan identification to discover disease- and/or tissue-specific glycosignature in the brain.[259]

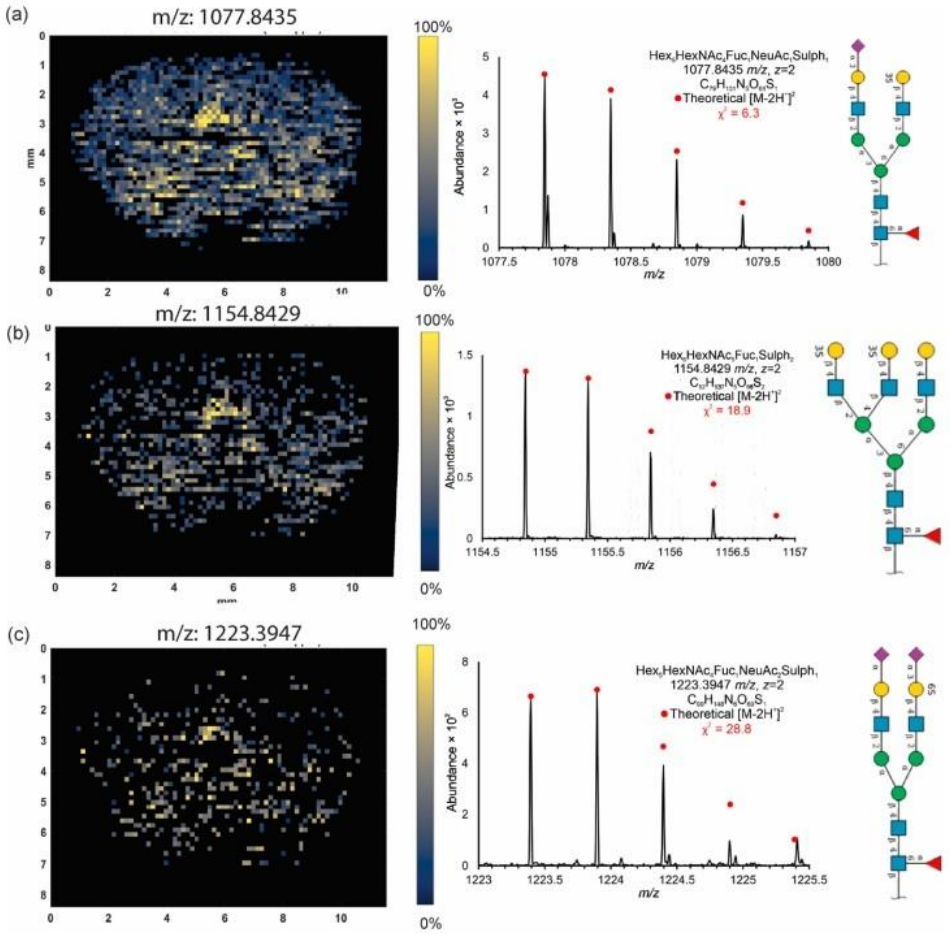

Figure 15. Detection of sulfated brain N-glycans. (a−c) Ion images of three representative sulfated N-glycans with a complete isotopic distribution for the respective charge-state (z = 2) and the glycan structure and composition. The sulfated glycans show higher concentration and enhanced detection in the myelin-enriched corpus callosum. Reproduced with permission Samal et al (2023), ACS

It has been demonstrated that N-glycan MSI methods are incredibly effective and helpful in providing information on N-glycan co-localization with tissue histopathology. N-glycan MSI's capacity to distinguish between isomers, new glycans, and complicated structures keeps expanding thanks to developments in equipment, data processing, and the integration of other methodologies. Because MSI research directly studies metabolic processes in tissue samples, it has helped to better understand the biological genesis and clinical features of various carcinomas. Regarding glycosylation, MSI's ongoing advancements and broader applications should provide additional insight into the molecular pathways behind various diseases and maladies. Clinical research laboratories are expected to integrate glycan-MSI systems for early disease detection and monitoring by identifying glycosyl molecular fingerprints in the following years.

Single cell analysis

Cells are the most basic structural and functional units of life, and as such, they are prone to a wide range of factors that can alter their metabolism, differentiation, and proliferation. As a result, even individual cells within the same organism exhibit a notable degree of variability.[267-270] Despite sharing the same genetic composition, homologous cells might differ in terms of their concentration and chemical composition.[271-273] Because population cell analysis yields only averaged data, information regarding cellular individuality is often unavailable.[273,274] Thus, accurate information on individual cells in each microenvironment can be obtained by comprehending cellular morphology and makeup at the single-cell level. In addition to being vital for studying cell signaling and the physiological pathologies of diseases, the contrasting information offered by numerous distinct cells is essential for explaining cell differences as well as assisting in the search for biomarkers that may help determine serious medical conditions early in life.[275-277] Nevertheless, because of the tiny sample volumes needed and the complexity of the chemicals found in these cellular environments, it can be exceedingly difficult to recognize and evaluate the chemical makeup and contents contained within individual cells.[278-281] Single-cell RNA sequencing has emerged as an increasingly significant technique for biological and medical research. Fluorescence microscopy and flow cytometry[282-285] are the two most widely used techniques for single-cell investigation.[286,287] It is difficult to accurately determine the components of cells because of the narrow linear range of the fluorescent signal, and spectral interference prevents the operation of several channels for the detection of different dyes at the same time. Furthermore, cellular reactions to competing species can differ based on the physiological state of the associated cells.[288] The dynamics of metabolite expression, which results in notable concentration changes throughout the growth of a culture or bloom, necessitate the use of rapid and high-throughput technologies.[289,290]

Due to additional advantages including minimal sample consumption, high throughput, and multiplexed detection, which allow for quantitative, qualitative, and spatially resolved cellular-level research, MS techniques are well suited for single-cell analysis.[291,292] The use of ambient mass spectrometry (AMS) in analytical science has grown to be beneficial. Its capacity to facilitate the quick analysis of a range of samples—typically in their natural condition or with little sample preparation—is what has led to its surge in popularity and visible applications. Relevant data from empirical investigations on single cell analysis using ambient mass spectrometry imaging is included in Table 4.

Table 4. Empirical studies on single cell analysis with AMSI

Author	Domain	Sample	Ionization	Analyzer	Metabolites	AT
Xi et al (2020)	Biological	HeLa cells	IR-MALDESI	Orbitrap-MS	Phospholipids	NA
Pareek et al (2020)	Biological	HeLa cells	GCIB-SIMS	TOF	Purinosome	NA
Taylor et al (2021)	Plant biology	*Allium cepa* and *Fittonia argyroneura* cells	LAESI	Obritrap-MS	Catechol, furoic acid, phthalide, lysine Glycineamideribonucleotide	NA
Stopka et al (2021)	Plant biology	Allium cepa cells	f-LAESI	QTOF	malate, disaccharides, glutamate, and citrate	NA
Meng et al (2021)	Drugs and nanomaterials	HeLa cells	LA	ICP-MSI	NA	Bright field mircoscopy
Tamura et al (2019)	Biomedical	ccRCC tissue sample	DESI	QTOF	azelaic acid, palmitoleic acid, linoleic acid, oleic acid	H&E stain
Vijayalakshmi et al (2020)	Biomedical		DESI	Orbitrap-MS	small metabolites, fatty acids and lipids	H&E stain
Benussan et al (2020)	Biomedical	ADC & SCC tissue sample	DESI	Orbitrap-MS	asglycerophosphoglycerols (PG), glycerophosphoinositols (PI), glycerophosphoserines (PS), glycerophosphoethanolamines (PE), and fatty acids (FA)	H&E stain
Tian et al (2022)	Biomedical	liver tissue samples	DESI	QTOF	fatty acids (FA), phosphatidylinositols (PIs), phosphatidylserines (PSs), lysophosphatidylserines (LPSs), phosphatidic acids (PAs), lysophosphatidic acids (LPAs)	H&E stain, AP-MALDI, Immunostain
Li et al (2021)	Drug distribution	HeLa cells cultivated with proflavine & methylthioninium chloride	MLF-LDPI	TOF	NA	NA
Hieta et al (2021)	Plant biology	plant tissue samples	LAAPPI	micrOTOF	flavonol glycosides, fatty acids (FA), fatty acid esters, galactolipids, and glycosphingolipids,	NA

AT – alternate techniques; TOF – time of flight; QTOF – quadrupole time of flight

AMS and single-cell analysis

The heterogeneity of lipids and the limited sample sizes collected from a single cell make it difficult to classify the lipidome in detail for individual cells. The Patern-Büchi (PB) reaction in conjunction with MS is one of the best techniques for the comprehensive detection and comparative quantification of lipids at the carbon-carbon double bond "C=C" location and sn-position levels. 145-148[293-296] The MS approach has been found to be able to determine the C-C locations of lipids in a single cell when used in conjunction with the PB reaction. However, there has never been a comparative quantification of isoforms, and their precise biological significance has not been established. 149[297]

To assess the lipidomic profile of individual cells, Li et al. (2021) created a general technique that allows for high structural selectivity. Before single-cell evaluation, lipids are retained inside

the cell during batch treatments using a technique called cell fixation.[298] Lipids' fatty acyl chains are verified by tandem MS, while their C=C and sn-locations are ascertained by batch photochemical functionalization and individual-cell droplet treatment, respectively. Single-cell MS analysis is made possible by the combination of electro-migration and droplet-assisted electrospray ionization, or "DAESI," which is simple to use yet maximizes sample consumption. Utilizing lipid C=C or sn-location isomer quantitation on 160 cells, four distinct types of breast cancer cells were successfully identified.[298]

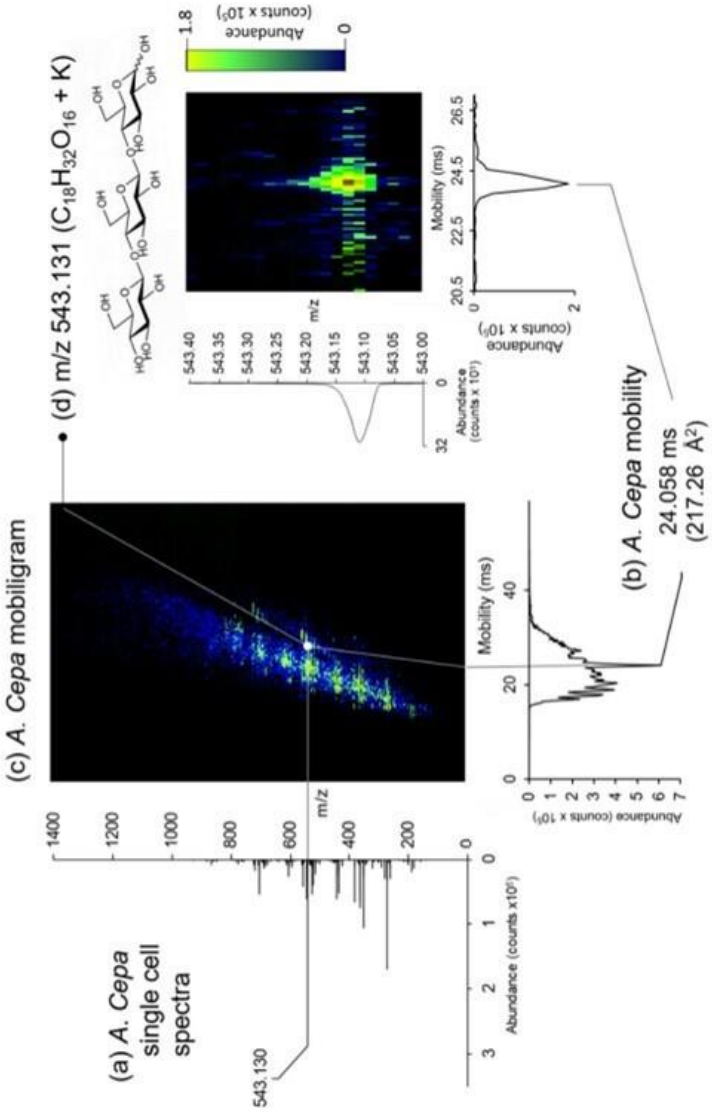

Figure 16. Example LAESI-DTIMS analysis of a single A. Cepa cell. (a) Spectrum with the saccharide peak labeled, (b) the corresponding mobility graph, and the (c) mobiligram showing detected species (green/yellow). (d) Spectrum and mobility graph of m/z 543.131 (C18H32O16 + K, Trisaccharide) with corresponding mobiligram. Reproduced with permission from Taylor et al.[153]

Taylor et al. (2021) paired a drift-tube ion mobility mass spectrometer, or "DTIMS," with a LAESI microscope. This allowed for precise mass measurements as well as the separation of isobaric ions and the calculation of the cross sections of ion collisions.[299] After computing the mobiligram (Figure 16d), the authors were able to identify the trisaccharide.[299] It is highly probable that this value is cellotriose based on comparisons with DTCCS values found in a metabolite repository in a DTIMS system.[300] It is expected that cellotriose will be an essential component in A. cepa because cellulose is the major polysaccharide in onion skins and a necessary component of cell walls.[299] These findings highlight the importance of ion mobility in improving structural predictions.

In a recent study, Stopka et al. (2021) demonstrated a dual-mode imaging system that utilizes simultaneous brightfield and fluorescent imaging paired with f-LAESI-MS for enhanced single-cell analysis.[301] Through the use of an etched optical fiber to drive the laser to the analyte's surface, fiber-based LAESI-MS (f-LAESI-MS) has made the biggest strides in SC analysis. To demonstrate the selective targeting of a certain cell type, frozen root nodules from soybean plants infected with GFP-labeled rhizobia for 21 days were sectioned. By using fluorescence and brightfield pictures, one may differentiate between infected and uninfected cells based on the fluorescence, size, and lack of fluorescence, respectively. Many metabolites, such as malate, disaccharides, glutamate, and citrate, were found in each kind of cell because of comparing the mass spectra of the two cell types. The difference is especially noticeable in the lipid area, where membrane lipids are substantially more plentiful in infected cells.[301] However, enormous environmental noise and spectral sophistication may arise due to the lack of orthogonal separation in ambient analytic techniques such as LAESI-MS.[302]

Single-cell analysis has drawn more interest from researchers across a range of biological fields because of its effectiveness as a tool for understanding the mechanisms governing cellular and molecular patterns. The empirical studies presented in Table 3 demonstrate the value of the imaging and micro sampling methods for examining the components of cells at varying degrees of chemical reactivity and spatial resolution. The growing technological needs associated with the research of cellular environments and single cells further underscore the need for MS systems with better capabilities, particularly regarding detectability in addition to time and spatial resolution.

Pharmaceutical research

When developing new pharmaceutical compositions and medication substances, it is critical to be able to monitor the distribution and progression of the drugs in preclinical studies using more basic in vitro models or in vivo treatment studies.[303] All forms of imaging, including fluorescence microscopy, which uses luminous markers to provide potential drug selectivity, benefit greatly from the exceptional spatial clarity that microscopes provide.[303] But when selectivity is achieved through tagging, a number of issues arise. When a fluorophore is attached to a molecular structure, it changes the molecular structure's chemical and biological properties significantly. This can cause an organism to react differently than it would if the molecular structure weren't labeled. Furthermore, only a limited number of chemicals are observable at once.[303] Some of these issues are addressed, for example, while examining via autoradiography, where radioactive tags are used in place of fluorescent tags. Nevertheless, the manufacturing of

chemicals and the handling of radiolabeled molecules are quite expensive and resource-intensive processes. [303] Moreover, the radioactive label is what is seen in autoradiography rather than the designated molecule because many drugs undergo final transformations in the body before being eliminated.

The domains of basic research on drug delivery and various stages of the drug discovery and development process have witnessed an increase in the use of AMSI. The capacity of AMSI to ascertain the concentrations of the initial drug and its metabolites throughout dosed samples without losing spatial data facilitates precise monitoring of a drug's pharmacological processes, including intake, distribution, metabolism, and discharge. A few of the numerous phenotypes that AMSI may simultaneously analyze include lipids, glycans, and proteins. Every single one of these compounds has a specific biological function and distribution pattern throughout the body. The application of AMSI in pharmacy has progressed beyond conventional tissue analysis to the initial phases of drug discovery and development. This includes investigating the relationship between structure and function, utilizing high-throughput techniques for in vitro analysis, and conducting ex vivo studies on single cells or tumor spheroids. Furthermore, a vast array of endogenous compounds that could serve as tissue diagnostics can be examined concurrently, providing an extremely detailed assessment of the specimen. An overview of the MSI application's characteristics, drug type, specimen, ambient ionization method, MS analyzer, and additional analytical methodologies is provided in Table 5.

Application of AMSI in pharmaceutical research

DESI-MSI

One important advantage of MSI is its ability to evaluate drugs that are constrained in space and their derivatives at the same time.[304] It has been shown that such findings are particularly important for studies on drug toxicology because the drug and its metabolites can localize to different organs and have different toxicological effects.[305] LC-MS has been widely used to identify drug metabolic fingerprints in biofluids, such as plasma, urine, or whole tissue homogenates, in studies examining the chemical degradation of acetaminophen (APAP).[306,307] While such an investigation sheds some light on the prevalence of drugs and their derivatives, it does not address particular differences in drug metabolism between different tissues or the levels of localized drug-derived byproducts that may be hazardous for certain areas inside organs. Traditionally, radiolabels or antibodies have been used to identify the localization of medications.[308,309] That being said, these methods often overlook other metabolites that could build up in the tissue and cause detrimental effects.[310-313]

In the C57BL/6J mouse model, Akakpo et al. (2022) highlighted the spatial mapping of APAP breakdown inside the liver following APAP overload and showed alterations brought on by 4-methylpyrazole (4MP) treatment.[314]The distribution and propagation of oxidative and nonoxidative metabolites were assessed in mouse liver slices following varying doses of APAP.[314] The spatial distribution of signal intensity was significantly changed by 4MP therapy, and the changes were clearly correlated with the amount of metabolites in the tissues. With a 50-micron spatial resolution, the study provided a novel label- and matrix-free methodology with

exceptional sensitivity for assessing regional variations in APAP metabolite levels following 4MP therapy.[314]

Table 5. List of empirical studies reviewed on ambient MSI in pharmaceutical research.

Authors	Application	Drug	Sample	Q	Ionization	Analyzer	ST
Guo et al (2021)	Drug distribution	Fluoropezil (DC20)	Rat brain coronal tissue	yes	DESI-MSI	IMS	LC-ESI-MS
Danhorn et al (2022)	Drug distribution	Terfenadine, losartan, diphenhydramine and dextromethorphan	Rat kidney and liver tissues	yes	DESI-MSI	Q-Orbitrap	MALDI-MSI
Yamamoto et al (2021)	Drug distribution & spatial localization	Ciclesonide	Rat lung tissue	yes	DESI-MSI	TOF	LC-MS, H&E staining
Akakpo et al (2022)	Spatial localization, hepatotoxicity & drug distribution	4-methyl pyrazole aka (4MP, Fomepizole)	Mice liver tissue	yes	DESI-MSI	Q-TOF	LC-MS
Liu et al (2022)	pharmacometabolomics, drug metabolism & distribution	Olanzapine (OLZ)	Brain tissue	no	AFADESI-MSI	Q-Orbitrap	H&E staining
Jin et al (2023)	Drug targets for central nervous system	sedative-hypnotic drug candidate YZG-331	Rat sagittal brain tissue	yes	AFADESI-MSI	Q-Orbitrap	LC-MS, H&E staining, Nissl staining
Li et al (2023)	metabolism & hepatotoxicity	Amiodarone (AMI)	HepG2 spheroids	no	AFADESI-MSI	Q-Orbitrap	H&E staining & IHC
Luo et al (2019)	Spatial metabolomics	sedative-hypnotic drug candidates YZG-331 and YZG-330	rat whole body tissue sections	no	AFADESI-MSI	Q-Orbitrap	NA
Brown et al (2020)	drug metabolism	Diclofenac	Liver and kidney tissues	yes	nano-DESI-MSI	Q-Orbitrap	LC-MS
Matsumoto et al (2020)	Brain distributions	Geissoschizine methyl ether (GM)	brain sagittal tissue section	yes	DESI-MSI	FT-ICR & Q-TOF	MALDI-MSI, LC-MS
Quartier et al (2021)	drug distribution, drug penetration pathways	econazole nitrate (ECZ),D-α-tocopheryl succinate polyethylene glycol 1000 (TPGS)	Porcine skin section	no	DESI-MSI	TOF	NA
Vallianatou et al (2018)	drug interactivity	Propranolol, loperamide	mouse brain tissue	yes	DESI-MSI	Q-Orbitrap	MALDI, H&E staining
Colclough et al (2021)	blood brain barrier, metastatic brain disease	Osimertinib	rat brain tissue	yes	DESI-MSI	Q-Orbitrap	LC-MS,H&E staining
Zhang et al (2020)	Targeting efficiency	Paclitaxel derivatives	Xenografted tumor	yes	AFADESI-MSI	Q-Orbitrap	H&E staining

Table 5. (Continued)

Authors	Application	Drug	Sample	Q	Ionization	Analyzer	ST
Kokesch-Himmelreich et al (2022)	Targeting efficiency	Clofazimine, moxifloxacin, bedaquiline, pyrazinamide, rifampicin	Necrotic Granulomas	no	AP-MALDI	Q-Orbitrap	H&E staining
Morosi et al (2022)	Drug distribution	Pioglitazone	neoplastic and normal liver tissues	yes	AP-MALDI	Q-Orbitrap	HPLC-UV
Pang et al (2021)	metabolic network mapping	Scopolamine	rat brain tissue	no	AFADESI-MSI	Q-Orbitrap	H&E staining
Holm et al (2022)	drug metabolism	Cyclosporine	whole body mouse kidney and intestine	yes	DESI-MSI	Q-Orbitrap	MALDI-MSI
Gao et al (2022)	Drug distribution	Uncaria alkaloids	brain tissue	yes	DESI-MSI	Q-TOF	H&E staining
Lin et al (2020)	Disease biomarker	NA	lung tissue & luminal B breast tumor tissue		nano-DESI-MSI	TOF	MALDI-MSI & IHC
Islam et al (2022)	drug metabolism	imipramine, chloroquine	Sagittal sections of mice kidneys and brains	yes	AP-MALDI-MSI	Q-TOF, FT-ICR	DESI-MSI, MALDI-MSI, H&E staining, LC-MS
Tan et al (2023)	chemical composition	Radix Aconiti	R-TBC, H-TBC, and F-TBC	yes	DESI-MSI	Q-TOF	HPTLC

Q – quantification; NA – not applicable; ST- supplementary techniques; Q-TOF – quadrupole time of flight; FT-ICR – fourier transform ion cyclotron resonance; TOF – time of flight.

AFADESI-MSI

Liu et al. (2022) evaluated the effects of olanzapine (OLZ) on the brain tissue segments using a temporo-spatial pharmacometabolomic technique and AFADESI-MSI to gain a deeper understanding of the molecular processes that medications perform on the microregions of the central nervous system (CNS).[315] The AFADESI-MSI-based temporo-spatial pharmacometabolomic approach has the advantage of precisely measuring molecular phenomena both in situ and micro-regionally, as well as detecting changes in endogenous and exogenous chemical levels within different CNS microregions.[315] The results of this study clearly revealed the drug's pharmacokinetics and its byproduct, 2-hydroxymethyl OLZ, in many rat brain regions.[315]

Amiodarone [AMI], an antiarrhythmic drug that is commonly administered, has been connected to cirrhosis, steatohepatitis, and liver fibrosis.[316] Several investigations have connected drug-induced liver damage to AMI metabolism[317,318], but the precise biochemical mechanisms underlying this association are still unclear. In a recent work, Li et al. (2023) utilized AFADESI-

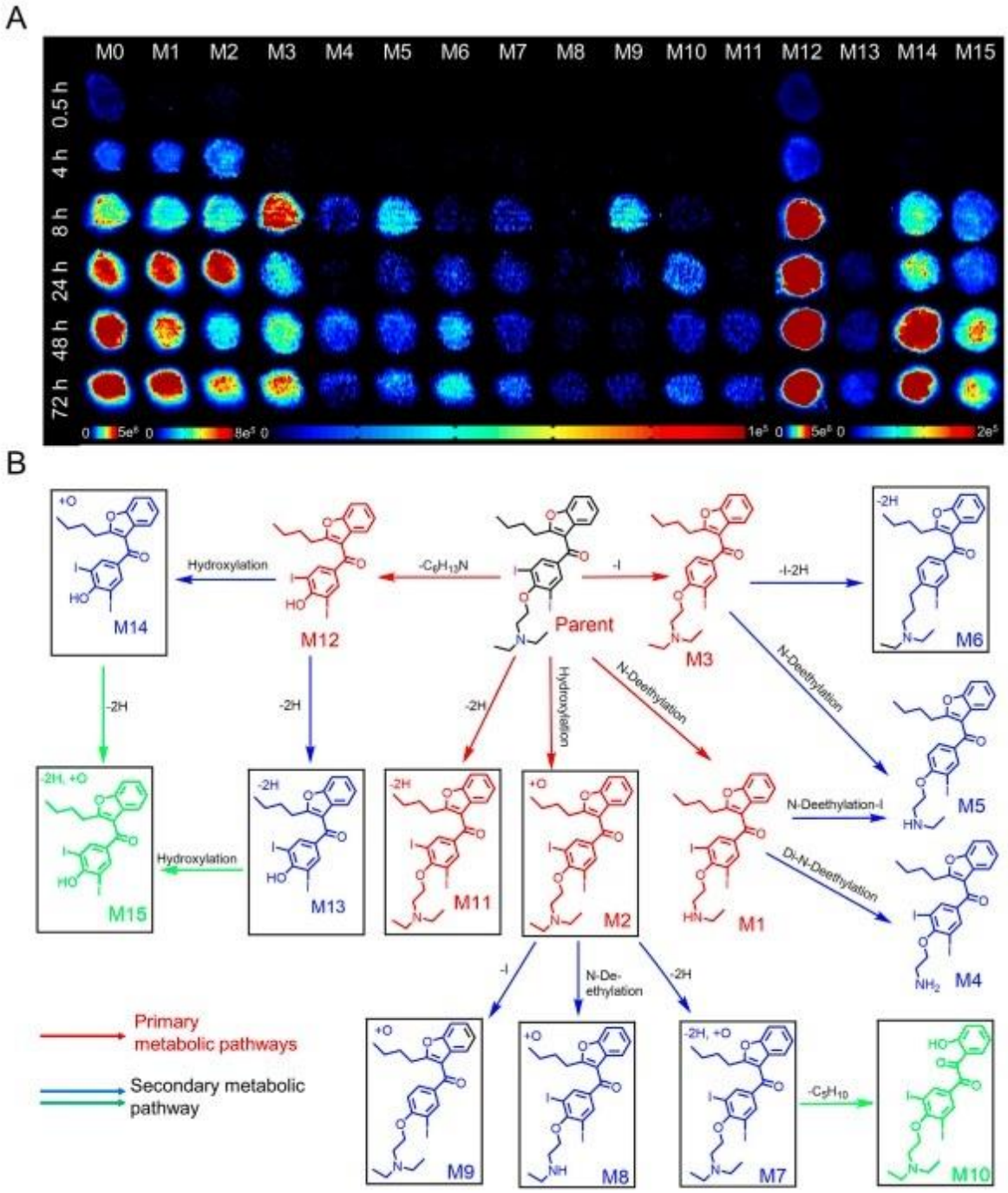

Figure 17. Time-dependent penetration and metabolism of amiodarone (AMI) in HepG2 spheroids analyzed using airflow-assisted desorption electrospray ionization-mass spectrometry imaging (AFADESI-MSI). (A) AFADESI-MS images of AMI and metabolite distribution at different treatment times. HepG2 spheroids were treated with 50 mM AMI for 0.5, 4, 8, 24, 48, and 72 h. (B) Postulated metabolic pathways of AMI in the HepG2 spheroids. Reproduced with permission Li et al (2023), ELSEVIER.

MSI with 3D HepG2 spheroids to evaluate the damage to the liver and metabolism of AMI.[319] Using AMI as a model drug, the spatial and temporal characteristics of extrinsic drug disintegration during AMI therapy were examined to determine potential drug metabolic pathways. Following AMI medication at different intervals, 15 metabolites of AMI involved in metabolic processes were identified, and AMI's metabolic routes have been suggested according to the spatiotemporal behavior features of these metabolites (Figure 17).[319] Then, it was feasible to identify the spatial and temporal variations in the metabolic alterations triggered by drug intake within spheroids using metabolomic evaluation.[319] The two primary metabolic pathways that were disrupted were arachidonic acid and glycerophospholipid metabolism, which were highly indicative of the underlying cause of AMI liver injury.[319]

nano DESI-MSI

Glutaronidation, a stage II metabolic pathway, is a common process that medications and xenobiotics go through to increase their solubility for excretion. To reduce swelling and discomfort, diclofenac, an anti-steroidal and non-inflammatory medication, is frequently used.[320-323] In humans, diclofenac glucuronide is mainly excreted from the body through the kidneys, whereas in lab animals, it is mainly removed through the bile.[324,325] Both in humans and animals, diclofenac acyl glucuronide [DCG] has been linked to intestinal damage and liver toxicity.[321-323,326,327] It has been proposed that adverse reactions and poor treatment responses are brought on by the derivatives of diclofenac's.

Sanchez et al. (2022) used nanoDESI-MSI.14 to examine the spatial distribution of diclofenac and its metabolites in mouse kidney and liver tissues. Signal measurements were at least one order of magnitude higher with selective ion monitoring ("SIM"), with mass-to-charge intervals localized on the low-abundance ions of interest.[328] Results demonstrate that DCG is confined to the inner medulla while hydroxy diclofenac is limited to the kidney cortex (Figure 23).[328] It appears that the toxic metabolite is exiting the tissue because DCG is present in the medulla. On the other hand, constant amounts of diclofenac, hydroxy diclofenac, and the DCG derivative were found in the liver tissue. Semiquantitative analysis verified that the metabolite-to-diclofenac concentrations found in nano-DESI and LC-MS investigations were consistent.[328]

AP-MALDI

The common transmissible illness that causes tuberculosis (TB) is Mycobacterium tuberculosis [Mtb]. People who have tuberculosis infections develop necrotic granulomas in the affected organ, which is typically the lungs.[329] The primary component of TB treatment is antibiotic-based regimens, which usually last for more than a year.[330] Long-term TB treatment regimens promote the development of therapy-resistant Mtb strains, which subsequently raises the demand for novel anti-TB medications and in vivo preclinical testing of potential new treatments.[331] Since mtb is still present in the caseum of necrotic granulomas, TB patients need to be treated with TB medications that can enter the granulomas' central core.

Himmelreich et al. (2022) developed an AP-MALDI-MSI procedure to investigate the absorption and uptake patterns of anti-TB drugs (clofazimine [CFZ], pyrazinamide [PZA], and rifampicin [RIF]) within mouse lung tissue.[332] An atypical animal model that closely paralleled the

pathophysiology of tuberculosis in humans was used in the study. Distinct concentrations of PZA and RIF have been observed within the tumors of Mtb-infected mice, providing further evidence to support the microhistological features of mouse tumors with a spatial accuracy of 30 microns.[332] The study validates the distribution properties of CFZ and PZA in TB patients' tumors, supporting the suitability of the animal model for the development of experimental anti-TB drugs.[332] The information indicates that CFZ can enter the granuloma and accumulate inside the macrophages' cellular components. The results acquired suggest that the imaging technique presented in the paper increases the predictive power of experimental animal research.[332]

Conclusion and perspectives

Pros and cons of the most common ionization sources

While several ionization sources were employed across the empirical studies surveyed, the most utilized were AFADESI, MALDI, and DESI. The following passages will present how the three ionization sources fair against each other. The advantages and shortcomings of the ionization techniques MALDI, DESI, and AFADESI are compared in Table 6.

Table 6. Ionization sources comparison

Technique	MALDI-MSI	DESI-MSI	AFADESI-MSI
Environment	Vacuum	Ambient	Ambient
Maximum spatial resolution	~1.4 micron	~50-200 micron	~100 micron
Sample type	Frozen or FFPE	Frozen or FFPE	Frozen or FFPE
Pros	Higher spatial resolution Ideal for small specimens Reliable results	High throughput Atmospheric conditions Minimal sample preparation Swift analysis	Atmospheric conditions Minimal sample preparation Varying field of coverage Better sensitivity and resolution over DESI-MSI
Cons	Tedious sample preparation process Non-ambient conditions	Low spatial resolution and sensitivity	Low reproducibility

FFPE – formalin-fixed, paraffin-embedded.

Despite determining the relative abundances of molecules, spatial metabolomics provides the opportunity to determine their localizations. This allows for a direct correlation between modifications in small molecules and anatomical features. As a result, it may result in the evolution of customized care, expedited diagnostic methods, and enhanced comprehension of complicated illnesses.[333] Because spatial metabolomics preserves the spatial information of metabolites, it demands several small molecules to be thoroughly analyzed concurrently. More molecules can be identified at once using MSI than with traditional staining methods because it constitutes a label-free, highly effective technology.[334]

MALDI is a widely utilized ionization technique associated with MSI because it offers a great balance between sensitivity, spatial resolution, and sample preparation.[334] In a recent investigation, 1.4 μm of spatial resolution was obtained using atmospheric pressure (AP)-MALDI.[335] However, to achieve a higher spatial resolution, the ion yield frequently drops as the laser's focusing region reduces in dimension.[334,336] Therefore, to conduct spatial metabolomics

studies, researchers need to keep figuring out how to strike a compromise between achieving sufficient signal intensities and improving spatial resolutions. Furthermore, some investigations have demonstrated that MALSI-MSI has trouble identifying compounds with low molecular weights. This is due to the matrix ions' chemical properties, which may conflict with metabolite representations and resemble several metabolite ions of lower weight.[337,338]

In contrast to MALDI, DESI doesn't warrant a matrix. Thus, it is not subject to the typically substantial risk of spatial allocation error resulting from sample displacement associated with the MALDI approach.[339,340] Because DESI requires little preparation, it also makes the specimens available for observation and other procedures during the analysis.[339] Furthermore, in comparison to MALDI-MSI (30–50 μm), DESI-MSI has a lower spatial resolution because of factors including the composition of the solvent, the size of the capillaries, and the gas flow rate.[341] Recent investigations have used nano-DESI-MSI to overcome these constraints and reach higher spatial resolutions (10 μm), highlighting future directions for DESI-MSI.[342,343]

In addition to reaping the advantages of DESI-MSI, AFADESI-MSI can achieve an extremely broad spectrum of the metabolites under investigation. It can identify thousands of compounds at once in untargeted research.[344] This technology can also be used to visualize whole-body sections.[345] This coverage substantially broadens the expected value of spatial metabolomics by enabling the simultaneous investigation and comparison of a variety of metabolites. In addition, by precisely adjusting the distance that exists between the ion transport tubing and the MSI inlet, AFADESI is able to attain picomolar sensitivity.[346]

The following classes illustrate how MSI, as a multimodal molecular visualization tool, might be enhanced.

Spatial resolution

This is yet another crucial MSI metric that helps assess the accuracy with which an ion image may be obtained to extract more complex spatial data. Because a smaller sample size typically translates into a relatively limited molecule concentration and the accompanying signal output provides a constant ionization efficiency, this is typically a paradoxical problem conjugating with the sensitivity.[347,348]

Sensitivity

To acquire chemical profiles, even from the sub-micron impact zone, without experiencing a significant reduction in sensitivity, a more sensitive in situ soft ionization technique must be further developed. The development of new sample-mounting nanomaterials, well-crafted secondary ionization, complex ion-focusing lens systems, less complex sample pre-processing, and chemical derivatization are areas that require ongoing effort.

Functional imaging

An MSI experiment's mass spectral profile is more than just a collection of isolated, insignificant peaks; there are biological relationships between these peaks. The drug-phenotype relationship

and the spatially defined molecular composition, environment, and biological function may be elucidated by these bio-informative relations. By evaluating and organizing the gathered large data, MSI can also be used as a functional imaging technique to view biological activities, including biomolecular function, enzyme catalysis, autophagy, ferroptosis, proliferation, and metastasis.[349]

Data acquisition

The most common method for collecting MSI data now is still the microprobe-based line-by-line scan mode, which might take hours or even a whole day to finish for bigger samples or when an ultrahigh-resolution image is needed. The MSI operating efficiency will undoubtedly increase with rapid microscopic snapshot-mode MSI data acquisition.[350]

Deep learning

To understand the chemical profile pattern and guide accurate spatial recognition, deep learning has already been developed.[351] More advanced data science approaches and computational tools, like spatial genomics and transcriptomics, are anticipated to make it easier to integrate spatial multi-omics data.

Open access to omics database

To facilitate unrestricted communication and investigation among MSI researchers, an open-access MSI information system ought to be advocated and facilitated.[352] An open-access spatial omics database with a molecular phenotypic atlas of important organs and cancer tissue is also anticipated. Of course, the entire MSI and spatial omics groups need to collaborate and work together on this. It is essential not just for the MSI community but also for the broader spatial omics community's multimodality imaging analysis across MS images, along with additional molecular imaging methods.

Although there is constant development of improved MSI technologies, the evolution of spatial metabolomics is hindered by issues with mass and spatial resolutions. Although the field is still underdeveloped, it holds enormous potential for improving diagnostic and therapeutic techniques as well as understanding drug metabolism.

References

1. Michno, W., Wehrli, P.M., Blennow, K., Zetterberg, H. and Hanrieder, J. Molecular imaging mass spectrometry for probing protein dynamics in neurodegenerative disease pathology. *Journal of neurochemistry*,2019,151,488.

2. Banerjee S. Empowering clinical diagnostics with mass spectrometry. ACS omega. 2020,5,2041.

3. Yan, Z., Cheng, C. and Liu, S.Applications of mass spectrometry in analyses of steroid hormones. In *LC-MS in Drug Bioanalysis*, Boston, MA: Springer US.2012, pp. 251-286.

4. Wu, C., Dill, A.L., Eberlin, L.S., Cooks, R.G. and Ifa, D.R. Mass spectrometry imaging under ambient conditions. *Mass spectrometry reviews*, 2013,*32*,218.

5. Chughtai, K. and Heeren, R.M.Mass spectrometric imaging for biomedical tissue analysis. *Chemical reviews*,2010,*110*,237.

6. McDonnell, L.A. and Heeren, R.M.Imaging mass spectrometry. *Mass spectrometry reviews*,2007,*26*, 606.

7. Pacholski, M.L. and Winograd, N.Imaging with mass spectrometry. *Chemical reviews*,1999,*99*, 2977.

8. Vickerman, J.C.Molecular imaging and depth profiling by mass spectrometry—SIMS, MALDI or DESI?. *Analyst*,2011,*136*,2199.

9. Vidova, V., Volný, M., Lemr, K. and Havlíček, V.Surface analysis by imaging mass spectrometry. *Collection of Czechoslovak Chemical Communications*,2009,*74*,1101.

10. Gao, L., Zhang, Z., Wu, W., Deng, Y., Zhi, H., Long, H., Lei, M., Hou, J., Wu, W. and Guo, D.A. Quantitative imaging of natural products in fine brain regions using desorption electrospray ionization mass spectrometry imaging (DESI-MSI): Uncaria alkaloids as a case study. *Analytical and Bioanalytical Chemistry*,2022,*414*,999.

11. Spengler, B., 2015. Mass spectrometry imaging of biomolecular information. *Analytical chemistry*,2015,*87*,64.

12. Ajith, A., Sthanikam, Y. and Banerjee, S.Chemical analysis of the human brain by imaging mass spectrometry. *Analyst*, 2021,*146*,5451.

13. Mattson, M.P. and Chan, S.L.Dysregulation of cellular calcium homeostasis in Alzheimer's disease: bad genes and bad habits. *Journal of Molecular Neuroscience*,2001,*17*,205.

14. Fujita, K.A., Ostaszewski, M., Matsuoka, Y., Ghosh, S., Glaab, E., Trefois, C., Crespo, I., Perumal, T.M., Jurkowski, W., Antony, P.M. and Diederich, N.Integrating pathways of Parkinson's disease in a molecular interaction map. *Molecular neurobiology*,2014,*49*,88.

15. Prickett, T.D. and Samuels, Y. Molecular pathways: dysregulated glutamatergic signaling pathways in cancer. *Clinical Cancer Research*,2012,*18*,4240.

16. Telias M. Molecular mechanisms of synaptic dysregulation in fragile X syndrome and autism spectrum disorders. *Frontiers in molecular neuroscience*,2019;12,51.

17. Shimma, S.Mass Spectrometry Imaging. *Mass Spectrometry*,2022,*11*,A0102.

18. Römpp, A. and Spengler, B.Mass spectrometry imaging with high resolution in mass and space. *Histochemistry and cell biology*,2013,*139*,759.

19. Spraggins, J.M., Djambazova, K.V., Rivera, E.S., Migas, L.G., Neumann, E.K., Fuetterer, A., Suetering, J., Goedecke, N., Ly, A., Van de Plas, R. and Caprioli, R.M.High-performance

molecular imaging with MALDI trapped ion-mobility time-of-flight (timsTOF) mass spectrometry. *Analytical chemistry*,2019,*91*,14552.

20. Schwartz, S.A., Reyzer, M.L. and Caprioli, R.M.Direct tissue analysis using matrix-assisted laser desorption/ionization mass spectrometry: practical aspects of sample preparation. *Journal of Mass Spectrometry*,2003,*38*,699.

21. Pietrowska, M., Gawin, M., Polańska, J. and Widłak, P.Tissue fixed with formalin and processed without paraffin embedding is suitable for imaging of both peptides and lipids by MALDI-IMS. *Proteomics*,2016,*16*,1670.

22. Buck, A., Ly, A., Balluff, B., Sun, N., Gorzolka, K., Feuchtinger, A., Janssen, K.P., Kuppen, P.J., van de Velde, C.J., Weirich, G. and Erlmeier, F.High-resolution MALDI-FT-ICR MS imaging for the analysis of metabolites from formalin-fixed, paraffin-embedded clinical tissue samples. *The Journal of pathology*,2015,*237*,123.

23. Urban, C., Buck, A., Siveke, J.T., Lordick, F., Luber, B., Walch, A. and Aichler, M., 2018. PAXgene fixation enables comprehensive metabolomic and proteomic analyses of tissue specimens by MALDI MSI. *Biochimica et Biophysica Acta (BBA)-General Subjects*,2018,*1862*,51.

24. Gorzolka, K. and Walch, A.MALDI mass spectrometry imaging of formalin-fixed paraffin-embedded tissues in clinical research, 2014.

25. Longuespée, R., Fléron, M., Pottier, C., Quesada-Calvo, F., Meuwis, M.A., Baiwir, D., Smargiasso, N., Mazzucchelli, G., De Pauw-Gillet, M.C., Delvenne, P. and De Pauw, E., 2014. Tissue proteomics for the next decade? Towards a molecular dimension in histology. *OMICS: A Journal of Integrative Biology*,2014,*18*,539.

26. Monroe, E.B., Jurchen, J.C., Koszczuk, B.A., Losh, J.L., Rubakhin, S.S. and Sweedler, J.V. Massively parallel sample preparation for the MALDI MS analyses of tissues. *Analytical chemistry*,2006,*78*,6826.

27. Zimmerman, T.A., Monroe, E.B. and Sweedler, J.V. Adapting the stretched sample method from tissue profiling to imaging. *Proteomics*,2008,*8*,3809.

28. Kaletaş, B.K., van der Wiel, I.M., Stauber, J., Dekker, L.J., Güzel, C., Kros, J.M., Luider, T.M. and Heeren, R.M.Sample preparation issues for tissue imaging by imaging MS. *Proteomics*,2009, *9*,2622.

29. Beavis, R.C., Chait, B.T. and Fales, H.M.Cinnamic acid derivatives as matrices for ultraviolet laser desorption mass spectrometry of proteins. *Rapid Communications in Mass Spectrometry*,1989,*3*,432.

30. Zavalin, A., Yang, J., Hayden, K., Vestal, M. and Caprioli, R.M.Tissue protein imaging at 1 μm laser spot diameter for high spatial resolution and high imaging speed using transmission geometry MALDI TOF MS. *Analytical and bioanalytical chemistry*,2015,*407*,2337.

31. Beavis, R.C., Chaudhary, T. and Chait, B.T. α-Cyano-4-hydroxycinnamic acid as a matrix for matrixassisted laser desorption mass spectromtry. *Organic mass spectrometry*,1992,*27*,156.

32. Hanrieder, J., Ekegren, T., Andersson, M. and Bergquist, J., 2013. MALDI imaging of post-mortem human spinal cord in amyotrophic lateral sclerosis. *Journal of neurochemistry*,2013,*124*,695.

33. Alexandrov, T.MALDI imaging mass spectrometry: statistical data analysis and current computational challenges. *BMC bioinformatics*,2012,*13*,S11.

34. Chambers, M.C., Maclean, B., Burke, R., Amodei, D., Ruderman, D.L., Neumann, S., Gatto, L., Fischer, B., Pratt, B., Egertson, J. and Hoff, K., 2012. A cross-platform toolkit for mass spectrometry and proteomics. *Nature biotechnology*,2012,*30*,918.

35. Bokhart, M.T., Nazari, M., Garrard, K.P. and Muddiman, D.C.MSiReader v1. 0: evolving open-source mass spectrometry imaging software for targeted and untargeted analyses. *Journal of The American Society for Mass Spectrometry2017*, *29*,8.

36. Bemis, K.D., Harry, A., Eberlin, L.S., Ferreira, C., van de Ven, S.M., Mallick, P., Stolowitz, M. and Vitek, O.Cardinal: an R package for statistical analysis of mass spectrometry-based imaging experiments. *Bioinformatics*,2015,*31*,2418.

37. Källback, P., Nilsson, A., Shariatgorji, M. and Andrén, P.E.msIQuant–quantitation software for mass spectrometry imaging enabling fast access, visualization, and analysis of large data sets. *Analytical chemistry*,2016,*88*,4346.

38. Römpp, A., Schramm, T., Hester, A., Klinkert, I., Both, J.P., Heeren, R.M., Stöckli, M. and Spengler, B., 2011. imzML: Imaging Mass Spectrometry Markup Language: A common data format for mass spectrometry imaging. *Data Mining in Proteomics: From Standards to Applications*,2011,205.

39. Deininger S.-O., Ebert M. P., Fuetterer A., Gerhard M. and Roecken C. MALDI imaging combined with hierarchical clustering as a new tool for the interpretation of complex human cancers. J. Proteome Res,2008, 7, 5230.

40. Henderson A., Fletcher J. S. and Vickerman J. C. comparison of PCA and MAF for ToF-SIMS image interpretation. Surf. Interface Anal,2009,41, 666.

41. Graham D. J. and Castner D. G. Multivariate analysis of ToF SIMS data from multicomponent systems: the why, when, and how. Biointerphases,2012, 7, 49.

42. Hanrieder J., Malmberg P., Lindberg O. R., Fletcher J. S. and Ewing A. G. Time-of-flight secondary ion mass spectrometry based molecular histology of human spinal cord tissue and motor neurons. Anal. Chem,2013a,85, 8741.

43. De Sio G., Smith A. J., Galli M., Garancini M., Chinello C., Bono F., Pagni F. and Magni F. A MALDI-mass spectrometry imaging method applicable to different formalin-fixed paraffin embedded human tissues. Mol. BioSyst,2015,11,1507.

44. Race A. M., Palmer A. D., Dexter A., Steven R. T., Styles I. B. and Bunch J. SpectralAnalysis: software for the masses. Anal. Chem,2016,88,9451.

45. Norris J. L., Cornett D. S., Mobley J. A., Andersson M., Seeley E. H., Chaurand P. and Caprioli R. M. Processing MALDI mass spectra to improve mass spectral direct tissue analysis. Int. J. Mass Spectrom,2007,260, 212.

46. Tarolli J. G., Jackson L. M. and Winograd N. Improving secondary ion mass spectrometry image quality with image fusion. J. Am. Soc. Mass Spectrom,2014,25, 2154.

47. Piqueras Solsona S., Maeder M., Tauler R. and de Juan A. (2017) A new matching image preprocessing for image data fusion. Chemometr. Intell. Lab. Syst,2017, 164,32.

48. Porta Siegel, T., Hamm, G., Bunch, J., Cappell, J., Fletcher, J.S. and Schwamborn, K.Mass spectrometry imaging and integration with other imaging modalities for greater molecular understanding of biological tissues. *Molecular imaging and biology*,2018,*20*,888.

49. Levenson, R.M., Borowsky, A.D. and Angelo, M. Immunohistochemistry and mass spectrometry for highly multiplexed cellular molecular imaging. *Laboratory Investigation*,2015,*95*,397.

50. Clift, C.L., Drake, R.R., Mehta, A. and Angel, P.M. Multiplexed imaging mass spectrometry of the extracellular matrix using serial enzyme digests from formalin-fixed paraffin-embedded tissue sections. *Analytical and bioanalytical chemistry*,2021,*413*,2709.

51. Angel, P.M., Baldwin, H.S., Sen, D.G., Su, Y.R., Mayer, J.E., Bichell, D. and Drake, R.R. Advances in MALDI imaging mass spectrometry of proteins in cardiac tissue, including the heart valve. *Biochimica et Biophysica Acta (BBA)-Proteins and Proteomics*,2017,*1865*,927.

52. Woodin, C.L., Maxon, M. and Desaire, H. Software for automated interpretation of mass spectrometry data from glycans and glycopeptides. *Analyst*,2013,*138*,2793.

53. Damerell, D., Ceroni, A., Maass, K., Ranzinger, R., Dell, A. and Haslam, S.M. Annotation of glycomics MS and MS/MS spectra using the GlycoWorkbench software tool. *Glycoinformatics*, 2015,3.

54. Cooper, C.A., Gasteiger, E. and Packer, N.H., 2001. GlycoMod–a software tool for determining glycosylation compositions from mass spectrometric data. *PROTEOMICS: International Edition*,2001,*1*, 340.

55. Alocci, D., Mariethoz, J., Gastaldello, A., Gasteiger, E., Karlsson, N.G., Kolarich, D., Packer, N.H. and Lisacek, F. GlyConnect: glycoproteomics goes visual, interactive, and analytical. *Journal of proteome research*,2018,*18*,664.

56. Tiemeyer, M., Aoki, K., Paulson, J., Cummings, R.D., York, W.S., Karlsson, N.G., Lisacek, F., Packer, N.H., Campbell, M.P., Aoki, N.P. and Fujita, A. GlyTouCan: an accessible glycan structure repository. *Glycobiology*,2017,*27*,915.

57. McDowell, C.T., Lu, X., Mehta, A.S., Angel, P.M. and Drake, R.R. Applications and continued evolution of glycan imaging mass spectrometry. *Mass Spectrometry Reviews*,2023,42,674.

58. Gustafsson, J.O., Oehler, M.K., Ruszkiewicz, A., McColl, S.R. and Hoffmann, P. MALDI imaging mass spectrometry (MALDI-IMS)—application of spatial proteomics for ovarian cancer classification and diagnosis. *International journal of molecular sciences*,2011,*12*,773.

59. Tuck, M., Grélard, F., Blanc, L. and Desbenoit, N. MALDI-MSI towards multimodal imaging: challenges and perspectives. *Frontiers in Chemistry*,2022,*10*,904688.

60. Norris, J.L. and Caprioli, R.M. Analysis of tissue specimens by matrix-assisted laser desorption/ionization imaging mass spectrometry in biological and clinical research. *Chemical reviews*,2013,*113*,2309.

61. Kaya, I., Sämfors, S., Levin, M., Borén, J. and Fletcher, J.S. Multimodal MALDI imaging mass spectrometry reveals spatially correlated lipid and protein changes in mouse heart with acute myocardial infarction. *Journal of the American Society for Mass Spectrometry*,2020,*31*,2133.

62. Neumann, E.K., Migas, L.G., Allen, J.L., Caprioli, R.M., Van de Plas, R. and Spraggins, J.M. Spatial metabolomics of the human kidney using MALDI trapped ion mobility imaging mass spectrometry. *Analytical Chemistry*,2020,*92*,13084.

63. Kompauer, M., Heiles, S. and Spengler, B. Atmospheric pressure MALDI mass spectrometry imaging of tissues and cells at 1.4-μm lateral resolution. *Nature methods*,2017,*14*,90.

64. Ščupáková, K., Balluff, B., Tressler, C., Adelaja, T., Heeren, R.M., Glunde, K. and Ertaylan, G. Cellular resolution in clinical MALDI mass spectrometry imaging: the latest advancements and current challenges. *Clinical Chemistry and Laboratory Medicine (CCLM)*,2020,*58*,914.

65. Soltwisch, J., Heijs, B., Koch, A., Vens-Cappell, S., Höhndorf, J. and Dreisewerd, K. MALDI-2 on a trapped ion mobility quadrupole time-of-flight instrument for rapid mass spectrometry imaging and ion mobility separation of complex lipid profiles. *Analytical Chemistry*,2020,*92*,8697.

66. De Hoffmann, E. and Stroobant, V., 2007. *Mass spectrometry: principles and applications*. John Wiley & Sons.

67. Oberacher, H. On the use of different mass spectrometric techniques for characterization of sequence variability in genomic DNA. *Analytical and bioanalytical chemistry*,2008,*391*,135.

68. Kaltashov, I.A., Zhang, M., Eyles, S.J. and Abzalimov, R.R. Investigation of structure, dynamics and function of metalloproteins with electrospray ionization mass spectrometry. *Analytical and bioanalytical chemistry*,2006,*386*,472.

69. Nielen, M.W. MALDI time-of-flight mass spectrometry of synthetic polymers. *Mass Spectrometry Reviews*,1999,*18*,309.

70. Fenn, J.B., Mann, M., Meng, C.K., Wong, S.F. and Whitehouse, C.M.Electrospray ionization for mass spectrometry of large biomolecules. *Science*,1989,*246*,64.

71. Hillenkamp, F., Karas, M., Beavis, R.C. and Chait, B.T. Matrix-assisted laser desorption/ionization mass spectrometry of biopolymers. *Analytical chemistry*,1991,*63*,1193A.

72. Cole, R.B. ed. Electrospray and MALDI mass spectrometry: fundamentals, instrumentation, practicalities, and biological applications, 2011.

73. Kuck, D. Reactive Intermediates. MS Investigations in Solution. Edited by Leonardo S. Santos,2010.

74. Alberici, R.M., Simas, R.C., Sanvido, G.B., Romão, W., Lalli, P.M., Benassi, M., Cunha, I.B. and Eberlin, M.N. Ambient mass spectrometry: bringing MS into the "real world". *Analytical and bioanalytical chemistry*,2010,*398*,265.

75. Weston, D.J. Ambient ionization mass spectrometry: current understanding of mechanistic theory; analytical performance and application areas. *Analyst*, 2010,*135*,661.

76. Wiseman, J.M., Ifa, D.R., Song, Q. and Cooks, R.G. Tissue imaging at atmospheric pressure using desorption electrospray ionization (DESI) mass spectrometry. *Angewandte Chemie International Edition*,2006,*45*,7188.

77. Santagata, S., Eberlin, L.S., Norton, I., Calligaris, D., Feldman, D.R., Ide, J.L., Liu, X., Wiley, J.S., Vestal, M.L., Ramkissoon, S.H. and Orringer, D.A. Intraoperative mass spectrometry mapping of an onco-metabolite to guide brain tumor surgery. *Proceedings of the National Academy of Sciences*,2014,*111*,11121.

78. Banerjee, S. and Mazumdar, S. Electrospray ionization mass spectrometry: a technique to access the information beyond the molecular weight of the analyte. *International journal of analytical chemistry*, *2012*.

79. Fenn, J.B., Mann, M., Meng, C.K., Wong, S.F. and Whitehouse, C.M. Electrospray ionization for mass spectrometry of large biomolecules. *Science*,1989,*246*,64.

80. Nguyen, S.N., Sontag, R.L., Carson, J.P., Corley, R.A., Ansong, C. and Laskin, J. Towards high-resolution tissue imaging using nanospray desorption electrospray ionization mass spectrometry coupled to shear force microscopy. *Journal of the American Society for Mass Spectrometry*,2017,*29*, 316.

81. Unsihuay, D., Qiu, J., Swaroop, S., Nagornov, K.O., Kozhinov, A.N., Tsybin, Y.O., Kuang, S. and Laskin, J. Imaging of triglycerides in tissues using nanospray desorption electrospray ionization (Nano-DESI) mass spectrometry. *International journal of mass spectrometry*,2020,*448*,116269.

82. Li, X., Hu, H., Yin, R., Li, Y., Sun, X., Dey, S.K. and Laskin, J. High-Throughput Nano-DESI Mass Spectrometry Imaging of Biological Tissues Using an Integrated Microfluidic Probe. *Analytical Chemistry*,2022,*94*,9690.

83. Lu, H., Zhang, H., Chingin, K., Xiong, J., Fang, X. and Chen, H. Ambient mass spectrometry for food science and industry. *TrAC Trends in Analytical Chemistry*,2018,*107*,99.

84. Chen, H., Wortmann, A., Zhang, W. and Zenobi, R. Rapid in vivo fingerprinting of nonvolatile compounds in breath by extractive electrospray ionization quadrupole time-of-flight mass spectrometry. *Angewandte Chemie*,2007,*119*,586.

85. Ding, J., Yang, S., Liang, D., Chen, H., Wu, Z., Zhang, L. and Ren, Y. Development of extractive electrospray ionization ion trap mass spectrometry for in vivo breath analysis. *Analyst*,2009,*134*,2040.

86. Gamez, G., Zhu, L., Disko, A., Chen, H., Azov, V., Chingin, K., Krämer, G. and Zenobi, R. Real-time, in vivo monitoring and pharmacokinetics of valproic acid via a novel biomarker in exhaled breath. *Chemical Communications*,2011,*47*,4884.

87. He, M.J., Pu, W., Wang, X., Zhang, W., Tang, D. and Dai, Y. Comparing DESI-MSI and MALDI-MSI mediated spatial metabolomics and their applications in cancer studies. *Frontiers in Oncology*,2022,*12*,891018.

88. Luo Z, HeJ, Chen Y, He J, Gong T, Tang F, et al. Air Flow-Assisted Ionization Imaging Mass Spectrometry Method for Easy Whole-Body Molecular Imaging Under Ambient Conditions. *Anal Chem*,2013, 85,2977.

89. 45. Sun C, Li T, Song X, Huang L, Zang Q, Xu J, et al. Spatially Resolved Metabolomics to Discover Tumor-Associated Metabolic Alterations. *Proc Natl Acad Sci U.S.A*,2019,116,52.

90. He J, Sun C, Li T, Luo Z, Huang L, Song X, et al. A Sensitive and Wide Coverage Ambient Mass Spectrometry Imaging Method for Functional Metabolites Based Molecular Histology. *Adv Sci*,2018,5,1800250

91. Tang F, Chen Y, He J-M, Luo Z-G, Abliz Z, Wang X-H. Design and Performance of Air Flow-Assisted Ionization Imaging Mass Spectrometry System. *Chin Chem Lett*,2014,25,687.

92. Nemes, P. and Vertes, A. Laser ablation electrospray ionization for atmospheric pressure, in vivo, and imaging mass spectrometry. *Analytical chemistry*,2007,*79*,8098.

93. Sampson, J.S., Hawkridge, A.M. and Muddiman, D.C., 2006. Generation and detection of multiply-charged peptides and proteins by matrix-assisted laser desorption electrospray ionization (MALDESI) Fourier transform ion cyclotron resonance mass spectrometry. *Journal of the American Society for Mass Spectrometry*,2006,*17*,1712.

94. Nemes, P., Woods, A.S. and Vertes, A. Simultaneous imaging of small metabolites and lipids in rat brain tissues at atmospheric pressure by laser ablation electrospray ionization mass spectrometry. *Analytical chemistry*,2010,*82*,982.

95. Hu, B., So, P.K., Chen, H. and Yao, Z.P. Electrospray ionization using wooden tips. *Analytical chemistry*,2011,*83*,8201.

96. Fincher, J.A., Korte, A.R., Reschke, B., Morris, N.J., Powell, M.J. and Vertes, A. Enhanced sensitivity and metabolite coverage with remote laser ablation electrospray ionization-mass spectrometry aided by coaxial plume and gas dynamics. *Analyst*,2017,*142*,157.

97. Compton, L.R., Reschke, B., Friend, J., Powell, M. and Vertes, A. Remote laser ablation electrospray ionization mass spectrometry for non-proximate analysis of biological tissues. *Rapid Communications in Mass Spectrometry*,2015,*29*,67.

98. Nazari, M. and Muddiman, D.C. Polarity switching mass spectrometry imaging of healthy and cancerous hen ovarian tissue sections by infrared matrix-assisted laser desorption electrospray ionization (IR-MALDESI). *Analyst*,2016,*141*,595.

99. Bokhart, M.T., Manni, J., Garrard, K.P., Ekelöf, M., Nazari, M. and Muddiman, D.C. IR-MALDESI mass spectrometry imaging at 50 micron spatial resolution. *Journal of the American Society for Mass Spectrometry*,2017,*28*,2099.

100. Ajith, A., Sthanikam, Y. and Banerjee, S. Chemical analysis of the human brain by imaging mass spectrometry. *Analyst*,2021,*146*,5451.

101. Taylor, J.P., Hardy, J. and Fischbeck, K.H. Toxic proteins in neurodegenerative disease. *science*,2002,*296*,1991.

102. Hanrieder, J., Phan, N.T., Kurczy, M.E. and Ewing, A.G., 2013. Imaging mass spectrometry in neuroscience. *ACS chemical neuroscience*,2013,*4*,666.

103. Michno, W., Wehrli, P.M., Blennow, K., Zetterberg, H. and Hanrieder, J., 2019. Molecular imaging mass spectrometry for probing protein dynamics in neurodegenerative disease pathology. *Journal of neurochemistry*,2019,*151*,488.

104. Evans, C.L., Potma, E.O., Puoris' haag, M., Côté, D., Lin, C.P. and Xie, X.S., 2005. Chemical imaging of tissue in vivo with video-rate coherent anti-Stokes Raman scattering microscopy. *Proceedings of the national academy of sciences*,2005,*102*,16807.

105. Schmid, T., Opilik, L., Blum, C. and Zenobi, R., 2013. Nanoscale chemical imaging using tip-enhanced Raman spectroscopy: a critical review. *Angewandte Chemie International Edition*,2013,*52*,5940.

106. Eberlin, L.S., Ferreira, C.R., Dill, A.L., Ifa, D.R. and Cooks, R.G. Desorption electrospray ionization mass spectrometry for lipid characterization and biological tissue imaging. *Biochimica et Biophysica Acta (BBA)-Molecular and Cell Biology of Lipids*,2011,*1811*,946.

107.Lacor, P.N., Buniel, M.C., Chang, L., Fernandez, S.J., Gong, Y., Viola, K.L., Lambert, M.P., Velasco, P.T., Bigio, E.H., Finch, C.E. and Krafft, G.A. Synaptic targeting by Alzheimer's-related amyloid β oligomers. *Journal of Neuroscience*,2004,*24*,10191.

108. Palop, J.J. and Mucke, L. Amyloid-β–induced neuronal dysfunction in Alzheimer's disease: from synapses toward neural networks. *Nature neuroscience*,2010,*13*,812.

109. Nasrabady, S.E., Rizvi, B., Goldman, J.E. and Brickman, A.M. White matter changes in Alzheimer's disease: a focus on myelin and oligodendrocytes. *Acta neuropathologica communications*,2018,*6*,1.

110. Bartzokis, G. Age-related myelin breakdown: a developmental model of cognitive decline and Alzheimer's disease. *Neurobiology of aging*,2004,*25*,5.

111. Collins-Praino, L.E., Francis, Y.I., Griffith, E.Y., Wiegman, A.F., Urbach, J., Lawton, A., Honig, L.S., Cortes, E., Vonsattel, J.P.G., Canoll, P.D. and Goldman, J.E. Soluble amyloid beta levels are elevated in the white matter of Alzheimer's patients, independent of cortical plaque severity. *Acta neuropathologica communications*,2014,*2*,1.

112. Di Paolo, G. and Kim, T.W. Linking lipids to Alzheimer's disease: cholesterol and beyond. *Nature Reviews Neuroscience*,2011,*12*,284.

113. Mitew, S., Kirkcaldie, M.T., Halliday, G.M., Shepherd, C.E., Vickers, J.C. and Dickson, T.C. Focal demyelination in Alzheimer's disease and transgenic mouse models. *Acta neuropathologica*,2010,*119*,567.

114. Palavicini, J.P., Wang, C., Chen, L., Hosang, K., Wang, J., Tomiyama, T., Mori, H. and Han, X., 2017. Oligomeric amyloid-beta induces MAPK-mediated activation of brain cytosolic and calcium-independent phospholipase A2 in a spatial-specific manner. *Acta neuropathologica communications*,2017,*5*,1.

115. Yang, D.S., Stavrides, P., Saito, M., Kumar, A., Rodriguez-Navarro, J.A., Pawlik, M., Huo, C., Walkley, S.U., Saito, M., Cuervo, A.M. and Nixon, R.A., 2014. Defective macroautophagic turnover of brain lipids in the TgCRND8 Alzheimer mouse model: prevention by correcting lysosomal proteolytic deficits. *Brain*,2014,*137*,3300.

116. Michno, W., Wehrli, P.M., Koutarapu, S., Marsching, C., Minta, K., Ge, J., Meyer, S.W., Zetterberg, H., Blennow, K., Henkel, C. and Oetjen, J. Structural amyloid plaque polymorphism is associated with distinct lipid accumulations revealed by trapped ion mobility mass spectrometry imaging. *Journal of Neurochemistry*,2022,*160*,482.

117. Špolcová, A., Mikulášková, B., Holubová, M., Nagelová, V., Pirnik, Z., Zemenová, J., Haluzík, M., Železná, B., Galas, M.C. and Maletínská, L. Anorexigenic lipopeptides ameliorate central insulin signaling and attenuate tau phosphorylation in hippocampi of mice with monosodium glutamate-induced obesity. *Journal of Alzheimer's Disease*,2015,*45*,823.

118. Wehrli, P.M., Ge, J., Michno, W., Koutarapu, S., Dreos, A., Jha, D., Zetterberg, H., Blennow, K. and Hanrieder, J. Correlative Chemical Imaging and Spatial Chemometrics Delineate Alzheimer Plaque Heterogeneity at High Spatial Resolution. *JACS Au*,2023,*3*,762.

119. Louis, D.N., Perry, A., Wesseling, P., Brat, D.J., Cree, I.A., Figarella-Branger, D., Hawkins, C., Ng, H.K., Pfister, S.M., Reifenberger, G. and Soffietti, R. The 2021 WHO classification of tumors of the central nervous system: a summary. *Neuro-oncology*,2021,*23*,1231.

120. Tiek, D.M., Khatib, S.A., Trepicchio, C.J., Heckler, M.M., Divekar, S.D., Sarkaria, J.N., Glasgow, E. and Riggins, R.B. Estrogen-related receptor β activation and isoform shifting by cdc2-like kinase inhibition restricts migration and intracranial tumor growth in glioblastoma. *The FASEB Journal*,2019,*33*,13476.

121. Verhaak, R.G., Hoadley, K.A., Purdom, E., Wang, V., Qi, Y., Wilkerson, M.D., Miller, C.R., Ding, L., Golub, T., Mesirov, J.P. and Alexe, G. Integrated genomic analysis identifies clinically relevant subtypes of glioblastoma characterized by abnormalities in PDGFRA, IDH1, EGFR, and NF1. *Cancer cell*,2010,*17*,98.

122. Neftel, C., Laffy, J., Filbin, M.G., Hara, T., Shore, M.E., Rahme, G.J., Richman, A.R., Silverbush, D., Shaw, M.L., Hebert, C.M. and Dewitt, J. An integrative model of cellular states, plasticity, and genetics for glioblastoma. *Cell*,2019,*178*,835.

123. Wang, Q., Hu, B., Hu, X., Kim, H., Squatrito, M., Scarpace, L., Decarvalho, A.C., Lyu, S., Li, P., Li, Y. and Barthel, F. Tumor evolution of glioma-intrinsic gene expression subtypes associates with immunological changes in the microenvironment. *Cancer cell*,2018,*33*,152.

124. Lim, M., Xia, Y., Bettegowda, C. and Weller, M. Current state of immunotherapy for glioblastoma. *Nature reviews Clinical oncology*,2018,*15*,422.

125. Gabrusiewicz, K., Rodriguez, B., Wei, J., Hashimoto, Y., Healy, L.M., Maiti, S.N., Thomas, G., Zhou, S., Wang, Q., Elakkad, A. and Liebelt, B.D. Glioblastoma-infiltrated innate immune cells resemble M0 macrophage phenotype. *JCI insight*,2016,*1*.

126. Gielen, P.R., Schulte, B.M., Kers-Rebel, E.D., Verrijp, K., Petersen-Baltussen, H.M., Ter Laan, M., Wesseling, P. and Adema, G.J. Increase in both CD14-positive and CD15-positive myeloid-derived suppressor cell subpopulations in the blood of patients with glioma but predominance of CD15-positive myeloid-derived suppressor cells in glioma tissue. *Journal of neuropathology & experimental neurology*,2015,*74*,390.

127. Mi, Y., Guo, N., Luan, J., Cheng, J., Hu, Z., Jiang, P., Jin, W. and Gao, X. The emerging role of myeloid-derived suppressor cells in the glioma immune suppressive microenvironment. *Frontiers in Immunology*,2020,*11*,737.

128. Platten, M., Nollen, E.A., Röhrig, U.F., Fallarino, F. and Opitz, C.A. Tryptophan metabolism as a common therapeutic target in cancer, neurodegeneration and beyond. *Nature reviews Drug discovery*,2019,*18*,379.

129. Gutiérrez-Vázquez, C. and Quintana, F.J. Regulation of the immune response by the aryl hydrocarbon receptor. *Immunity*,2018,*48*,19.

130. Opitz, C.A., Litzenburger, U.M., Sahm, F., Ott, M., Tritschler, I., Trump, S., Schumacher, T., Jestaedt, L., Schrenk, D., Weller, M. and Jugold, M. An endogenous tumour-promoting ligand of the human aryl hydrocarbon receptor. *Nature*,2011,*478*,197.

131. Panitz, V., Končarević, S., Sadik, A., Friedel, D., Bausbacher, T., Trump, S., Farztdinov, V., Schulz, S., Sievers, P., Schmidt, S. and Jürgenson, I. Tryptophan metabolism is inversely regulated in the tumor and blood of patients with glioblastoma. *Theranostics*,2021,*11*,9217.

132. Capper, D., Jones, D.T., Sill, M., Hovestadt, V., Schrimpf, D., Sturm, D., Koelsche, C., Sahm, F., Chavez, L., Reuss, D.E. and Kratz, A. DNA methylation-based classification of central nervous system tumours. *Nature*,2018,*555*,469.

133. Deighton, R.F., McGregor, R., Kemp, J., McCulloch, J. and Whittle, I.R. Glioma pathophysiology: insights emerging from proteomics. *Brain Pathology*,2010,*20*,691.

134. Dilillo, M., Ait-Belkacem, R., Esteve, C., Pellegrini, D., Nicolardi, S., Costa, M., Vannini, E., Graaf, E.D., Caleo, M. and McDonnell, L. Ultra-high mass resolution MALDI imaging mass spectrometry of proteins and metabolites in a mouse model of glioblastoma. *Scientific reports*,2017,*7*,603.

135. Kalinina, J., Peng, J., Ritchie, J.C. and Van Meir, E.G. Proteomics of gliomas: initial biomarker discovery and evolution of technology. *Neuro-oncology*,2011,*13*,926.

136. Djuric, U., Lam, K.B., Kao, J., Batruch, I., Jevtic, S., Papaioannou, M.D. and Diamandis, P. Defining protein pattern differences among molecular subtypes of diffuse gliomas using mass spectrometry*[S]. *Molecular & Cellular Proteomics*,2019,*18*,2029.

137. Yanovich-Arad, G., Ofek, P., Yeini, E., Mardamshina, M., Danilevsky, A., Shomron, N., Grossman, R., Satchi-Fainaro, R. and Geiger, T., 2021. Proteogenomics of glioblastoma associates molecular patterns with survival. *Cell reports*,2021,*34*.

138. Abuhusain, H.J., Matin, A., Qiao, Q., Shen, H., Kain, N., Day, B.W., Stringer, B.W., Daniels, B., Laaksonen, M.A., Teo, C. and McDonald, K.L. A metabolic shift favoring sphingosine 1-phosphate at the expense of ceramide controls glioblastoma angiogenesis. *Journal of Biological Chemistry*,2013,*288*,37355.

139. O'Neill, K.C., Liapis, E., Harris, B.T., Perlin, D.S. and Carter, C.L. Mass spectrometry imaging discriminates glioblastoma tumor cell subpopulations and different microvascular formations based on their lipid profiles. *Scientific Reports*,2022,*12*,17069.

140. Beghi, E., Giussani, G., Nichols, E., Abd-Allah, F., Abdela, J., Abdelalim, A., Abraha, H.N., Adib, M.G., Agrawal, S., Alahdab, F. and Awasthi, A., 2019. Global, regional, and national burden of epilepsy, 1990–2016: a systematic analysis for the Global Burden of Disease Study. *The Lancet Neurology*,2016,*18*,357.

141. Blümcke, I., Aronica, E., Miyata, H., Sarnat, H.B., Thom, M., Roessler, K., Rydenhag, B., Jehi, L., Krsek, P., Wiebe, S. and Spreafico, R. International recommendation for a

comprehensive neuropathologic workup of epilepsy surgery brain tissue: a consensus Task Force report from the ILAE Commission on Diagnostic Methods. *Epilepsia*,2016,*57*,348.

142. Stafstrom, C.E. and Carmant, L. Seizures and epilepsy: an overview for neuroscientists. *Cold Spring Harbor perspectives in medicine*,2015,*5*.

143. Amini, E., Rezaei, M., Mohamed Ibrahim, N., Golpich, M., Ghasemi, R., Mohamed, Z., Raymond, A.A., Dargahi, L. and Ahmadiani, A. A molecular approach to epilepsy management: from current therapeutic methods to preconditioning efforts. *Molecular neurobiology*,2015,*52*,492.

144. Banerjee, S. Ambient ionization mass spectrometry imaging for disease diagnosis: Excitements and challenges. *Journal of biosciences*,2018,*43*,731.

145. Ajith, A., Mondal, S., Chattopadhyay, S., Kumar, A., Sthanikam, Y., Chacko, A.G., Prabhu, K., Chacko, G., Vanjare, H.A., Rajesh, R.V. and Banerjee, S. Mass spectrometry imaging deciphers dysregulated lipid metabolism in the human hippocampus affected by temporal lobe epilepsy. *ACS chemical neuroscience*,2021,*12*,4187.

146. Jankovic, J. Parkinson's disease: clinical features and diagnosis. *Journal of neurology, neurosurgery & psychiatry*,2008,*79*,368.

147. Lang, A.E. and Lozano, A.M. Parkinson's disease. *New England Journal of Medicine*,1998,*339*,1130.

148. Marín, C., Bonastre, M., Mengod, G., Cortés, R. and Rodríguez-Oroz, M.C. From unilateral to bilateral parkinsonism: Effects of lateralization on dyskinesias and associated molecular mechanisms. *Neuropharmacology*,2015,*97*,365.

149. Sgroi, S., Capper-Loup, C., Paganetti, P. and Kaelin-Lang, A. Enkephalin and dynorphin neuropeptides are differently correlated with locomotor hypersensitivity and levodopa-induced dyskinesia in parkinsonian rats. *Experimental neurology*,2016,*280*,80.

150. Hulme, H., Fridjonsdottir, E., Gunnarsdottir, H., Vallianatou, T., Zhang, X., Wadensten, H., Shariatgorji, R., Nilsson, A., Bezard, E., Svenningsson, P. and Andrén, P.E. Simultaneous mass spectrometry imaging of multiple neuropeptides in the brain and alterations induced by experimental parkinsonism and L-DOPA therapy. *Neurobiology of Disease*,2020,*137*,104738.

151. Gerfen, C.R., McGinty, J.F. and Young, W.S. Dopamine differentially regulates dynorphin, substance P, and enkephalin expression in striatal neurons: in situ hybridization histochemical analysis. *Journal of Neuroscience*,1991,*11*,1016.

152. Capper-Loup, C. and Kaelin-Lang, A. Locomotor velocity and striatal adaptive gene expression changes of the direct and indirect pathways in parkinsonian rats. *Journal of Parkinson's disease*,2013,*3*,341.

153. Ahlskog, J.E. and Muenter, M.D. Frequency of levodopa-related dyskinesias and motor fluctuations as estimated from the cumulative literature. *Movement disorders: official journal of the Movement Disorder Society*,2001,*16*,448.

154. Tanaka, H., Kannari, K., Maeda, T., Tomiyama, M., Suda, T. and Matsunaga, M. Role of serotonergic neurons in L-DOPA-derived extracellular dopamine in the striatum of 6-OHDA-lesioned rats. *Neuroreport*,1999,*10*,631.

155. Carta, M., Carlsson, T., Kirik, D. and Björklund, A. Dopamine released from 5-HT terminals is the cause of L-DOPA-induced dyskinesia in parkinsonian rats. *Brain*,2007,*130*,1819.

156. Rylander, D., Parent, M., O'Sullivan, S.S., Dovero, S., Lees, A.J., Bezard, E., Descarries, L. and Cenci, M.A. Maladaptive plasticity of serotonin axon terminals in levodopa-induced dyskinesia. *Annals of neurology*,2010,*68*,619.

157. Beaudoin-Gobert, M., Epinat, J., Metereau, E., Duperrier, S., Neumane, S., Ballanger, B., Lavenne, F., Liger, F., Tourvielle, C., Bonnefoi, F. and Costes, N. Behavioural impact of a double dopaminergic and serotonergic lesion in the non-human primate. *Brain*,2015,*138*,2632.

158. Bastide, M.F., Meissner, W.G., Picconi, B., Fasano, S., Fernagut, P.O., Feyder, M., Francardo, V., Alcacer, C., Ding, Y., Brambilla, R. and Fisone, G. Pathophysiology of L-dopa-induced motor and non-motor complications in Parkinson's disease. *Progress in neurobiology*,2015,*132*,96.

159. Fridjonsdottir, E., Shariatgorji, R., Nilsson, A., Vallianatou, T., Odell, L.R., Schembri, L.S., Svenningsson, P., Fernagut, P.O., Crossman, A.R., Bezard, E. and Andrén, P.E. Mass spectrometry imaging identifies abnormally elevated brain l-DOPA levels and extrastriatal monoaminergic dysregulation in l-DOPA–induced dyskinesia. *Science Advances*,2021,*7*,eabe5948.

160. McLaughlin, N., Bielinski, T.M., Tressler, C.M., Barton, E., Glunde, K. and Stumpo, K.A. Pneumatically sprayed gold nanoparticles for mass spectrometry imaging of neurotransmitters. *Journal of the American Society for Mass Spectrometry*,2020,*31*,2452.

161. McGranahan N, Swanton C. Clonal heterogeneity and tumor evolution: past, present, and the future. *Cell*. **2017**,168,613-28.

162. Baylin SB, Jones PA. Epigenetic determinants of cancer. Cold Spring Harbor perspectives in biology. **2016**,8,a019505.

163. Mazor T, Pankov A, Song JS, Costello JF. Intratumoral heterogeneity of the epigenome. *Cancer cell*. **2016**,29,440-51.

164. Mikkilineni L, Whitaker-Menezes D, Domingo-Vidal M, Sprandio J, Avena P, Cotzia P, Dulau-Florea A, Gong J, Uppal G, Zhan T, Leiby B. Hodgkin lymphoma: A complex metabolic ecosystem with glycolytic reprogramming of the tumor microenvironment. *InSeminars in oncology* **2017**;44:218-225.

165. Hsieh JJ, Purdue MP, Signoretti S, Swanton C, Albiges L, Schmidinger M, Heng DY, Larkin J, Ficarra V. Renal cell carcinoma. *Nature reviews Disease primers*. **2017**;3:1-9.

166. Fitzmaurice C, Allen C, Barber RM, Barregard L, Bhutta ZA, Brenner H, Dicker DJ, Chimed-Orchir O, Dandona R, Dandona L, Fleming T. Global, regional, and national cancer incidence, mortality, years of life lost, years lived with disability, and disability-adjusted life-years for 32 cancer groups, 1990 to 2015: a systematic analysis for the global burden of disease study. *JAMA oncology*. **2017**;3:524-48.

167. Motzer RJ, Hutson TE, Tomczak P, Michaelson MD, Bukowski RM, Oudard S, Negrier S, Szczylik C, Pili R, Bjarnason GA, Garcia-del-Muro X. Overall survival and updated results for sunitinib compared with interferon alfa in patients with metastatic renal cell carcinoma. *Journal of clinical oncology*. **2009**;27:3584.

168. Motzer RJ, Escudier B, Oudard S, Hutson TE, Porta C, Bracarda S, Grünwald V, Thompson JA, Figlin RA, Hollaender N, Urbanowitz G. Efficacy of everolimus in advanced renal cell carcinoma: a double-blind, randomised, placebo-controlled phase III trial. *The Lancet*. **2008**;372:449-56.

169. Hudes G, Carducci M, Tomczak P, Dutcher J, Figlin R, Kapoor A, Staroslawska E, Sosman J, McDermott D, Bodrogi I, Kovacevic Z. Temsirolimus, interferon alfa, or both for advanced renal-cell carcinoma. *New England Journal of Medicine*. **2007**;356:2271-81.

170. Rini BI, Escudier B, Tomczak P, Kaprin A, Szczylik C, Hutson TE, Michaelson MD, Gorbunova VA, Gore ME, Rusakov IG, Negrier S. Comparative effectiveness of axitinib versus sorafenib in advanced renal cell carcinoma (AXIS): a randomised phase 3 trial. *The Lancet*. **2011**;378:1931-9.

171. Wettersten HI, Aboud OA, Lara Jr PN, Weiss RH. Metabolic reprogramming in clear cell renal cell carcinoma. *Nature Reviews Nephrology*. **2017**;13:410-9.

172. Hakimi AA, Pham CG, Hsieh JJ. A clear picture of renal cell carcinoma. *Nature genetics*. **2013**;45:849-50.

173. Saito K, Arai E, Maekawa K, Ishikawa M, Fujimoto H, Taguchi R, Matsumoto K, Kanai Y, Saito Y. Lipidomic signatures and associated transcriptomic profiles of clear cell renal cell carcinoma. *Scientific reports*. **2016**;6:1-2.

174. Vijayalakshmi K, Shankar V, Bain RM, Nolley R, Sonn GA, Kao CS, Zhao H, Tibshirani R, Zare RN, Brooks JD. Identification of diagnostic metabolic signatures in clear cell renal cell carcinoma using mass spectrometry imaging. *International journal of cancer*. **2020**;147:256-65.

175. Emoto K, Toyama-Sorimachi N, Karasuyama H, Inoue K, Umeda M. Exposure of phosphatidylethanolamine on the surface of apoptotic cells. *Experimental cell research*. **1997**;232:430-4.

176. Zhang J, Li SQ, Lin JQ, Yu W, Eberlin LS. Mass Spectrometry Imaging Enables Discrimination of Renal Oncocytoma from Renal Cell Cancer Subtypes and Normal Kidney

TissuesMass Spectrometry Imaging of Renal Oncocytoma and Carcinomas. *Cancer research*. **2020**;80:689-98.

177. Ridge CA, Pua BB, Madoff DC. Epidemiology and staging of renal cell carcinoma. *InSeminars in interventional radiology* **2014** Mar (Vol. 31, No. 01, pp. 003-008). Thieme Medical Publishers.

178. Yu JS, Chen YT, Chiang WF, Hsiao YC, Chu LJ, See LC, Wu CS, Tu HT, Chen HW, Chen CC, Liao WC. Saliva protein biomarkers to detect oral squamous cell carcinoma in a high-risk population in Taiwan. *Proceedings of the National Academy of Sciences*. **2016**;113:11549-54.

179. Wang Q, Gao P, Wang X, Duan Y. The early diagnosis and monitoring of squamous cell carcinoma via saliva metabolomics. *Scientific Reports*. **2014**;4:1-9.

180. Ye G, Liu Y, Yin P, Zeng Z, Huang Q, Kong H, Lu X, Zhong L, Zhang Z, Xu G. Study of induction chemotherapy efficacy in oral squamous cell carcinoma using pseudotargeted metabolomics. *Journal of proteome research*. **2014**;13:1994-2004.

181. Sugimoto M, Wong DT, Hirayama A, Soga T, Tomita M. Capillary electrophoresis mass spectrometry-based saliva metabolomics identified oral, breast and pancreatic cancer-specific profiles. *Metabolomics*. **2010**;6:78-95.

182. Vaysse PM, Demers I, van den Hout MF, van de Worp W, Anthony IG, Baijens LW, Tan BI, Lacko M, Vaassen LA, van Mierlo A, Langen RC. Evaluation of the Sensitivity of Metabolic Profiling by Rapid Evaporative Ionization Mass Spectrometry: Toward More Radical Oral Cavity Cancer Resections. *Analytical Chemistry*. **2022**;94:6939-47.

183. Heng YJ, Lester SC, Tse GM, Factor RE, Allison KH, Collins LC, et al. The molecular basis of breast cancer pathological phenotypes. *J Pathol* **2017**;241: 375–91

184. Wishart DS. Is cancer a genetic disease or a metabolic disease? EBioMedicine 2015;2:478–9.

185. Boroughs LK, DeBerardinis RJ. Metabolic pathways promoting cancer cell survival and growth. Nat Cell Biol 2015;17:351–9.

186. DeBenardinis RJ, Lum JJ, Hatzivassiliou G, Thompson CB. The biology of cancer: metabolic reprogramming fuels cell growth and proliferation. *Cell Metab* **2008**;7:11–20.

187. Cai Y, Crowther J, Pastor T, Abbasi LA, Baietti MF, De Troyer M, et al. Loss of chromosome 8p governs tumor progression and drug response by altering lipid metabolism. *Cancer Cell* **2016**;29:751–66.

188. Song X, Chen H, Zare RN. Conductive polymer spray ionization mass spectrometry for biofluid analysis. *Analytical chemistry*. **2018**;90:12878-85.

189. Song Y, Zhang Y, Xie S, Song X. Screening and diagnosis of triple negative breast cancer based on rapid metabolic fingerprinting by conductive polymer spray ionization mass

spectrometry and machine learning. *Frontiers in Cell and Developmental Biology*. **2022**;10:1075810.

190. Aramaki S, Tsuge S, Islam A, Eto F, Sakamoto T, Oyama S, Li W, Zhang C, Yamaguchi S, Takatsuka D, Hosokawa Y. Lipidomics-based tissue heterogeneity in specimens of luminal breast cancer revealed by clustering analysis of mass spectrometry imaging: A preliminary study. *Plos one*. **2023**;18:e0283155.

191. Mondal S, Sthanikam Y, Kumar A, Nandy A, Chattopadhyay S, Koner D, Rukmangadha N, Narendra H, Banerjee S. Mass Spectrometry Imaging of Lumpectomy Specimens Deciphers Diacylglycerols as Potent Biomarkers for the Diagnosis of Breast Cancer. *Analytical Chemistry*. **2023**.

192. Torre LA, Bray F, Siegel RL, Ferlay J, Lortet-Tieulent J, Jemal A. Global cancer statistics, 2012. CA: *a cancer journal for clinicians*. **2015**;65:87-108.

193. Chadwick G, Varagunam M, Brand C, Riley SA, Maynard N, Crosby T, Michalowski J, Cromwell DA. Coding of Barrett's oesophagus with high-grade dysplasia in national administrative databases: a population-based cohort study. *BMJ open*. **2017**;7:e014281.

194. Hanahan D, Weinberg RA. The hallmarks of cancer. *cell*. **2000**;100:57-70.

195. Kroemer G, Pouyssegur J. Tumor cell metabolism: cancer's Achilles' heel. *Cancer cell*. **2008**;13:472-82.

196. Holmes E, Wilson ID, Nicholson JK. Metabolic phenotyping in health and disease. *Cell*. **2008**;134:714-7.

197. Lewis A, Wishart DS, Guo AC, Gautam B, Tzur D, Sobsey CA, Shaykhutdinov R, Fradette R, De Souza A, Cruz JA, Xiong Y. HMDB: A knowledgebase for the human metabolome.

198. Xie D, Seremwe M, Edwards JG, Podolsky R, Bollag WB. Distinct effects of different phosphatidylglycerol species on mouse keratinocyte proliferation. *PLoS One*. **2014**;9:e107119.

199. Frankell AM, Jammula S, Li X, Contino G, Killcoyne S, Abbas S, Perner J, Bower L, Devonshire G, Ococks E, Grehan N. The landscape of selection in 551 esophageal adenocarcinomas defines genomic biomarkers for the clinic. Nature genetics. **2019**;51:506-16.

200. Abbassi-Ghadi N, Antonowicz SS, McKenzie JS, Kumar S, Huang J, Jones EA, Strittmatter N, Petts G, Kudo H, Court S, Hoare JM. De novo lipogenesis alters the phospholipidome of esophageal adenocarcinoma. Cancer Research. **2020**;80:2764-74.

201. Ohtsubo K, Marth JD. Glycosylation in cellular mechanisms of health and disease. Cell. 2006;126:855.

202. Xu C, Ng DT. Glycosylation-directed quality control of protein folding. Nature reviews Molecular cell biology. 2015;16:742.

203. Vagin O, Kraut JA, Sachs G. Role of N-glycosylation in trafficking of apical membrane proteins in epithelia. American Journal of Physiology-Renal Physiology. 2009;296:F459.

204. Delorme E, Lorenzini T, Giffin J, Martin F, Jacobsen F, Boone T, Elliott S. Role of glycosylation on the secretion and biological activity of erythropoietin. Biochemistry. 1992;31:9871

205. Rudd PM, Elliott T, Cresswell P, Wilson IA, Dwek RA. Glycosylation and the immune system. Science. 2001;291:2370-6.

206. Wolfert MA, Boons GJ. Adaptive immune activation: glycosylation does matter. Nature chemical biology. 2013;9:776-84.

207. Marth JD, Grewal PK. Mammalian glycosylation in immunity. Nature Reviews Immunology. 200;8:874-87.

208. Twine SM, Reid CW, Aubry A, McMullin DR, Fulton KM, Austin J, Logan SM. Motility and flagellar glycosylation in Clostridium difficile. Journal of bacteriology. 2009;191:7050-62.

209. Varki, A. & Gagneux, P. in Essentials of glycobiology (eds rd et al.) 77–88 (Cold Spring Harbor Laboratory Press. Copyright 2015–2017 by Te Consortium of Glycobiology Editors, La Jolla, California. All rights reserved, 2015).

210. Cummings RD. The repertoire of glycan determinants in the human glycome. Molecular BioSystems. 2009;5:1087.

211. Reitsma S, Slaaf DW, Vink H, Van Zandvoort MA, oude Egbrink MG. The endothelial glycocalyx: composition, functions, and visualization. Pflügers Archiv-European Journal of Physiology. 2007;454:345.

212. Stanley P, Wuhrer M, Lauc G, Stowell SR, Cummings RD. Structures common to different glycans. Essentials of Glycobiology [Internet]. 4th edition. 2022.

213. Mereiter S, Balmaña M, Campos D, Gomes J, Reis CA. Glycosylation in the era of cancer-targeted therapy: where are we heading?. Cancer cell. 2019;36:6.

214. Mulloy B, Dell A, Stanley P, H. Prestegard J. Structural Analysis of Glycans. 2017. In: Varki A, Cummings RD, Esko JD, Stanley P, Hart GW, Aebi M, Darvill AG, Kinoshita T, Packer NH, Prestegard JH, Schnaar RL, Seeberger PH, editors. Essentials of Glycobiology [Internet]. 3rd ed. Cold Spring Harbor (NY): Cold Spring Harbor Laboratory Press; 2015–2017. Chapter 50. PMID: 28876844.

215. Litwin MS, Tan HJ. The diagnosis and treatment of prostate cancer: a review. Jama. 2017;317:2532.

216. Santoni M, Piva F, Scarpelli M, Cheng L, Lopez-Beltran A, Massari F, Iacovelli R, Berardi R, Santini D, Montironi R. The origin of prostate metastases: emerging insights. Cancer and Metastasis Reviews. 2015;34:765.

217. West CA, Liang H, Drake RR, Mehta AS. New enzymatic approach to distinguish fucosylation isomers of N-linked glycans in tissues using MALDI imaging mass spectrometry. Journal of proteome research. 2020;19:2989.

218. Blaschke CR, Hartig JP, Grimsley G, Liu L, Semmes OJ, Wu JD, Ippolito JE, Hughes-Halbert C, Nyalwidhe JO, Drake RR. Direct N-glycosylation profiling of urine and prostatic fluid glycoproteins and extracellular vesicles. Frontiers in Chemistry. 2021;9:734280.

219. van Gils MP, Cornel EB, Hessels D, Peelen WP, Witjes JA, Mulders PF, Rittenhouse HG, Schalken JA. Molecular PCA3 diagnostics on prostatic fluid. The Prostate. 2007;67:881.

220. Laxman B, Morris DS, Yu J, Siddiqui J, Cao J, Mehra R, Lonigro RJ, Tsodikov A, Wei JT, Tomlins SA, Chinnaiyan AM. A first-generation multiplex biomarker analysis of urine for the early detection of prostate cancer. Cancer research. 2008;68:645.

221. Linxweiler J, Junker K. Extracellular vesicles in urological malignancies: an update. Nature reviews Urology. 2020;17:11.

222. Song W, Zhou X, Benktander JD, Gaunitz S, Zou G, Wang Z, Novotny MV, Jacobson SC. In-depth compositional and structural characterization of N-glycans derived from human urinary exosomes. Analytical chemistry. 2019;91:13528.

223. Hanzawa K, Tanaka-Okamoto M, Murakami H, Mukai M, Takahashi H, Omori T, Ikezawa K, Ohkawa K, Ohue M, Miyamoto Y. Investigation of acidic free-glycans in urine and their alteration in cancer. Glycobiology. 2021;31:391.

224. Pace CL, Angel PM, Drake RR, Muddiman DC. Mass Spectrometry Imaging of N-Linked Glycans in FFPE Human Prostate by Infrared Matrix-Assisted Laser Desorption Electrospray Ionization. Journal of proteome research. 2022;21:243.

225. Powell AK, Harvey DJ. Stabilization of sialic acids in N-linked oligosaccharides and gangliosides for analysis by positive ion matrix-assisted laser desorption/ionization mass spectrometry. Rapid communications in mass spectrometry. 1996;10:1027.

226. Everest-Dass AV, Briggs MT, Kaur G, Oehler MK, Hoffmann P, Packer NH. N-glycan MALDI imaging mass spectrometry on formalin-fixed paraffin-embedded tissue enables the delineation of ovarian cancer tissues. Molecular & Cellular Proteomics. 2016;15:3003.

227. Kuo JC, Gandhi JG, Zia RN, Paszek MJ. Physical biology of the cancer cell glycocalyx. Nature Physics. 2018;14:658.

228. Zhang Z, Wuhrer M, Holst S. Serum sialylation changes in cancer. Glycoconjugate journal. 2018;35:139.

229. Paulson JC, Colley KJ. Glycosyltransferases. Structure, localization, and control of cell type-specific glycosylation. J Biol Chem. 1989;264:17615.

230. Stencel-Baerenwald JE, Reiss K, Reiter DM, Stehle T, Dermody TS. The sweet spot: defining virus–sialic acid interactions. Nature Reviews Microbiology. 2014;12:739.

231. Bertozzi CR. A decade of bioorthogonal chemistry. Accounts of chemical research. 2011;44:651.

232. Lopez Aguilar A, Briard JG, Yang L, Ovryn B, Macauley MS, Wu P. Tools for studying glycans: recent advances in chemoenzymatic glycan labeling. ACS chemical biology. 2017;12:611.

233. Cioce A, Malaker SA, Schumann B. Generating orthogonal glycosyltransferase and nucleotide sugar pairs as next-generation glycobiology tools. Current Opinion in Chemical Biology. 2021;60:66.

234. Lu X, McDowell CT, Blaschke CR, Liu L, Grimsley G, Wisniewski L, Gao C, Mehta AS, Haab BB, Angel PM, Drake RR. Bioorthogonal Chemical Labeling Probes Targeting Sialic Acid Isomers for N-Glycan MALDI Imaging Mass Spectrometry of Tissues, Cells, and Biofluids. Analytical Chemistry. 2023;95:7475.

235. McDowell CT, Klamer Z, Hall J, West CA, Wisniewski L, Powers TW, Angel PM, Mehta AS, Lewin DN, Haab BB, Drake RR. Imaging mass spectrometry and lectin analysis of N-linked glycans in carbohydrate antigen–defined pancreatic cancer tissues. Molecular & Cellular Proteomics. 2021;20.

236. Blaschke CR, Hartig JP, Grimsley G, Liu L, Semmes OJ, Wu JD, Ippolito JE, Hughes-Halbert C, Nyalwidhe JO, Drake RR. Direct N-glycosylation profiling of urine and prostatic fluid glycoproteins and extracellular vesicles. Frontiers in Chemistry. 2021;9:734280.

237. Laughlin ST. Agard NJ Baskin JM Carrico IS Chang PV Ganguli AS Hangauer MJ Lo A. Prescher JA Bertozzi CR Metabolic labeling of glycans with azido sugars for visualization and glycoproteomics. Methods Enzymol. 2006;415:230.

238. Holst S, Heijs B, De Haan N, Van Zeijl RJ, Briaire-de Bruijn IH, Van Pelt GW, Mehta AS, Angel PM, Mesker WE, Tollenaar RA, Drake RR. Linkage-specific in situ sialic acid derivatization for N-glycan mass spectrometry imaging of formalin-fixed paraffin-embedded tissues. Analytical chemistry. 2016;88:5904.

239. Blaschke CR, McDowell CT, Black AP, Mehta AS, Angel PM, Drake RR. Glycan imaging mass spectrometry: progress in developing clinical diagnostic assays for tissues, biofluids, and cells. Clinics in laboratory medicine. 2021;41:247.

240. Mehta A, Herrera H, Block T. Glycosylation and liver cancer. Advances in cancer research. 2015;126:257.

241. Blomme B, Van Steenkiste C, Callewaert N, Van Vlierberghe H. Alteration of protein glycosylation in liver diseases. Journal of hepatology. 2009;50:592.

242. Comunale MA, Lowman M, Long RE, Krakover J, Philip R, Seeholzer S, Evans AA, Hann HW, Block TM, Mehta AS. Proteomic analysis of serum associated fucosylated glycoproteins in the development of primary hepatocellular carcinoma. Journal of proteome research. 2006;5:308.

243. DelaCourt A, Black A, Angel P, Drake R, Hoshida Y, Singal A, Lewin D, Taouli B, Lewis S, Schwarz M, Fiel MI. N-glycosylation patterns correlate with hepatocellular carcinoma genetic subtypes. Molecular Cancer Research. 2021;19:1868.

244. Sandhu DS, Roberts LR. Diagnosis and management of cholangiocarcinoma. Current gastroenterology reports. 2008;10:43.

245. Brindley PJ, Bachini M, Ilyas SI, Khan SA, Loukas A, Sirica AE, Teh BT, Wongkham S, Gores GJ. Cholangiocarcinoma. Nature reviews Disease primers. 2021;7:65.

246. Ochoa-Rios S, Blaschke CR, Wang M, Peterson KD, DelaCourt A, Grauzam SE, Lewin D, Angel P, Roberts LR, Drake R, Mehta AS. Analysis of n-linked glycan alterations in tissue and serum reveals promising biomarkers for intrahepatic cholangiocarcinoma. Cancer Research Communications. 2023;3:383.

247. Bray FF, Ferlay J, Soerjomataram I, Siegel RL, Torre LA, Jemal AJ. Erratum: Global cancer statistics 2018: GLOBOCAN estimates of incidence and mortality worldwide for 36 cancers in 185 countries. Ca Cancer J Clin. 2020;70:313.

248. Wanyama FM, Blanchard V. Glycomic-based biomarkers for ovarian cancer: Advances and challenges. Diagnostics. 2021;11:643.

249. Briggs MT, Condina MR, Ho YY, Everest-Dass AV, Mittal P, Kaur G, Oehler MK, Packer NH, Hoffmann P. MALDI mass spectrometry imaging of early-and late-stage serous ovarian cancer tissue reveals stage-specific N-glycans. Proteomics. 2019;19:1800482.

250. Grzeski M, Taube ET, Braicu EI, Sehouli J, Blanchard V, Klein O. In situ N-glycosylation signatures of epithelial ovarian cancer tissue as defined by MALDI mass spectrometry imaging. Cancers. 2022;14:1021.

251. Bray F, Ferlay J, Soerjomataram I, Siegel RL, Torre LA, Jemal A. Global cancer statistics 2018: GLOBOCAN estimates of incidence and mortality worldwide for 36 cancers in 185 countries. CA: a cancer journal for clinicians. 2018;68:394.

252. Bray F, Jemal A, Grey N, Ferlay J, Forman D. Global cancer transitions according to the Human Development Index (2008–2030): a population-based study. The lancet oncology. 2012;13:790.

253. de Freitas Junior JC, Morgado-Díaz JA. The role of N-glycans in colorectal cancer progression: Potential biomarkers and therapeutic applications. Oncotarget. 2016;7:19395.

254. Holst S, Deuss AJ, Van Pelt GW, Van Vliet SJ, Garcia-Vallejo JJ, Koeleman CA, Deelder AM, Mesker WE, Tollenaar RA, Rombouts Y, Wuhrer M. N-glycosylation profiling of colorectal cancer cell lines reveals association of fucosylation with differentiation and caudal type homebox 1 (CDX1)/Villin mRNA expression. Molecular & Cellular Proteomics. 2016;15:124.

255. de Vroome SW, Holst S, Girondo MR, van der Burgt YE, Mesker WE, Tollenaar RA, Wuhrer M. Serum N-glycome alterations in colorectal cancer associate with survival. Oncotarget. 2018;9:30610.

256. Boyaval F, Dalebout H, Van Zeijl R, Wang W, Fariña-Sarasqueta A, Lageveen-Kammeijer GS, Boonstra JJ, McDonnell LA, Wuhrer M, Morreau H, Heijs B. High-mannose N-glycans as malignant progression markers in early-stage colorectal cancer. Cancers. 2022;14:1552.

257. Rebelo AL, Gubinelli F, Roost P, Jan C, Brouillet E, Van Camp N, Drake RR, Saldova R, Pandit A. Complete spatial characterisation of N-glycosylation upon striatal neuroinflammation in the rodent brain. Journal of Neuroinflammation. 2021;18:1.

258. Scott H, Panin VM. N-glycosylation in regulation of the nervous system. Glycobiology of the nervous system. 2014:367.

259. Samal J, Palomino TV, Chen J, Muddiman DC, Segura T. Enhanced Detection of Charged N-Glycans in the Brain by Infrared Matrix-Assisted Laser Desorption Electrospray Ionization Mass Spectrometric Imaging. Analytical Chemistry. 2023.

260. Fukuda M, Hiraoka N, Akama TO, Fukuda MN. Carbohydrate-modifying sulfotransferases: structure, function, and pathophysiology. Journal of Biological Chemistry. 2001;276:47747.

261. Yu SY, Wu SW, Hsiao HH, Khoo KH. Enabling techniques and strategic workflow for sulfoglycomics based on mass spectrometry mapping and sequencing of permethylated sulfated glycans. Glycobiology. 2009;19:1136.

262. Lei M, Mechref Y, Novotny MV. Structural analysis of sulfated glycans by sequential double-permethylation using methyl iodide and deuteromethyl iodide. Journal of the American Society for Mass Spectrometry. 2009;20:1660.

263. Harker A. Social dysfunction: The effects of early trauma and adversity on socialization and brain development. InThe neurobiology of brain and behavioral development 2018 Jan 1 (pp. 439-467). Academic Press.

264. Yoshimura T, Hayashi A, Handa-Narumi M, Yagi H, Ohno N, Koike T, Yamaguchi Y, Uchimura K, Kadomatsu K, Sedzik J, Kitamura K. GlcNAc6ST-1 regulates sulfation of N-glycans and myelination in the peripheral nervous system. Scientific reports. 2017;7:42257.

265. Nave KA, Trapp BD. Axon-glial signaling and the glial support of axon function. Annu. Rev. Neurosci.. 2008;31:535.

266. Quarles RH. Comparison of CNS and PNS myelin proteins in the pathology of myelin disorders. Journal of the neurological sciences. 2005;228:187

267. Coskun, A.F., Eser, U. and Islam, S., 2016. Cellular identity at the single-cell level. *Molecular BioSystems*, *12*(10), pp.2965-2979.

268. Griffiths, J.A., Scialdone, A. and Marioni, J.C., 2018. Using single-cell genomics to understand developmental processes and cell fate decisions. *Molecular systems biology*, *14*(4), p.e8046.

269. Gutierrez, G.D., Gromada, J. and Sussel, L., 2017. Heterogeneity of the pancreatic beta cell. *Frontiers in genetics*, *8*, p.22.

270. Gustavsson, A.K., van Niekerk, D.D., Adiels, C.B., Goksör, M. and Snoep, J.L., 2014. Heterogeneity of glycolytic oscillatory behaviour in individual yeast cells. *FEBS letters*, *588*(1), pp.3-7.

271. Ren, S.C., Qu, M. and Sun, Y.H., 2013. Investigating intratumour heterogeneity by single-cell sequencing. *Asian journal of andrology*, *15*(6), p.729.

272. Evans, C.R. and Ling, J., 2018. Visualizing translational errors: one cell at a time. *Current genetics*, *64*(3), pp.551-554.

273. Cao, Z. and Wu, S., 2017. Current research development of single cell genome in urological tumor. *The International Journal of Biochemistry & Cell Biology*, *90*, pp.167-171.

274. Haselgrübler, T., Haider, M., Ji, B., Juhasz, K., Sonnleitner, A., Balogi, Z. and Hesse, J., 2014. High-throughput, multiparameter analysis of single cells. *Analytical and Bioanalytical Chemistry*, *406*, pp.3279-3296.

275. Chattopadhyay, P.K., Gierahn, T.M., Roederer, M. and Love, J.C., 2014. Single-cell technologies for monitoring immune systems. *Nature immunology*, *15*(2), pp.128-135.

276. Li, G., Dzilic, E., Flores, N., Shieh, A. and Wu, S.M., 2017. Strategies for the acquisition of transcriptional and epigenetic information in single cells. *Journal of Thoracic Disease*, *9*(Suppl 1), p.S9.

277. Kelsey, G., Stegle, O. and Reik, W., 2017. Single-cell epigenomics: Recording the past and predicting the future. *Science*, *358*(6359), pp.69-75.

278. Shaw, R., Tian, X. and Xu, J., 2021. Single-cell transcriptome analysis in plants: advances and challenges. *Molecular Plant*, *14*(1), pp.115-126.

279. Kodzius, R. and Gojobori, T., 2016. Single-cell technologies in environmental omics. *Gene*, *576*(2), pp.701-707.

280. Hu, P., Zhang, W., Xin, H. and Deng, G., 2016. Single cell isolation and analysis. *Frontiers in cell and developmental biology*, *4*, p.116.

281. Heath, J.R., Ribas, A. and Mischel, P.S., 2016. Single-cell analysis tools for drug discovery and development. *Nature reviews Drug discovery*, *15*(3), pp.204-216.

282. Muñoz, H.E., Li, M., Riche, C.T., Nitta, N., Diebold, E., Lin, J., Owsley, K., Bahr, M., Goda, K. and Di Carlo, D., 2018. Single-cell analysis of morphological and metabolic heterogeneity in Euglena gracilis by fluorescence-imaging flow cytometry. *Analytical chemistry*, *90*(19), pp.11280-11289.

283. Miura, T., Mikami, H., Isozaki, A., Ito, T., Ozeki, Y. and Goda, K., 2018. On-chip light-sheet fluorescence imaging flow cytometry at a high flow speed of 1 m/s. *Biomedical optics express*, *9*(7), pp.3424-3433.

284. McKinnon, K.M., 2018. Flow cytometry: an overview. *Current protocols in immunology*, *120*(1), pp.5-1.

285. Frelinger III, A.L., 2018. Using flow cytometry to monitor glycoprotein IIb-IIIa activation. *Platelets*, *29*(7), pp.670-676.

286. Taruc, K., Yin, C., Wootton, D.G. and Heit, B., 2018. Quantification of efferocytosis by single-cell fluorescence microscopy. *JoVE (Journal of Visualized Experiments)*, (138), p.e58149.

287. Alber, A.B. and Suter, D.M., 2018. Single-cell quantification of protein degradation rates by time-lapse fluorescence microscopy in adherent cell culture. *JoVE (Journal of Visualized Experiments)*, (132), p.e56604.

288. Zenobi, R., 2013. Single-cell metabolomics: analytical and biological perspectives. *Science*, *342*(6163), p.1243259.

289. Barofsky, A., Simonelli, P., Vidoudez, C., Troedsson, C., Nejstgaard, J.C., Jakobsen, H.H. and Pohnert, G., 2010. Growth phase of the diatom Skeletonema marinoi influences the metabolic profile of the cells and the selective feeding of the copepod Calanus spp. *Journal of Plankton Research*, *32*(3), pp.263-272.

290. Vidoudez, C. and Pohnert, G., 2012. Comparative metabolomics of the diatom Skeletonema marinoi in different growth phases. *Metabolomics*, *8*, pp.654-669.

291. Polat, A.N. and Özlü, N., 2014. Towards single-cell LC-MS phosphoproteomics. *Analyst*, *139*(19), pp.4733-4749.

292. Ong, T.H., Tillmaand, E.G., Makurath, M., Rubakhin, S.S. and Sweedler, J.V., 2015. Mass spectrometry-based characterization of endogenous peptides and metabolites in small volume samples. *Biochimica et Biophysica Acta (BBA)-Proteins and Proteomics*, *1854*(7), pp.732-740.

293. Ma, X. and Xia, Y., 2014. Pinpointing double bonds in lipids by Paternò-Büchi reactions and mass spectrometry. *Angewandte Chemie International Edition*, *53*(10), pp.2592-2596.

294. Murphy, R.C., Okuno, T., Johnson, C.A. and Barkley, R.M., 2017. Determination of double bond positions in polyunsaturated fatty acids using the photochemical Paterno-Buchi reaction with acetone and tandem mass spectrometry. *Analytical chemistry*, *89*(16), pp.8545-8553.

295. Zhao, X., Zhang, W., Zhang, D., Liu, X., Cao, W., Chen, Q., Ouyang, Z. and Xia, Y., 2019. A lipidomic workflow capable of resolving sn-and C Created by potrace 1.16, written by Peter Selinger 2001-2019 C location isomers of phosphatidylcholines. *Chemical Science*, *10*(46), p.10740.

296. Cao, W., Cheng, S., Yang, J., Feng, J., Zhang, W., Li, Z., Chen, Q., Xia, Y., Ouyang, Z. and Ma, X., 2020. Large-scale lipid analysis with C= C location and sn-position isomer resolving power. *Nature communications*, *11*(1), p.375.

297. Zhu, Y., Wang, W. and Yang, Z., 2020. Combining Mass Spectrometry with Paternò–Büchi Reaction to Determine Double-Bond Positions in Lipids at the Single-Cell Level. *Analytical chemistry*, *92*(16), pp.11380-11387.

298. Li, Z., Cheng, S., Lin, Q., Cao, W., Yang, J., Zhang, M., Shen, A., Zhang, W., Xia, Y., Ma, X. and Ouyang, Z., 2021. Single-cell lipidomics with high structural specificity by mass spectrometry. *Nature Communications*, *12*(1), p.2869.

299. Taylor, M.J., Liyu, A., Vertes, A. and Anderton, C.R., 2021. Ambient single-cell analysis and native tissue imaging using laser-ablation electrospray ionization mass spectrometry with increased spatial resolution. *Journal of the American Society for Mass Spectrometry*, *32*(9), pp.2490-2494.

300. Zheng, X., Aly, N.A., Zhou, Y., Dupuis, K.T., Bilbao, A., Paurus, V.L., Orton, D.J., Wilson, R., Payne, S.H., Smith, R.D. and Baker, E.S., 2017. A structural examination and collision cross section database for over 500 metabolites and xenobiotics using drift tube ion mobility spectrometry. *Chemical science*, *8*(11), pp.7724-7736.

301. Stopka, S.A., Wood, E.A., Khattar, R., Agtuca, B.J., Abdelmoula, W.M., Agar, N.Y., Stacey, G. and Vertes, A., 2021. High-throughput analysis of tissue-embedded single cells by mass spectrometry with bimodal imaging and object recognition. *Analytical Chemistry*, *93*(28), pp.9677-9687.

302. Kulkarni, P., Wilschut, R.A., Verhoeven, K.J., van der Putten, W.H. and Garbeva, P., 2018. LAESI mass spectrometry imaging as a tool to differentiate the root metabolome of native and range-expanding plant species. *Planta*, *248*, pp.1515-1523.

303. Granborg JR, Handler AM, Janfelt C. Mass spectrometry imaging in drug distribution and drug metabolism studies–Principles, applications and perspectives. TrAC Trends in Analytical Chemistry. 2022;146:116482.

304. Yamamoto E, Taquahashi Y, Kuwagata M, Saito H, Matsushita K, Toyoda T, Sato F, Kitajima S, Ogawa K, Izutsu KI, Saito Y. Visualizing the spatial localization of ciclesonide and its metabolites in rat lungs after inhalation of 1-μm aerosol of ciclesonide by desorption electrospray ionization-time of flight mass spectrometry imaging. International Journal of Pharmaceutics. 2021;595:120241.

305. Goodwin RJ, Nilsson A, Mackay CL, Swales JG, Johansson MK, Billger M, Andrén PE, Iverson SL. Exemplifying the screening power of mass spectrometry imaging over label-based technologies for simultaneous monitoring of drug and metabolite distributions in tissue sections. Journal of biomolecular screening. 2016;21(2):187-93.

306. Akakpo JY, Ramachandran A, Duan L, Schaich MA, Jaeschke MW, Freudenthal BD, Ding WX, Rumack BH, Jaeschke H. Delayed treatment with 4-methylpyrazole protects against acetaminophen hepatotoxicity in mice by inhibition of c-Jun N-terminal kinase. Toxicological Sciences. 2019;170(1):57-68

307. Akakpo JY, Ramachandran A, Kandel SE, Ni HM, Kumer SC, Rumack BH, Jaeschke H. 4-Methylpyrazole protects against acetaminophen hepatotoxicity in mice and in primary human hepatocytes. Human & Experimental Toxicology. 2018;37(12):1310-22.

308. McEwen A, Henson C. Quantitative whole-body autoradiography: past, present and future. Bioanalysis. 2015;7(5):557-68.

309. Solon EG. Use of radioactive compounds and autoradiography to determine drug tissue distribution. Chemical research in toxicology. 2012;25(3):543-55.

310. Prideaux B, Stoeckli M. Mass spectrometry imaging for drug distribution studies. Journal of proteomics. 2012;75(16):4999-5013.

311. Karlsson O, Hanrieder J. Imaging mass spectrometry in drug development and toxicology. Archives of toxicology. 2017;91:2283-94.

312. Ho YN, Shu LJ, Yang YL. Imaging mass spectrometry for metabolites: technical progress, multimodal imaging, and biological interactions. Wiley Interdisciplinary Reviews: Systems Biology and Medicine. 2017;9(5):e1387.

313. Balluff B, McDonnell LA. Mass spectrometry imaging of metabolites. Clinical Metabolomics: Methods and Protocols. 2018:345-57.

314. Akakpo JY, Jaeschke MW, Etemadi Y, Artigues A, Toerber S, Olivos H, Shrestha B, Midey A, Jaeschke H, Ramachandran A. Desorption Electrospray Ionization Mass Spectrometry Imaging Allows Spatial Localization of Changes in Acetaminophen Metabolism in the Liver after Intervention with 4-Methylpyrazole. Journal of the American Society for Mass Spectrometry. 2022;33(11):2094-107.

315. Liu D, Huang J, Gao S, Jin H, He J. A temporo-spatial pharmacometabolomics method to characterize pharmacokinetics and pharmacodynamics in the brain microregions by using ambient mass spectrometry imaging. Acta Pharmaceutica Sinica B. 2022;12(8):3341-53.

316. Babatin M, Lee SS, Pollak PT. Amiodarone hepatotoxicity. Current vascular pharmacology. 2008;6(3):228-36.

317. Endo S, Toyoda Y, Fukami T, Nakajima M, Yokoi T. Stimulation of human monocytic THP-1 cells by metabolic activation of hepatotoxic drugs. Drug metabolism and pharmacokinetics. 2012;27(6):621-30.

318. Waldhauser KM, Török M, Ha HR, Thomet U, Konrad D, Brecht K, Follath F, Krähenbühl S. Hepatocellular toxicity and pharmacological effect of amiodarone and amiodarone derivatives. Journal of pharmacology and experimental therapeutics. 2006;319(3):1413-23.

319. Li L, Zang Q, Li X, Zhu Y, Wen S, He J, Zhang R, Abliz Z. Spatiotemporal pharmacometabolomics based on ambient mass spectrometry imaging to evaluate the metabolism and hepatotoxicity of amiodarone in HepG2 spheroids. Journal of Pharmaceutical Analysis. 2023;13(5):483-93.

320. Stierlin H, Faigle JW, Sallmann A, Kung W, Richter WJ, Kriemler HP, Alt KO, Winkler T. Biotransformation of diclofenac sodium (Voltaren®) in animals and in man: I. Isolation and identification of principal metabolites. Xenobiotica. 1979;9(10):601-10.

321. Kenny JR, Maggs JL, Meng X, Sinnott D, Clarke SE, Park BK, Stachulski AV. Syntheses and characterization of the acyl glucuronide and hydroxy metabolites of diclofenac. Journal of medicinal chemistry. 2004;47(11):2816-25.

322. Daly AK, Aithal GP, Leathart JB, Swainsbury RA, Dang TS, Day CP. Genetic susceptibility to diclofenac-induced hepatotoxicity: contribution of UGT2B7, CYP2C8, and ABCC2 genotypes. Gastroenterology. 2007;132(1):272-81.

323. Sparidans RW, Lagas JS, Schinkel AH, Schellens JH, Beijnen JH. Liquid chromatography–tandem mass spectrometric assay for diclofenac and three primary metabolites in mouse plasma. Journal of Chromatography B. 2008;872(1-2):77-82.

324. Boelsterli UA. Diclofenac-induced liver injury: a paradigm of idiosyncratic drug toxicity. Toxicology and applied pharmacology. 2003;192(3):307-22.

325. Regan SL, Maggs JL, Hammond TG, Lambert C, Williams DP, Park BK. Acyl glucuronides: the good, the bad and the ugly. Biopharmaceutics & drug disposition. 2010;31(7):367-95.

326. Bort R, Macé K, Boobis A, Gómez-Lechón MJ, Pfeifer A, Castell J. Hepatic metabolism of diclofenac: role of human CYP in the minor oxidative pathways. Biochemical pharmacology. 1999;58(5):787-96.

327. Vaz AD, Wang WW, Bessire AJ, Sharma R, Hagen AE. A rapid and specific derivatization procedure to identify acyl-glucuronides by mass spectrometry. Rapid Communications in Mass Spectrometry. 2010;24(14):2109-21.

328. Sanchez DM, Brown HM, Yin R, Chen B, Vavrek M, Cancilla MT, Zhong W, Shyong B, Zhang NR, Li F, Laskin J. Mass spectrometry imaging of diclofenac and its metabolites in tissues using nanospray desorption electrospray ionization. Analytica Chimica Acta. 2022;1233:340490.

329. World Health Organization. Global tuberculosis report 2020: executive summary. InGlobal tuberculosis report 2020: executive summary 2020.

330. Horsburgh Jr CR, Barry III CE, Lange C. Treatment of tuberculosis. New England Journal of Medicine. 2015;373(22):2149-60.

331. Dartois V. The path of anti-tuberculosis drugs: from blood to lesions to mycobacterial cells. Nature Reviews Microbiology. 2014;12(3):159-67.

332. Kokesch-Himmelreich J, Treu A, Race AM, Walter K, Hölscher C, Römpp A. Do anti-tuberculosis drugs reach their target?─ high-resolution matrix-assisted laser desorption/ionization mass spectrometry imaging provides information on drug penetration into necrotic granulomas. Analytical Chemistry. 2022;94(14):5483-92.

333. Schwamborn K, Caprioli RM. Molecular imaging by mass spectrometry—looking beyond classical histology. Nature Reviews Cancer. 2010 Sep;10(9):639-46.

334. Li T, He J, Mao X, Bi Y, Luo Z, Guo C, Tang F, Xu X, Wang X, Wang M, Chen J. In situ biomarker discovery and label-free molecular histopathological diagnosis of lung cancer by ambient mass spectrometry imaging. Scientific reports. 2015 Sep 25;5(1):14089.

335. Tuck M, Grélard F, Blanc L, Desbenoit N. MALDI-MSI towards multimodal imaging: challenges and perspectives. Frontiers in Chemistry. 2022 May 9;10:904688.

336. Kompauer M, Heiles S, Spengler B. Atmospheric pressure MALDI mass spectrometry imaging of tissues and cells at 1.4-μm lateral resolution. Nature methods. 2017 Jan;14(1):90-6.

337. Ščupáková K, Balluff B, Tressler C, Adelaja T, Heeren RM, Glunde K, Ertaylan G. Cellular resolution in clinical MALDI mass spectrometry imaging: the latest advancements and current challenges. Clinical Chemistry and Laboratory Medicine (CCLM). 2020 Jun 25;58(6):914-29.

338. Neumann EK, Migas LG, Allen JL, Caprioli RM, Van de Plas R, Spraggins JM. Spatial metabolomics of the human kidney using MALDI trapped ion mobility imaging mass spectrometry. Analytical Chemistry. 2020 Jul 15;92(19):13084-91.

339. Klein O, Haeckel A, Reimer U, Nebrich G, Schellenberger E. Multiplex enzyme activity imaging by MALDI-IMS of substrate library conversions. Scientific Reports. 2020 Sep 23;10(1):15522.

340. Luo Z, He J, Chen Y, He J, Gong T, Tang F, Wang X, Zhang R, Huang L, Zhang L, Lv H. Air flow-assisted ionization imaging mass spectrometry method for easy whole-body molecular imaging under ambient conditions. Analytical chemistry. 2013 Mar 5;85(5):2977-82.

341. Takats Z, Wiseman JM, Cooks RG. Ambient mass spectrometry using desorption electrospray ionization (DESI): instrumentation, mechanisms and applications in forensics, chemistry, and biology. Journal of mass spectrometry. 2005 Oct;40(10):1261-75.

342. Qi K, Wu L, Liu C, Pan Y. Recent advances of ambient mass spectrometry imaging and its applications in lipid and metabolite analysis. Metabolites. 2021 Nov 15;11(11):780.

343. Yin R, Kyle J, Burnum-Johnson K, Bloodsworth KJ, Sussel L, Ansong C, Laskin J. High spatial resolution imaging of mouse pancreatic islets using nanospray desorption electrospray ionization mass spectrometry. Analytical chemistry. 2018 May 2;90(11):6548-55.

344. Unsihuay D, Yin R, Sanchez DM, Yang M, Li Y, Sun X, Dey SK, Laskin J. High-resolution imaging and identification of biomolecules using Nano-DESI coupled to ion mobility spectrometry. Analytica Chimica Acta. 2021 Nov 22;1186:339085.

345. Sun C, Li T, Song X, Huang L, Zang Q, Xu J, Bi N, Jiao G, Hao Y, Chen Y, Zhang R. Spatially resolved metabolomics to discover tumor-associated metabolic alterations. Proceedings of the National Academy of Sciences. 2019 Jan 2;116(1):52-7.

346. He J, Sun C, Li T, Luo Z, Huang L, Song X, Li X, Abliz Z. A sensitive and wide coverage ambient mass spectrometry imaging method for functional metabolites based molecular histology. Advanced Science. 2018 Nov;5(11):1800250.

347. Van de Plas, R., Yang, J., Spraggins, J. and Caprioli, R.M., 2015. Image fusion of mass spectrometry and microscopy: a multimodality paradigm for molecular tissue mapping. *Nature methods*, *12*(4), pp.366-372.

348. Yan, X., Zhao, X., Zhou, Z., McKay, A., Brunet, A. and Zare, R.N., 2020. Cell-type-specific metabolic profiling achieved by combining desorption electrospray ionization mass spectrometry imaging and immunofluorescence staining. *Analytical chemistry*, *92*(19), pp.13281-13289.

349. Mellinger, A.L., Muddiman, D.C. and Gamcsik, M.P., 2022. Highlighting functional mass spectrometry imaging methods in bioanalysis. *Journal of proteome research*, *21*(8), pp.1800-1807.

350. Körber, A., Keelor, J.D., Claes, B.S., Heeren, R.M. and Anthony, I.G., 2022. Fast Mass Microscopy: Mass Spectrometry Imaging of a Gigapixel Image in 34 Minutes. *Analytical Chemistry*, *94*(42), pp.14652-14658.

351. Guo, L., Liu, X., Zhao, C., Hu, Z., Xu, X., Cheng, K.K., Zhou, P., Xiao, Y., Shah, M., Xu, J. and Dong, J., 2022. iSegMSI: an interactive strategy to improve spatial segmentation of mass spectrometry imaging data. *Analytical Chemistry*, *94*(42), pp.14522-14529.

352. Rübel, O., Greiner, A., Cholia, S., Louie, K., Bethel, E.W., Northen, T.R. and Bowen, B.P., 2013. OpenMSI: a high-performance web-based platform for mass spectrometry imaging. *Analytical chemistry*, *85*(21), pp.10354-10361.